A RAMAN SPECTROSCOPIC STUDY OF SOLID DISPERSIONS AND CO - CRYSTALS DURING THE PHARMACEUTICAL HOT MELT EXTRUSION PROCESS

Parineeta Namdeo BANEDAR

Submitted for the degree of

Doctor of Philosophy

Centre for Pharmaceutical Engineering Sciences

Faculty of Life Sciences

University of Bradford

2015

Abstract

Parineeta Namdeo BANEDAR

A RAMAN SPECTROSCOPIC STUDY OF SOLID DISPERSIONS AND CO-CRYSTALS DURING THE PHARMACEUTICAL HOT MELT EXTRUSION PROCESS

Keywords: Raman Spectroscopy, Process Analytical Technology, Hot Melt Extrusion, Solid Dispersions, Co-crystals

Process Analytical Technology (PAT) is framed with the objective of the design and development of processes to ensure predefined quality of the product at the end of manufacturing. PAT implementation includes better understanding of process, reduction in production time with use of in-line, at-line and on-line measurements, yield improvement and energy and cost reductions.

Hot Melt Extrusion process (HME) used in the present work is proving increasingly popular in industry for its continuous and green processing which is beneficial over traditional batch processing. The present work was focused on applications of Raman spectroscopy as off - line and in - line monitoring techniques as a PAT for production of pharmaceutical solid dispersions and co-crystals.

Solid dispersions (SDs) of the anti-convulsant Carbamazepine (CBZ) with two pharmaceutical grade polymers have been produced using HME at a

range of drug loadings and their amorphous nature confirmed using a variety of analytical techniques. Off-line and in-line Raman spectroscopy has been shown to be suitable techniques for proving preparation of these SDs. Through calibration curves generated from chemometric analysis in-line Raman spectroscopy was shown to be more accurate than off-line measurements proving the quantification ability of Raman spectroscopy as well as a PAT tool.

Pure co-crystals of Ibuprofen-Nicotinamide and Carbamazepine-Nicotinamide have been produced using solvent evaporation and microwave radiation techniques. Raman spectroscopy proved its superiority over off-line analytical techniques such as DSC, FTIR and XRD for co-crystal purity determination adding to its key advantage in its ability to be used as an in-line, non-destructive technique.

Acknowledgements

I take this opportunity to express my deep sense of gratitude to Dr. Tim Gough for showing the path and vision where research is all about enthusiasm, keen observation, creativity, hard work and patience. I am and will remain thankful to him forever for being there always, being motivational all the time and being supportive at every stage of my course.

I am thankful to Prof. Anant Paradkar for his suggestions and for the guidance during selection of this course at University of Bradford when I was planning to do PhD. Getting an opportunity to work in an interdisciplinary research environment at University of Bradford has eventually turned out as the most important and fruitful decision of my life. I gratefully acknowledge Dr. Adrian Kelly and Dr. Yee Li for their guidance during HME. I am thankful to Dr. Mohammad Isreb for his suggestions. My sincere thanks to Sue Baker from International office for her valuable suggestions. My special thanks to Anne Costigan for her help and support. My sincere thanks to Dr. Elaine Brown, Mr. Glen Thompson and all other Polymer IRC staff members. My sincere thanks to Dr. Anne Graham and Mrs. Shamim Haider from School of Life sciences for their support. I am thankful to all the non - teaching staff of the university especially, Dennis, Andrew, Pattie Grimshaw and Sahiba from analytical centre. I am also thankful to University of Bradford for offering on - campus jobs which helped me work and learn in a new professional environment. I am thankful to the student's union, University of Bradford services for arranging various activities for students.

I really feel fortunate to be a student of University of Bradford. My stay here in Bradford has helped me learn many things professionally and turned out as a significant learning experience of a lifetime. Fluctuating yet pleasant weather changes here in United Kingdom made me feel blessed to experience a different colour of life. After being a self-funded student with the support of my parents and education loan for almost first two years, I am thankful to my sponsor for funding my course since the end of second year.

I adequately express my deep sense of gratitude for my parents for being a reason of my being and unconditional support. I am thankful to everything and everyone being the reason for making me realise meaning of life in real sense which is a continuous learning process.

I am thankful to all my friends, colleagues, family members, new international friends and well - wishers.

Above all, I thank almighty God, the divine power in this world for showering infinite blessings and grace.

Parineeta

Bradford, England 2015

Dedicated to

Dr. Tim Gough

Table of Contents

Appendix A - 2

Simultaneous estimation of Carbamazepine and Iminostilbene by HPLC and calibration curve generation

List of Figures

List of Tables

List of abbreviations

API: Active Pharmaceutical Ingredient

CBZ: Carbamazepine

CoC/Co - C: Co – crystal

DSC: Differential Scanning Calorimetry

FTIR: Fourier Transform Infra - red

HME: Hot Melt Extrusion

HSM: Hot Stage Microscopy

IBU: Ibuprofen

NA: Nicotinamide

PAT: Process Analytical Technology

pm: physical mixtures

PXRD: Powder X - ray Diffractometry

QbD: Quality by Design

RS: Raman Spectroscopy

SD: Solid dispersion

TEC: Triethyl acetate

TGA: Thermo Gravimetric Analysis

Chapter 1 - Introduction

1.1. General Introduction

Since there is an increasing demand in the process optimization and product quality improvement within the pharmaceutical industries, less time consuming and novel analytical techniques are becoming a focus within related research.

Quality by Design (QbD) is a scientific and proactive approach to pharmaceutical development based on the concept that quality should be 'built-in' by proper design than being simply reliant on end product performance (ICH, 2009). Based on the QbD concept, Process Analytical Technology (PAT) applies innovative scientific and engineering principles for the assessment of pharmaceutical product design, analysis and process quality. It ensures a predefined quality of products after the production process which may improve production time, use of materials and energy utilized for production (Scott and Wilcock, 2006).

A review of the history of identification of polymorphic forms indicates the wide scale use of off-line analytical techniques such as Fourier Transform Infrared spectroscopy (FTIR), Nuclear Magnetic Resonance spectroscopy (NMR), Differential Scanning Calorimetry (DSC) and Powder X-ray Diffraction (PXRD) (Braatz, 2002). However, these analytical techniques do not provide continuous process information and may alter processing history. Near infrared (NIR) spectroscopy (Fevotte et al., 2004; Kobayashi et al., 2006) and Raman spectroscopy (Agarwal and Berglund, 2003; O'Brien et al., 2004; Wang et al., 2000) have been utilized for the characterization of crystal

form and conversion kinetics as PAT tools. Ability of the same methods for in - line studies along with their off - line characterization capacity is a novel application.

This report is concerned with the application of in - line Raman spectroscopy as a PAT technique for the assessment of solid dispersions during the hot melt extrusion (HME) process as well as the development of Raman as a technique for monitoring production of co-crystals using extrusion. The present work in this report focuses on applications of solid dispersions, co - crystals, HME and Raman spectroscopy along with discussion on the significance and challenges associated with the techniques.

1.2. Process Analytical Technology (PAT)

The design and development of processes to ensure predefined quality of the product at the end of manufacturing is the desired goal of PAT. The need and the challenge of the US FDA's (United States Food and Drug Administration) PAT initiative are of great concern for the manufacture of pharmaceutical formulations. PAT was introduced in 2004 by the US FDA for building inherent quality within pharmaceutical products (USFDA, 2005). PAT is a joint initiative of the Centre for Drug Evaluation and Research (CDER), Office of Regulatory Affairs (ORA) and the Centre for Veterinary Medicine (CVM) within the 'Current Good Manufacturing Practices (cGMPs) for the 21st Century' framework (FDA, 2004b).

The objective of PAT implementation includes better understanding of process, reduction in the production time with use of in-line, at-line and on-line measurements, yield improvement and cost reduction because of less energy consumption. The PAT framework consists of various tools for

pharmaceutical developments such as multivariate data acquisition and analysis tools, process analysers, process monitoring and continuous knowledge improvement tools. In multivariate analysis, the foundation for the product and process design is considered. Mathematical models can be used to assess reliability of this knowledge (Eriksson et al., 2001; FDA, 2004a).

The understanding of the interaction between process and product is the basis for the design of the process monitoring, process control and Quality Assurance (QA) strategies used in manufacturing. PAT is an integrated approach in which the results obtained from the real-time analysis of critical process control points are used to control the process in some way. During manufacturing, process parameters are adjusted (within clearly defined limits) to produce the desired product quality attributes at the process end-point. The automation systems required for this level of process control are available today and are used extensively in the chemical and petrochemical industries.

Methods used with PAT include Near-Infrared (NIR) spectroscopy, Raman spectroscopy, UV - visible spectrophotometry, Fourier Transform Infrared (FTIR) spectroscopy, X-Ray Powder Diffraction (XRPD), Terahertz Pulse (TP) spectroscopy, NIR microscopy, Acoustic Resonance (AR) spectrometry etc. The validation plan for a PAT system includes the validation of the process analyser hardware and software, software packages for data analysis, process control software, and IT systems for the management, storage and backup of results (FDA, 2002). These modern process analytical tools provide non -destructive methods for processing of materials and can

contain information related to the biological, physical, and chemical aspects of the materials being processed.

On-line monitoring

On-line monitoring involves the automated sampling by transport of the drug-polymer melt away from the main process, using a heated sample line, to a nearby analyzer for continuous analysis (Chalmers, 2000). This type of monitoring can be time consuming, and often results in perturbation of the process by removal of the melt stream. On - line methods of analysis therefore often involve samples which are not representative of the melt flow. Since on-line measurements are conducted away from the main process in a controlled measurement environment more stable analysis of the melt can be carried out, without being affected by fluctuations of temperature and pressures in the main process.

At - line monitoring

Here the sample is removed and isolated from the process stream and analyzed in the close proximity to the process stream.

In - line monitoring

During in - line monitoring, probes can be used which focus directly into the process through a suitable window or can be directly inserted into a process line. Such methods are often non-invasive allowing real - time, continuous process analysis of the melt without disturbing the process line. In - line monitoring for material characterisation during processing is continuously increasing both in use and scope with analytical techniques rapidly developing from conventional off - line laboratory based methods, to real - time analysis during processing (FDA, 2004a). Examples of process

analysers include process rheometers which can be used directly in or at the process flow and can be useful in material characterisation for determination of viscosity, composition and uniform mixing capacity.

1.3. Raman spectroscopy

1.3.1. Background

A series of experiments was performed by C.V. Raman and K.S. Krishnan which involved focusing sunlight onto samples of purified liquids or gases (Raman and Krishnan, 1928). The Raman effect was actually predicted some five years earlier by Smekal, and the same effect was also observed by Landsberg and Mandelstam at about the same time as Raman's discovery, but because Raman's paper represented the more thorough study, Raman was awarded the Nobel Prize in 1930 (Simonson, 2004). Raman spectroscopy is gaining more popularity in the area of pharmaceutical research. Since among all the spectroscopic techniques, Raman spectroscopy possesses a unique identity due to its specificity, high information content and ease of sampling (Kepa et al., 2012).

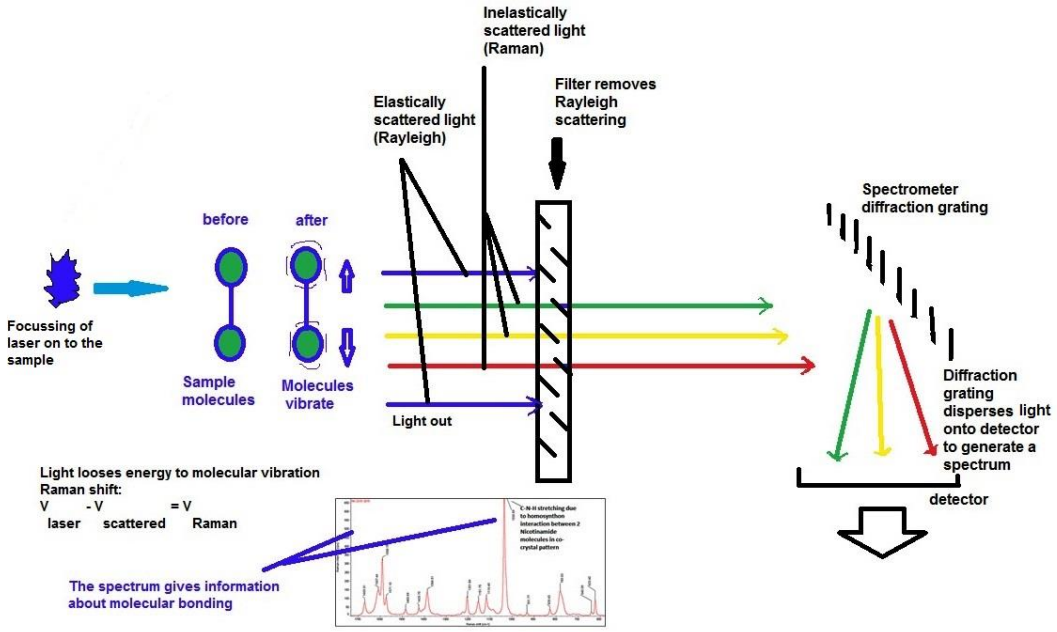

Fig.1.1. Raman spectroscopy (Adapted from Exeter, 2013).

1.3.2. Principle

The schematic presentation of Raman spectroscopy is given in Fig. 1.1. The Raman scattering technique is a vibrational molecular spectroscopy which derives from an inelastic light scattering process. It involves focusing a laser onto the sample and recording the energy profile of the scattered light. Unique spectra may be obtained due to excitation of the vibrational modes of the molecule and, for mixed samples, superimposition of the signals from each of the constituents may be observed (Kalantri et al., 2010). The energy of laser light produced by lasers used in Raman spectroscopy is higher than the energy required to bring molecules to a higher vibrational state.

During Raman study, at the same frequency (as that of energy), sample molecules scatter most of the energy. This identically scattered light is known as Rayleigh radiation. Light scattered by the molecules inelastically indicates the energy exchange between the incident light and the sample. This

inelastic scattering is termed as the Raman effect. The inelastic scattered radiation with probably lower energy than the incident radiation is known as Stokes radiation while the incident radiation with higher energy is called anti-Stokes radiation (Saerens et al., 2011). A typical modern Raman spectrophotometer is shown in Fig. 1.2.

Fig.1.2. DXR smart Raman spectrophotometer (780nm) by Thermo Scientific (Thermofisher.com)

1.3.3. Advantages of Raman spectroscopy

These include minimal or no sample preparation, fast collection of spectra, and high sensitivity to molecular geometry. Raman spectroscopy is a non-destructive method of analysis when correctly applied, so the same sample can be used in other analyses and is also a non-invasive method which can even work within sealed transparent containers (Fini, 2004). Small volumes of materials can be analysed, as the laser can be focused to a very small spot.

1.3.4. Challenges associated with Raman spectroscopy

Colored samples may undergo thermal or photochemical decomposition. Based on the sensitivity of the technique it can be concluded that it is most suited for studies of concentrated species (Bolton and Prasad, 1978). The same authors indicate that for low species concentration, it may be difficult to obtain quantitative information from Raman data. The cost of the equipment can be a limitation to the widespread adoption of Raman spectroscopy for routine analysis and high levels of fluorescence (intrinsic or caused by impurities) may also overlay the Raman bands making analysis difficult. This may sometimes be avoided by shifting the laser wavelength to the NIR spectral region however, if excitation intensities are too high, they may thermally decompose the sample (Saerens et al., 2011).

1.4. Extrusion

The word extrude means to push out in the process of extrusion wherein a material is forced by an extruder through an orifice die under set conditions such as temperature, pressure, rate of mixing and feed rate for producing a stable product of uniform shape and density (Saerens et al., 2011). Extrusion may be sub-classified into ram extrusion (Fig. 1.3), single screw extrusion and twin screw extrusion (Fig. 1.4).

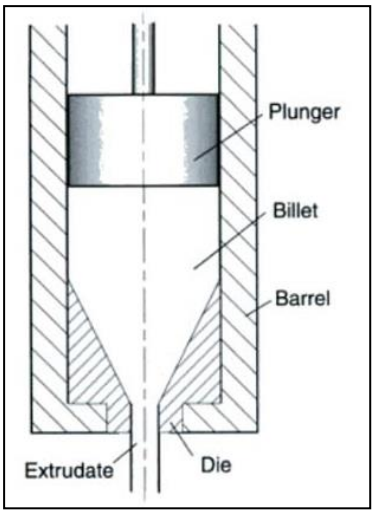

Fig.1.3. Ram extrusion (Rauwendaal, 2001)

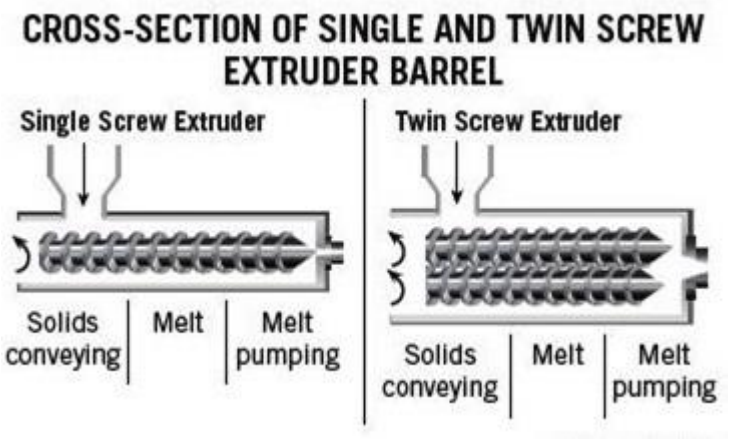

Fig.1.4. Cross section of single and twin screw extrusion (Particle sciences, 2011).

Single screw extrusion is not the preferred approach for the production of pharmaceutical formulations since it does not provide the high mixing capability of a twin screw machine. To achieve satisfactory dispersion and mixing of drugs with other ingredients may involve the breaking up of aggregates of the minor drug particles, meaning that a critical amount of

force must be applied during the process (Douglas et al., 2010). This force cannot be achieved with the single-screw, but the twin-screw extruder with its co-rotating or counter-rotating screws can provide the high energy necessary (Fig. 1.5). In addition, the versatility of a twin-screw extruder (process manipulation and optimisation) and the ability to accommodate various pharmaceutical formulations makes it much more favourable and hence it is the preferred choice for pharmaceuticals. Comparison points between single screw and twin screw extruders are listed in table 1.1. Another significant design variable is whether the two screws are intermeshing or non-intermeshing, the former being preferred due to the greater degree of conveying achievable and the shorter residence times**.** (I. and E., 2003). Screws and kneading elements are showed in Fig. 1.6.

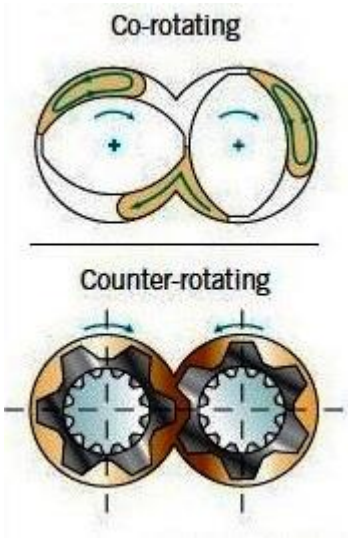

Fig.1.5. Co-rotating and counter-rotating screws (Particle sciences, 2011)

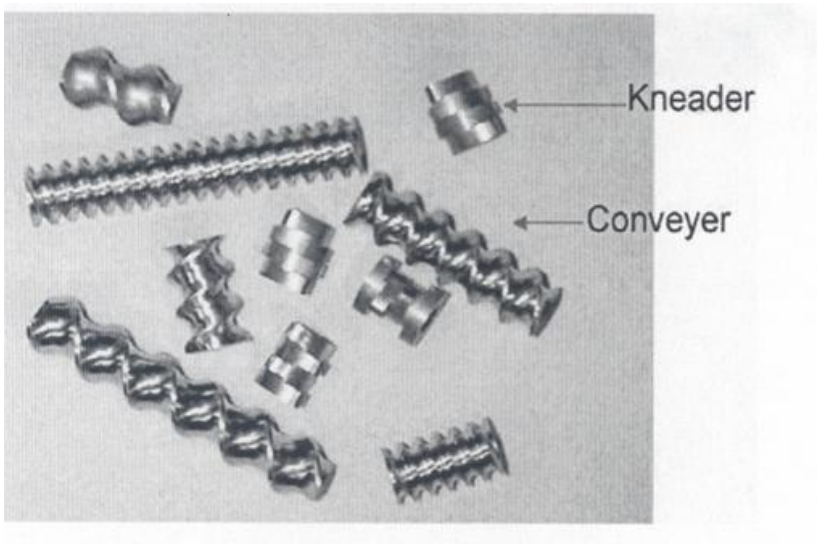

Fig. 1.6.Screw and kneading elements (Chokshi and Zia, 2004).

Sr. No.	**Single screw extruder**	**Twin screw extruder (TSE)**
1.	Used in simple profile extrusion and co-extrusion	Used in compounding profile and reactive extrusion
2.	Modular design of screw and barrel is rarely used, less flexibility	Often used with modular design of screw and barrel, great flexibility
3.	Prediction of extruder performance less difficult than for TSE	Prediction of extruder performance is often difficult
4.	Fair feeding, slippery additives tend to cause problems	Good feeding, can handle pellets, powder, liquids
5.	Fair degassing	Good degassing
6.	Fair melting, continuous solid melting mechanism	Good melting, dispersed solids melting mechanism
7.	Poor mixing ability	Good distributive mixing with

		effective mixing elements
8.	Not self-wiping, barrel is wiped but screw root and flight flanks are not	Intermeshing can have completely self-wiping characteristics
9.	Relatively inexpensive	Modular is very expensive
10.	Usually run between 10-150 rpm; high screw speeds possible but not often used	Co-rotating can run at very high screw speeds - up to 1400 rpm

Table 1.1. Comparison between twin screw and single screw extruder (Rauwendaal, 1986b).

1.5. Hot melt extrusion

Hot melt extrusion involves a platform supporting a drive system, an extrusion barrel, a rotating screw arrangement on a screw shaft and an extrusion die for the shape of the final product (Fig. 1.7.). The extrusion barrel is divided into different zones such as the feeding zone, the compression zone and the metering zone. In the feeding zone (where material enters the conveying screw arrangement) pressure is very low due to large screw flight depths and pitch allowing consistent feeding from the hopper (s) and gentle mixing of these materials. The basic function of the subsequent compression zone is to melt, homogenize and compress the extrudate so that it reaches the metering zone in a suitable form for extrusion. Finally the compounded / mixed material enters the die geometry allowing a controlled and continuous production process (Williams, 2010).

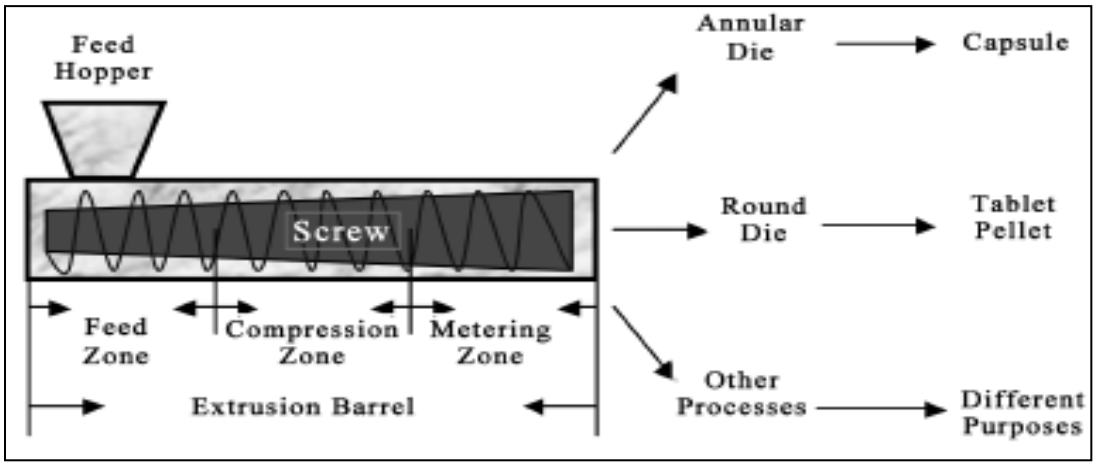

Fig.1.7. Hot melt extrusion process (Fevotte et al., 2004).

HME has been used successfully in many industries (plastic, food and rubber etc.) and has found recent applicability within the production of pharmaceutical formulations (Wilkinson and J., 1998). It has been proven that hot melt extrusion technology may improve the dissolution rate of poorly water-soluble drugs by forming solid dispersions and solid solutions (McGinity et al., 2001; Perissutti et al., 2002). A modern pharmaceutical grade hot melt extruder by Thermo Scientific is shown in Fig. 1.8.

Fig.1.8. Hot melt extruder (Thermo Scientific Pharma HME 16)

During in-line monitoring by Raman spectroscopy, one has to take into consideration processing as well as formulation parameters such as drug and polymer melt ratios, temperature, motor load, die and extruder geometries.

Advantages of HME over traditional pharmaceutical processing techniques can include:

1. It is a solvent-free process.
2. It has a short residence time.
3. It may enable superior mixing.
4. It can form solid dispersions of enhanced bioavailability and dissolution rate of drugs with poor water solubility.
5. It can produce products with controlled, sustained, modified and targeted drug release.
6. It allows in-line monitoring along with control of critical process parameters.
7. It can play an important role in masking the bitter taste of several APIs (Breitkreutz et al., 2003; Chokshi and Zia, 2004).

Various parameters such as screw configurations, temperature profiles, material feed rates, screw geometry and screw speed can influence the products extruded by the HME process.

1.6. Solid dispersions

The term solid dispersion is used to describe the dispersion of one or more active ingredients in an inert carrier or at solid state prepared by melting method (Chiou and Riegelmann, 1971; Lewis et al., 2009). The matrix material may be in either crystalline or amorphous form. The drug can be

dispersed molecularly, in amorphous particles or in crystalline particles. The formation of high surface area results in an increased dissolution rate and consequently, improves bioavailability. Solid dispersions may be classified as first generation, second generation and third generation solid dispersions.

In first generation solid dispersions, crystalline carriers have been used. Examples of such carriers include urea (Goldberg, 1966; Sekiguchi and Obi, 1961; Sekiguchi and Obi, 1964) and sugar (Goldberg, 1966). Levy and Kanig (Kanig, 1964) formulated solid dispersions containing mannitol as a carrier by preparation of solid solutions through molecular dispersions which showed faster dissolution of the carrier. Since first generation solid dispersions were not stable enough and might not be as effective as the amorphous formulations, second generation solid dispersions came into existence. The most common solid dispersions use amorphous carriers rather than crystalline. Due to the ability of polymeric carriers to formulate amorphous solid dispersions, they have been the most successful for solid dispersions. Polymorphic carriers are classified as natural product-based polymers and fully synthetic polymers. Natural polymers used include Hydroxypropylmethyl Cellulose (HPMC) (Ohara et al., 2005; Won et al., 2005), Ethyl Cellulose or Hydroxypropyl Cellulose (Tanaka et al., 2005) as well as Cyclodextrins (Rodier et al., 2005) while examples of used fully synthetic polymers are Povidone PVP (van Drooge et al., 2006), Polyethylene Glycols (PEG) (Chiou and Riegelmann, 1970) and Polymethacrylates (Ceballos, 2005). The drug is found to be in supersaturated state in the second generation solid dispersions due to its forceful solubilisation in the carrier (Tanaka et al., 2005) (Urbanetz, 2006). It

has been proved that these types of solid dispersions provide better wettability and dispersibility of the drug by the carrier (Damian et al., 2000).

1.6.1. Need for solid dispersions

The solid dispersion technique can provide different processing and excipient options that allow for flexibility while formulating oral delivery systems for poor water-soluble drugs compared with other dosage forms. The Biopharmaceutical Classification System (BCS) has categorised drugs exhibiting low aqueous solubility and high membrane permeability as class II drugs (Amidon et al., 1995). Solid dispersion technologies are especially promising for improving the oral absorption and bioavailability of these BCS class II drugs.

1.6.2. Applications of solid dispersions

Solid dispersions have various applications such as increasing the solubility of poorly soluble drugs thereby increasing the dissolution rate, absorption and bioavailability, stabilising unstable drugs against hydrolysis, oxidation, isomerisation, photo-oxidation and other decomposition procedures, reducing the side effects of certain drugs, masking of unpleasant taste and smell of drugs, improvement of drug release from ointment creams and gels, avoiding undesirable incompatibilities and obtaining a homogeneous distribution of a small amount of drug in solid state (Arunachalam et al., 2010; Lewis et al., 2009). The efficiency of taste masking by solid dispersions prepared by using hot melt extrusion has been evaluated. HME has been introduced for taste masking purposes of bitter APIs by use of taste masking polymers that create solid dispersions to prevent bitter drugs from

contacting taste buds of patient (Breitkreutz et al., 2003; Gryczke et al., 2011; Michalk et al., 2008; Witzleb et al., 2011).

1.6.3. Preparation of solid dispersions

Among the various methods used for solid dispersion preparations, melting and solid evaporation are the two prominent processes (Vasconcelos et al., 2007).

A. Melting (or Fusion) method

The term melting is preferred over fusion for the preparation of solid dispersions when the starting materials are crystalline in nature (Lewis et al., 2009). The first pharmaceutical solid dispersions containing sulfathiazole and urea were prepared by Sekiguchi and co-workers (Sekiguchi and Obi, 1961). This preparation consists of melting of sulfathiazole in the urea followed by its cooling and pulverization of the final product. For cooling and solidification of final products, various processes have been used such as ice bath agitation (Pokharkar et al., 2006; Sekiguchi and Obi, 1964) solidification on petri dishes at ambient temperature inside a desiccator (Li, 2006; Owusu-Ababio et al., 1998) as well as by immersing in liquid nitrogen (Yao et al., 2005). In spite of its frequent use, this melting or fusion method has some limitations (Lewis et al., 2009). These include degradation of several drugs by the use of high temperatures (Serajuddin, 1999), incompatibility of drug and matrix resulting in inhomogeneous solid dispersions. Such inhomogeneity can be avoided using surfactants (Damian et al., 2002).

Several modifications such as hot stage extrusion (Van den Mooter et al., 2006), Meltrex (Breitenbach and J., 2003) or melt agglomeration (Seo, 2003) have been introduced to avoid limitations of the fusion method. In the hot

stage extrusion method, reduction in processing temperature can be achieved through the use of carbon dioxide as a plasticizer (Verreck et al., 2007). This can allow the use of hot melt extrusion to thermolabile drugs (Verreck et al., 2006). It was observed that itraconazole or inutec solid dispersions prepared by hot stage extrusion resulted in glassy itraconazole while the same were partially glassy when prepared by a spray drying method. A patented solid dispersion manufacturing process, Meltrex, is based on the melting method. Solid dispersions can be prepared by melt agglomeration in a rotary process. In the case of solid dispersions prepared by HME, melt extrusion is found to offer the potential to shape the molten drug-polymer mixture into oral dosage forms, implants or ophthalmic inserts (Breitenbach, 2002). Also compared to the traditional fusion method, HME offers continuous production making it suitable for large scale production.

B. Solvent evaporation

This method of solid dispersion preparation involve the dissolution of the drug and polymer in a common solvent such as chloroform (Ahuja et al., 2007), ethanol (Yoshihashi et al., 2006) or a mixture of ethanol and dichloromethane (Tanaka et al., 2005). For instance, in the preparation of indomethacin solid dispersion, the drug and ethyl cellulose were dissolved in ethanol (Yoshihashi et al., 2006) and HPMC was suspended (Ohara et al., 2005). The thermal degradation of drugs or carriers can be avoided by using organic solvent evaporation since it can occur at low temperatures (Won et al., 2005). Preparation of solid dispersions by solvent evaporation can be achieved by several ways such as vacuum drying (Wang et al., 2005), slow evaporation of the solvent at low temperature, heating the mixture using a

hot plate (Desai, 2006) or by freeze-drying. Solid dispersion of diazepam and povidone was prepared by a spray drying method using liquid nitrogen followed by the lyophilization of the suspension obtained (van Drooge et al., 2006).

1.6.4. Advantages of solid dispersions (SDs)

- Particles with reduced particle size**:** molecular dispersions, such as SDs, represent the last state on particle size reduction, and after carrier dissolution the drug is molecularly dispersed in the dissolution medium.
- Particles with improved wettability, strong contribution to the enhancement of drug solubility is related to the drug wettability improvement verified in SDs.
- Particles with higher porosity - particles in SDs have been found to have a higher degree of porosity.
- Poorly water soluble crystalline drugs, when in the amorphous state tend to have higher solubility.

1.6.5. Challenges associated with solid dispersions

A major limitation of SDs is recrystallisation since amorphous systems are thermodynamically unstable and tend to change to a more stable state during recrystallisation. In this case, molecular mobility can be used to govern the stability of SDs. The efficient mixing of the drug and polymer in one solution can be challenging when their polarities are different. It may affect solubility of drug and polymer in the same solution. For minimisation of drug particle size in the solid dispersion, the drug and polymer have to be dispersed in the solvent as finely as possible (Hernandez-Trejo et al., 2005). Another challenge with the solvent method is to prevent phase separation as

crystallisation of either the drug or the polymer during solvent removal. Drying at high temperatures can speed up this process and reduce the time available for phase separation while at high temperatures - the molecular mobility of drug and polymer remaining high favouring phase separation (crystallisation). Commercial applications of solid dispersions are limited despite a good deal of research in this area. Some products marketed include: Cesamet (Lily), Nabilone in PVP, Gris-PEG (Novartis), Griseofulvin in PEG, Sporanox (Janseen Pharmaceutical / J&J), Itraconazole in HPMC and PEG 20000 sprayed on sugar spheres. Limitations influencing the successful commercialisation of SDs include the expensive and laborious manufacturing methods, characterisation reproducibility and difficulty in formulation dosage form incorporation, drug stability and scale-up of the manufacturing process.

1.7. Co-crystals (Co-Cs)

Introduction

A co-crystal can be termed as a crystalline structure formed by two different or molecular entities where intermolecular interactions are such as hydrogen bonding take place instead of ionic interactions (Djuris et al., 2013). Co-crystallisation is considered as an alternative approach in the formulation development for solubility improvement in pharmaceutical field. Pharmaceutical co-crystals can be applied in the field of pharmaceutical development in order to improve physical properties of the API such as solubility, stability and bioavailability without any change in their chemical composition (Sekhon, 2009).

A lot of research has been carried out on pharmaceutical co-crystals preparation, characterisation and their polymorphism. Pharmaceutical co-crystals are single- crystalline solids which involve an API and a co-crystal former (This co-former can be a drug or an excipient).Various pharmaceutical co-crystals have been reported in the literature such as those with Acetaminophen (Paracetamol), Aspirin, Ibuprofen etc (Sekhon, 2009).

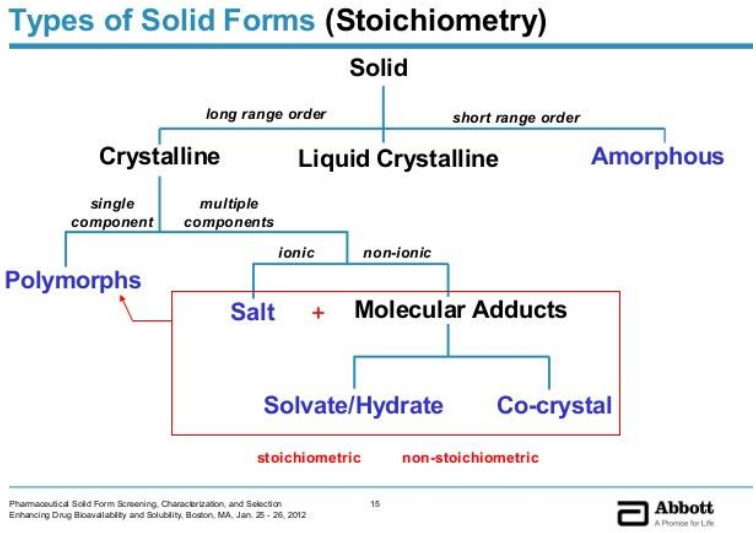

Fig. 1.9. Pharmaceutical solid forms (Abbott) (www.slideshare.net).

Methods of preparation of Co-Cs (Sekhon, 2009).

1. Slow solvent evaporation
2. Forced evaporation
3. Melting method
4. Mechano-chemical methods
5. Slurry conversion
6. Melt crystallisation

During the preparation of co-crystals, various conditions play an important role such as uptake of moisture, aqueous solubility of co-crystals, solubility and dissolution of co-crystal reactants etc.

1.8. Aim and objectives of present work

- To carry out in-line Raman spectroscopic studies of the preparation of solid dispersions during the hot melt extrusion process alongside complementary off-line analytical techniques such as X-ray diffraction (XRD) and Differential Scanning Calorimetry (DSC) was the main objective of the present work.

- The present work focuses on the suitability of Raman spectroscopy as a process analytical technique (PAT) tool for monitoring the stability of solid dispersions with active pharmaceutical ingredients in the polymer melt with respect to processing variables. In the present work, Raman spectroscopy has been used to understand the degradation mechanism of API during hot melt extrusion process.

- To perform a study of co-crystal properties through different methods of preparation of co-crystals and assess the suitability of Raman spectroscopy for in-line monitoring of the continuous production of co-crystals was an important objective.

1.9. Structure of thesis

Raman spectroscopic studies being the main objective of the present research work, the focus was on its implementation as a PAT technique. Present work describes with the results ability of Raman spectroscopy in

quantification of API. Carbamazepine being an API with low solubility and polymorphic nature was selected to be used in solid dispersion preparation with different polymers. Carbamazepine along with Kollidon VA64 and Soluplus has been used in the preparation of solid dispersions while Ibuprofen - Nicotinamide and Carbamazepine - Nicotinamide systems have been selected to be used in the present study which are discussed in detail in respective chapters.

This thesis is distributed into six chapters. Chapter one gives a general introduction of Process analytical techniques, Raman spectroscopy, hot melt extrusion, solid dispersions and co-crystals. Chapter two describes a literature review behind Raman spectroscopy in pharmaceuticals while chapter three describes the experimental techniques applied in the present work. Details about the DSC, TGA, XRD, FTIR, HSM and Raman spectroscopy including Process Raman probe used for In-line monitoring of solid dispersions have been discussed in this chapter. Details about materials and experimental methods are given in chapter four. Chapter five describes the results and discussion while conclusions are given in chapter six.

Chapter 2 - Literature Review

Spectroscopy is of great importance in pharmaceutical research and analysis. Vibrational spectroscopic methods including FTIR and Raman spectroscopy are applicable for drug characterisation especially in the structural elucidation of compounds.

2.1. Process Raman spectroscopy

In pharmaceuticals, Raman spectroscopy has been applicable in Quality assurance (QA), Quality control (QC), research and potential processes. It can be used as reaction monitoring tool for gaining information on the progress of reactions.

2.2. Raman spectroscopy applications

Raman spectroscopy has been found to be applicable in various areas of pharmaceutical research such as characterisation of drug materials, drug-excipient incompatibilities and formulation analysis (Spragg, 1995; Tensmeyer and Heathman, 1989).

For the study of polymers, Raman spectroscopy has been used for many years. It can provide information on molecular microstructure, polymer density, polymerisation, polymer orientation and crystallinity (Bower and Maddams, 1989). Initial applications of Raman spectroscopy for studying aqueous-phase emulsion polymerisation have been discussed (Al-Khanbashi et al., 1998). Raman analysis of many compounds of pharmaceutical interest has been reported (Cutmore and Skett, 1993).

The successful use of Raman spectroscopy has been reported along with a partial least squares method for on-line monitoring of polymerisation of emulsions (Bauer et al., 2000).

Raman spectroscopy can be used for dye uptake determination or measurement of the mechanical properties of polymer fibres (Wijk et al., 1999). Raman spectroscopy has been employed for measuring the residence time distributions of material in a twin screw extrusion process (Ward et al., 1996). Claybourn and co-workers applied Raman spectroscopy to measure spectra of acrylate containing copolymers by emulsion polymerisation (Claybourn et al., 1994).

Many reports have been found in literature about off- line laboratory analysis of fibres and films by using Raman spectroscopy for polyethylene (PE) and polypropylene (PP) (Arruebarren de Baez et al., 1995; Rull et al., 1993).

2.3. Raman spectroscopy for pharmaceutical industry

The pharmaceutical industry along with chemical industry started using Raman analysers for obtaining laboratory to pilot plant data and manufacturing process setting. For mapping active excipient distribution dispersive Raman spectroscopy is being used. Dispersive Raman spectroscopy has also been applied for reaction-monitoring, process monitoring and pilot-plant batch analysis.

The formulated products in pharmaceutical industries contain additives, binders, excipients, active material, dyes as well as identification marks. Often active materials are crystalline in nature and possess high Raman scattering tendency while the excipients have a low Raman scattering which

can lead to fluorescent spectra. FT- Raman spectroscopy by this means proved its applications in formulated product analysis. On the other hand dispersive Raman spectroscopy with visible excitation can be applicable for active ingredient monitoring during process (Frank, 1999). Quality control checks on incoming products at Colgate-Palmolive have been carried out using Raman spectroscopy (Frank, 1998).

For in-situ study of headspace gases in pharmaceuticals with vials Raman spectroscopy has been employed at the Wellcome Foundation in the United Kingdom (Gilbert et al., 1994). The same authors have described that Raman analysis has shown better C-H stretching modes than that of Infrared spectroscopy in pharmaceutical materials. For drug mapping of pharmaceutical formulations such as tablets, Raman spectroscopy (RS) has been used (Frank, 1999). For characterization of illicit drugs, due to its non-destructive nature and minimum sample requirements, Raman spectroscopy was found to be a preferred method (Hodges et al., 1989). The application of Raman and NIR spectroscopy for the in- process monitoring of drug synthesis process and crystallization was reported (Rasanen and Sandler, 2007). Use of RS for the in-line monitoring of the blending process of a binary mixture of diltiazem pellets and paraffinic wax beads has been reported. It has been investigated that Raman spectrometer also has applications in assessing powder mixture homogeneity (Wikstrom et al., 2005).

Raman spectroscopy has been applied for the quantitative, non-invasive probing of the bulk content of pharmaceutical capsules on the production line of (Eliasson et al., 2008). Confocal Raman microscope with an automated

stage has been used for producing high- resolution, three – dimensional maps of the multi- phase material composition (Andrew et al., 1998). Hydration-dehydration of carbamazepine and theophylline in the presence of excipients has been analyzed with Raman spectroscopy (Salameh and Taylor, 2006). Monitoring of non-isothermal seeded crystallization with phase transition was done by second degree method using Raman analysis (Hu et al., 2005). Bucindolol has been analyzed by Raman spectroscopy using a multivariate calibration (Niemczyk and Delgadolopez, 1998).

The Royal Pharmaceutical Society of Great Britain had hosted a new technologies forum meeting about the significance of Raman spectroscopy within the pharmaceutical industry. Due to its modern automation capability, spectral acquisition from small size samples its becoming an indispensable tool in pharmaceutical analysis.

A comparative study of NIR dispersive and FT - Raman analyzers for on- line monitoring of phosphorous trichloride have been carried out (Gervaso and Pelletier, 1997). RS has been used for the identification of polymorphic forms and crystallinity of various pharmaceuticals. The purpose behind the studies of polymorphism is understanding the various polymorphic forms of compounds and their thermodynamic stability which is significant in drug development process of pharmaceuticals. It has been observed that there can be differences between the Raman spectra between the amorphous and the crystalline forms of a compound (Langkilde, 1995; Langkilde et al., 1997). The stabilisation of amorphous indomethacin dimers in molecular dispersions with poly (vinyl pyrrolidone) (PVP) has been probed using Raman spectroscopy (Taylor and Zograti, 1997). Taylor and Zografi have used the

FT-Raman spectroscopic method to evaluate crystallinity of molecular substances in the homogeneous state (Taylor and Zograti, 1998). For testing levels of crystallinity of substances Raman spectroscopy has been suggested (Langkilde et al., 1997). In-situ Raman measurements of calcium carbonate polymorphic composition has been carried out in the presence of polymeric additives during the crystallisation process. Deeley et al. studied the difference between FTIR and Raman methods for detection of cortisone acetate polymorphism. Better results were obtained by Raman analysis (Deeley et al., 1991). Raman spectroscopy and FT-IR methods were found to be suitable for identification and quantitative determination of orthorhombic and monoclinic paracetamol in a powder mixture (Al-Zoubi et al., 2002). It has been shown that with high dosage paracetamol tablets and lufenuron tablets, identification of crystalline phases in drug products is possible with Raman spectroscopy (Szelagiewicz et al., 1999). Griesser and co-workers (Auer et al., 2003) investigated the use of near infrared FT-Raman spectroscopy for determination of polymorphic forms in various commercial drug products with polymorphic drug compounds. The same authors showed that thermodynamically stable polymorphic forms were found in drug products with meprobamate, sorbitol and carbamazepine (CBZ) while for solid dosage forms of acemetacin, phenylbutazone, famotidine and mannitol, metastable polymorphic forms were identified (Auer et al., 2003). Gorden, along with his co-workers, have carried out a thorough spectroscopic study of CBZ polymorphs. The Raman spectra of the two polymorphic forms of CBZ (forms III and I) were found to be different and it was found that a carboxamide group shows the prime structural difference between the two

forms. According to these authors the experimental spectra of CBZ revealed that IR is more polymorph sensitive than Raman spectroscopy (Strachan et al., 2004). Polymorphism of crystalline drugs is becoming a serious issue by means of combinatorial chemistry in the process of new drug discovery. New chemical entities (NCE) possess a large number of functional groups which may result in crystallisation of these drugs in many polymorphic forms. The solubilities and dissolution rates of different polymorphic forms will be different along with their absorption and bioavailability. Raman has also been applied for the quantitative detection of the polymorphic forms of ranitidine hydrochloride in tablets (Strachan et al., 2004). The solid state transformation of CBZ from form III to form I was studied by O'Brien and colleagues by using FT Raman spectroscopy (FTRS). They have also reported that FTRS can be used for non-destructive in-situ and at-line analysis of polymorphic drugs (O'Brien et al., 2004).

Tian et al. illustrated the use of RS to study the conversion of each polymorphic form of CBZ into its dihydrate. RS combined with partial least square analysis was used to generate quantitative models of binary and ternary mixtures of the different polymorphic forms of the dehydrate (Tian et al., 2006). Indomethacin has been used to illustrate the ability of FT-Raman to evaluate a low degree of crystallisation (Taylor and Zografi, 1997; Taylor and Zografi, 1998). Strachan et al. investigated the application of RS and Principal Component Analysis (PCA) of polymorphic mixtures of CBZ form III and I (Strachan et al., 2004).

2.4. Raman spectroscopy for in-line monitoring

Raman spectroscopy also enables in-line measurements and has previously been used during hot melt extrusion to monitor polymer melts (Alig et al., 2005; Barnes et al., 2005). To obtain in-process information related to the API, the polymorphic behaviour of the API and the homogeneity of content, PAT tools are of great importance. In-situ turbidity measurements have been found to be applicable for determination of polymorphic form transformation along with off-line spectroscopic studies (Barnes et al., 2008).

In-situ continuous qualitative analysis of the carbamazepine - nicotinamide co - crystallisation process has been carried out by Raman spectroscopy (Rodriguez-Hornedo, 2006).

A Raman spectroscopic method has been developed for in-line and real-time monitoring of the homogeneity of the powder mixing processes by de Beer and researchers in Ghent using Diltiazem Hydrochloride as the API under study (de Beer et al., 2008). The correctness of the conclusions from Raman spectroscopy was assured by the use of simultaneous NIR spectroscopy which ultimately enhances the certainty of the use of process analysers. In various publications, polymorphism has been studied and approximately 80% of marketed pharmaceuticals are found to exhibit polymorphism. In the case of the anti-retroviral drug Ritonavir from Abbott Laboratories, due to the sudden formation of an unknown, thermodynamically more stable and much less soluble crystalline polymorph, many final products failed dissolution tests which led to a financial loss of approximately 250 million dollars. This case indicates that insufficient understanding of crystallisation mechanisms

of the polymorphs could cause serious problems (Chemburkar et al., 2000). In-line monitoring of the crystal phase composition during the crystallisation process has been carried out by Raman spectroscopy. The polymorphic as well as pseudo-polymorphic composition of the crystals as a function of time can be obtained from in-line Raman spectroscopy which gives important kinetic information on the phase transformation between solid forms (Starbuck et al., 2002). Savolainen et al. used in-situ Raman spectroscopy in combination with either partial least squares discriminant analysis (PLS-DA) or partial least squares (PLS) regression analysis to monitor and quantify the solid phase transitions that take place during dissolution of CBZ (Savolainen et al., 2009). Demonstration of the suitability of RS as a PAT tool for in-line quantitative monitoring of active coatings with validation of the applied Raman analytical method in agreement with ICH guideline Q2 (ICH, 2009) has been carried out. Application of NIR Raman spectroscopy in identification of pharmaceuticals inside amber USP (the United States Pharmacopoeia) vials using a library of spectra has been reported (Al-Zoubi et al., 2002). In the end point detection of the blending of a binary pellet mixture have been carried out by Raman spectroscopy (Vergote et al., 2004). Using an immersion probe, in- line monitoring of low dose blend uniformity was determined by Raman spectroscopy. Romero-Torres et al. found applications of Raman spectroscopy for monitoring of pan coating in tablet manufacturing for determination of coat thickness (Romero et al., 2005). Similar types of work have been reported by Muller et al for monitoring active coating process using Raman spectroscopy (Muller and Knop, 2010). Mannitol phase behaviour during freeze drying has also been

monitored during in-line lyophillisation by Raman spectroscopy (Romero, 2007).

In-line Raman monitoring of fluid bed granulation using a univariate method has been reported (Walker and Bell, 2009). For controlled crystallisation of final formation in-line monitoring of lyophilisation have been demonstrated with the aid of Raman spectroscopy (de Waard et al., 2010). Mantanus and co-workers demonstrated the suitability of Raman mapping for evaluation of the API homogeneity within the drug reservoir (Mantanus et al., 2011). RS has also been implemented in a twin screw extrusion process to determine the concentration of Irganox additives in polypropylene (Alig et al., 2005). For off-line confirmation of drug dispersion within PEO and interaction with PEO in extrudates, RS has been used (Li et al., 2006). It is reported that solid state properties of SDs prepared by HME and solvent co-precipitation process can be compared by use of RS (Dong et al., 2007). The higher solubility of amorphous solids is found to be due to their higher energy and molecular mobility compared to their crystalline counterpart (Norman et al., 2011). Raman spectroscopy has been evaluated as a PAT tool to monitor the API concentration and polymer-drug melt solid state during pharmaceutical hot melt extrusion processes (Saerens et al., 2011). Recently Raman spectroscopy has been used to quantify polymorphic mixtures with methods ranging from simple univariate correlations to more complicated multivariate approaches (Croker et al., 2012).

2.5. Pharmaceutical co-crystals

It has been reported that co - crystallisation can be a better alternative for drug discovery processes in the pharmaceutical industry (Sekhon, 2009).

Various combinations of co - crystals have been reported in the literature. Synthesis of co-crystals of Piroxicam and carboxylic acids have been reported Co - crystals of Ibuprofen- Nicotinamide have been obtained by slurry conversion method by Soares and group (Soares and Carneiro, 2013). Polymorphism in Carbamazepine - Saccharin and Carbamazepine-Nicotinamide co-crystals has been reported in the literature (Porter et al., 2008). Polymorphs exhibit different stabilities and can convert from unstable forms to stable forms at certain temperatures range (Sreekanth et al., 2007). Polymorphism in co - crystals has been observed and reported. Co - crystals of Carbamazepine and Nicotinamide have been reported to exhibit in two polymorphic forms. Co - crystals of Carbamazepine and Saccharin have been reported to exhibit in two polymorphic forms (Porter et al., 2008). One more polymer - nucleated polymorph of Carbamazepine and Nicotinamide co-crystal has been reported (Rahman et al., 2011).

Researchers from the University of Bradford have reported a solvent free continuous co - crystallisation (SFCC) method for preparation of Ibuprofen and nicotinamide co-crystals and its monitoring using NIR as a PAT tool (Kelly et al., 2012). Impact of components used in co - crystals on decreasing solubility of the molecular complex to be crystallised is useful for nucleation and growth of co - crystals of Carbamazepine - Nicotinamide (Rodriguez - Hornedo, 2006). A method for Carbamazepine - Nicotinamide co-crystal generation pathways and kinetics using in-situ thermomicroscopy, spectroscopy and calorimetry studies has been reported (Rodriguez - Hornedo, 2006). Ali has reported solvent evaporation method for the preparation of Carbamazepine-Nicotinamide co-crystal using absolute

ethanol (Ali et al., 2014). A method (Fig. 2.1.) for synthesis of Carbamazepine - Nicotinamide co-crystals by a liquid - assisted grinding has been reported.

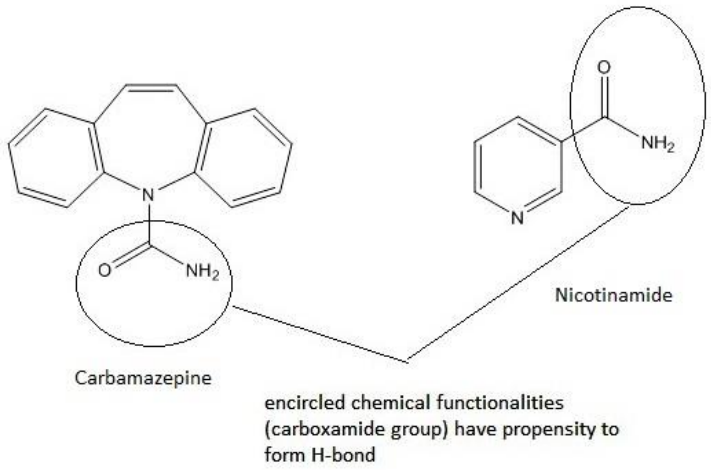

Fig.2.1. Carboxamide group H- bond interaction (Patil, 2014).

In-situ monitoring of Carbamazepine-Nicotinamide co-crystal intrinsic dissolution behaviour has been illustrated by Qiao (Qiao et al., 2013). It has been reported that formation of co-crystals occur due to hydrogen bonding between Carbamazepine and Nicotinamide since both provide hydrogen bonding donors and acceptors. In case of co-crystals of Carbamazepine - 4 - amino benzoic acid (1:1 and 2:1), it has been observed that more the content of co-formers, more the stability of co-crystals. By co-grinding of Carbamazepine with Saccharin or with Nicotinamide co-crystals were obtained (Zaworotko, 2008).

Chapter 3 - Experimental Techniques

Analysis of pharmaceuticals using various experimental techniques is of great importance especially in terms of confirmation of quality of formulations. Preliminary testing of starting materials, differences between properties of starting and end products give clear understanding of research methods. This chapter outlines the various experimental techniques used in this project including Thermo - Gravimetric Analysis (TGA), Differential Scanning Calorimetry (DSC), Powder X - ray Diffraction (PXRD), Rheology, Hot Stage Microscopy (HSM), High Performance Liquid Chromatography (HPLC), Fourier Transform Infra - red (FTIR) Spectroscopy and Raman Spectroscopy (RS). In Raman spectroscopy, DXR smart Raman spectrophotometer with universal platform for sampling (UPS) has been used for carrying out off - line Raman spectroscopic analysis whereas for in - line monitoring of solid dispersions during hot melt extrusion Process Raman probe by Inphotonics has been used.

3.1. Thermal Analysis

A. Thermo-Gravimetric Analysis (TGA)

TGA measures the amount and rate of change in the weight of a material as a function of temperature or time in a controlled atmosphere. TGA has been found useful in determination of the composition of multi-component systems, the thermal and oxidative stability of materials, the estimated lifetime of a product, decomposition kinetics of materials, the effect of reactive or corrosive atmospheres on materials, and also the moisture and volatile content of various materials (PerkinElmer, 2012). The Thermo - Gravimetric Analyser used in this project is shown in Figure 3.1.

Fig. 3.1. Thermo - Gravimetric Analyser (TGA Q5000 by TA Instruments)

(Eliasson et al., 2008).

The technique can characterise materials that exhibit weight loss or gain due to decomposition, oxidation, or dehydration. The typical TGA curve is shown in Fig. 3.2.

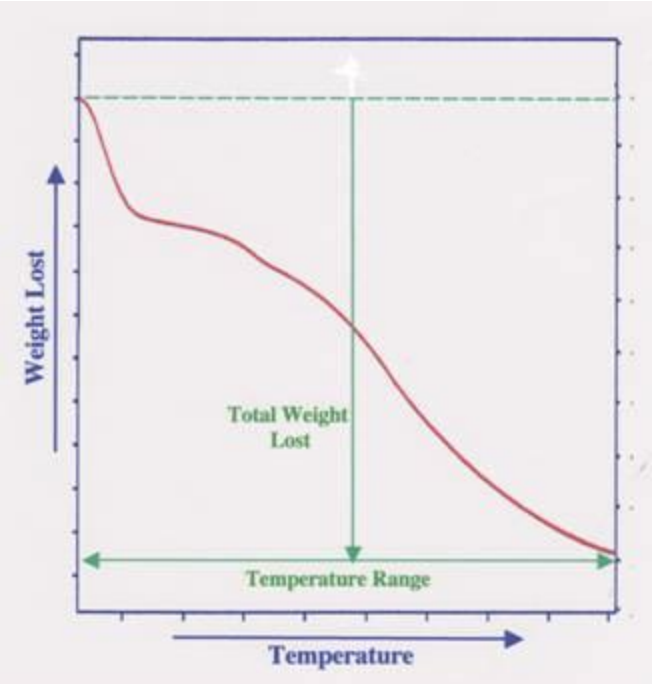

Fig. 3.2. Typical TGA curve (TA Instruments, 2012).

The instrument consists of several important parts such as the microbalance, furnace and thermocouples. During heating, an inert purge gas such as nitrogen or argon is used to prevent air-mediated oxidation or combustion. There are two separated sets of thermocouples, one is for measurement of sample temperature and usually located very close to the sample, while the other thermocouple measures the furnace temperature to facilitate steady and linear heating rate (Wilson and Haines, 2002).

In this project TGA has been used to quantify degradation of CBZ and Kollidon VA64 in CBZ - Kollidon VA64 SDs. Also to determine moisture content in SDs of CBZ and Kollidon VA64 TGA has been found useful. TGA

study of CBZ and NA also carried out along with their co - crystals for the confirmation of purity.

B. Differential Scanning Calorimetry (DSC)

DSC is utilised to quantify changes in a material's thermal properties (shifts in the melting point T_m and glass transition temperature T_g etc. as shown in Fig 3.6.) and can provide information on the 'form' of a substance during thermal processing. The Differential Scanning Calorimeters - Q2000 and Discovery DSC by TA Instruments used in this project are shown in Figure 3.3.

Fig. 3.3. Differential Scanning Calorimeters – a) Q2000 and b) Discovery DSC by TA Instruments

The temperatures of transformations, thermodynamics and kinetics of a process may be determined using DSC (Rutter, 2012). This technique is well established in the field of pharmaceuticals for thermal characterisation and has been found important in the assessment of amorphous and crystalline materials as well as in the characterisation of polymorphs and polymorphic transformations.

During DSC, transitions or energetic events are determined as a function of time and temperature against a standard reference. This happens as a result of heating and cooling of material or holding it isothermally for a length of time (Ford and Mann, 2012) (Cox, 1990). Instrument baseline heat flow has a significant impact on almost all differential scanning calorimetry (Ford and Mann, 2012). If instrument baseline is not correct, weak transitions such as glass transitions cannot be detected (Danley and Caulfield, 2015).

Glass transition (Tg) in polymers

The temperature at which a change in amorphous form of a material from a glossy to rubbery state occurs is known as glass transition temperature (Tg). Tg in semi- crystalline polymers can be observed by small fractions and hence glass transition of polymers is poorly visible in case of crystalline polymers which are 5% or less amorphous.

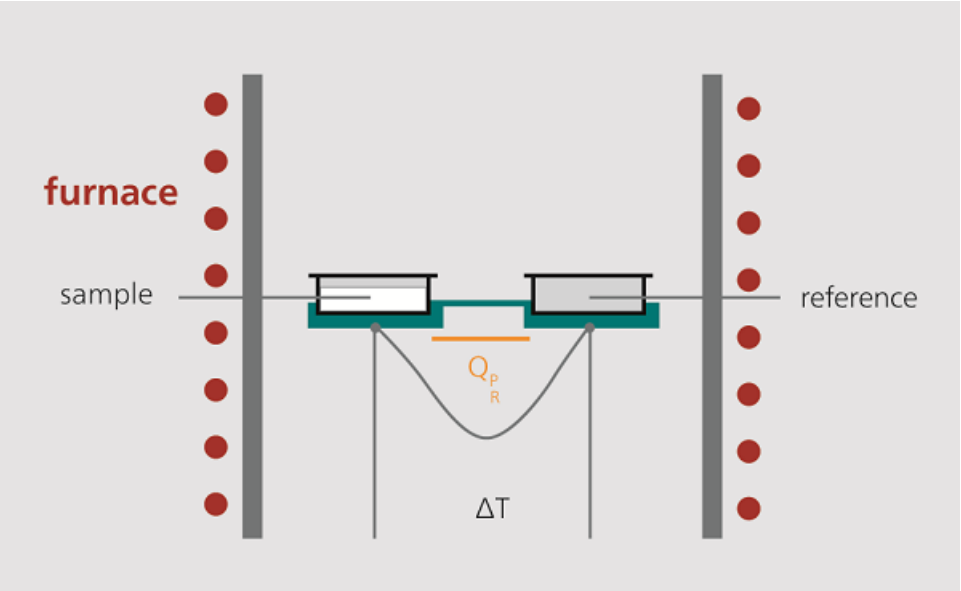

Fig.3.4. DSC measuring cell (Netzsch, 2015).

Measuring cell of DSC contains a furnace and an integrated sensor where positions are designated for sample and reference pans (Fig 3.4.).

The sensor area which plays an important role is attached to thermocouples or can be a part of thermocouple and due to this temperature difference between the sample and reference (DSC signal) allowing the absolute temperature of the sample or reference side to be recorded (Netzsch, 2015). Fig.3.5. shows transition enthalpy in DSC.

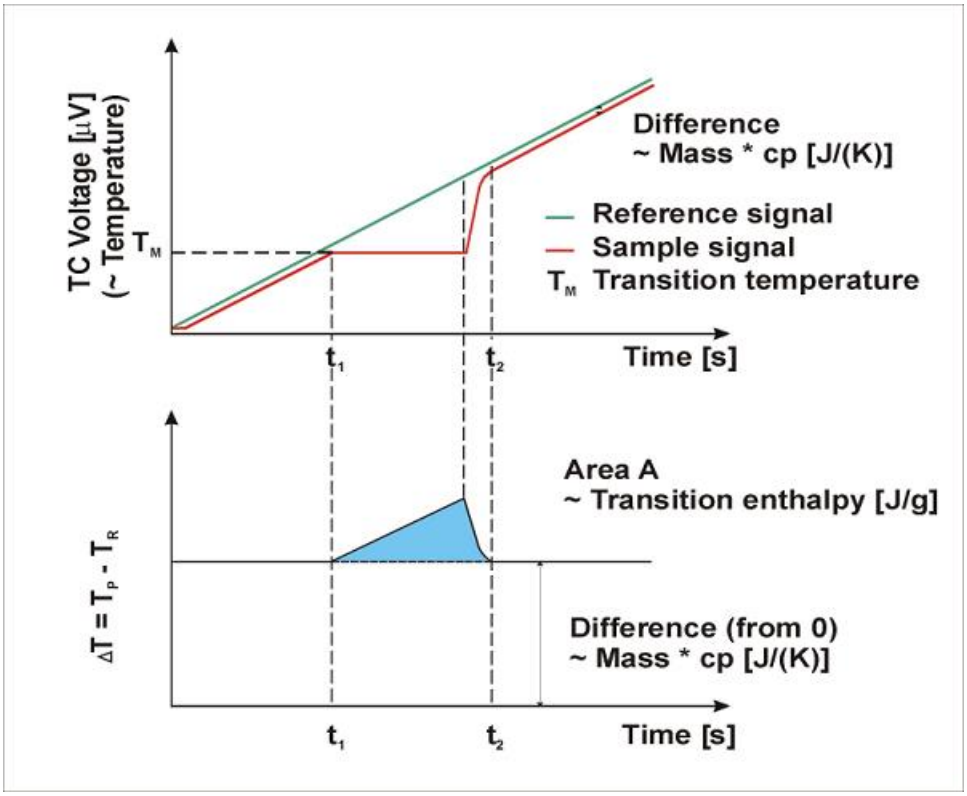

Fig 3.5. Graph showing transition enthalpy (DSC) (Netzsch, 2015).

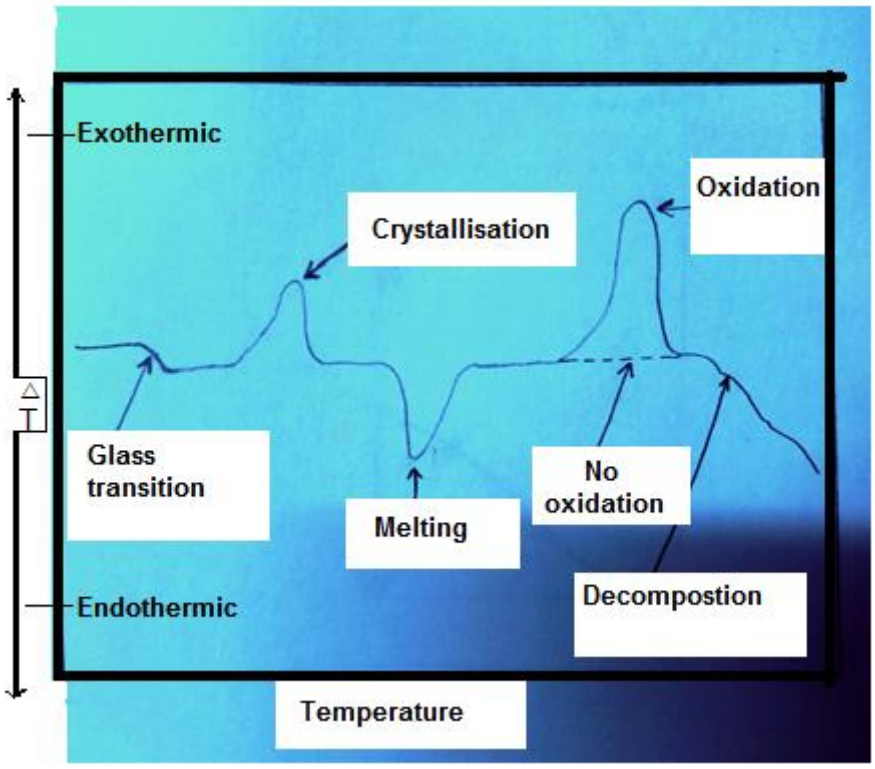

Fig. 3.6. Typical DSC curve (adapted from www.dscsolution.net).

Solids, liquids, powders, films and fibers of essentially any shape are encapsulated in metal pans and placed into a temperature and atmosphere-controlled environment where the measurement occurs. Sophisticated and easy to use software permits a quantitative analysis of transitions as a function of temperature and time. The temperature range for transitions in the different materials can often overlap and experience is required to create methods, which can assist with interpretation of results.

DSC measures only the sum or average value of the heat flow rate from overlapping processes which makes quantitative analysis of the individual processes impossible. For any DSC, the only way to improve sensitivity for detecting low energy transitions is to increase sample size and heating rate.

This however decreases resolution which is the ability to resolve a transition that occurs close to another in temperature. DSC thus cannot optimize both sensitivity and resolution in a single experiment (Thomas, 2005).

C. Modulated Differential Scanning Calorimetry (MDSC) In standard DSC, with a single heating rate, a single heat flow rate signal is produced, which is the sum of all heat flows occurring at any point in temperature or time. The operating principle of MDSC differs from standard DSC in that MDSC uses two simultaneous heating rates - a linear heating rate that provides information similar to standard DSC, and a sinusoidal or modulated heating rate that permits the simultaneous measurement of the sample's heat capacity. MDSC is superior to DSC since it can separate kinetic events. It also has the ability to resolve complex transitions into specific components which can improve data interpretation. One further benefit of MDSC is its ability to measure heat capacity changes during reactions under isothermal conditions and also the measurement of the initial crystallinity of polymers and other materials (Thomas, 2005).

In this project DSC has been utilised for confirmation of purity of APIs and polymers by means of their melting points, glass transition values and to find out differences in thermal changes in the starting materials (APIs, polymers along with their physical mixtures) and formulations after preparation. Purity of co - crystals of IBU - NA and CBZ - NA has been confirmed by analyzing their samples using DSC. Differences between samples of dilutions of IBU with IBU - NA co - crystals and samples of dilutions of CBZ with CBZ - NA co - crystals has been studied by DSC and from enthalpy values obtained from DSC, calibration curve has been generated which further compared with

Raman spectroscopic results for understanding sensitivity of analytical methods.

3.2. Rheology

3.2.1. General Introduction

Rheology is the science of deformation and flow (rheo = river in Greek). Rheological experiments not only reveal information about the flow behavior of liquids but also the deformation behavior of solids. Rheometry is the measuring technology used to determine rheological data. Both liquids and solids can be investigated using rotational and oscillatory rheometers. To characterize viscous behavior rotational tests are performed while to evaluate viscoelastic behavior creep tests, relaxation tests and oscillatory tests are performed (Mezger, 2006). A typical rheometer is shown in Fig.3.7.

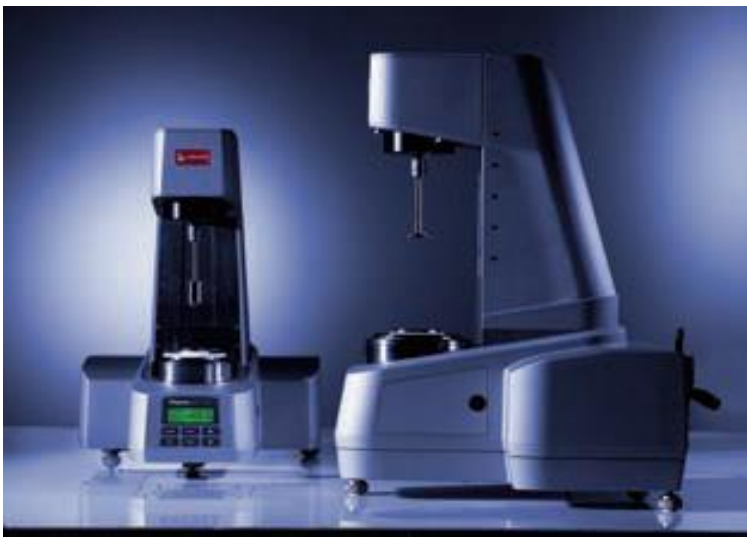

Fig. 3.7. Rheometer (Anton-Paar Physica MCR 301)

3.2.2. Viscoelasticity

Viscoelasticity is the property of a material to exhibit viscous and elastic behavior simultaneously. Viscoelastic materials tend to show delayed response on application and removal of load. For practical applications, viscous and elastic portions of a viscoelastic material are required to be in a balanced ratio.

Viscoelastic (VE) liquids: VE liquids tend to deform to a certain extent after release of this load. Examples of VE liquids include polymer melts and concentrated polymer solutions.

Viscoelastic solids: Complete reformation occurs in case of VE solids during prolonged testing periods. Examples of VE solids include gels, chemically cross-linked materials, concentrate dispersions etc. (Mezger, 2006).

3.2.3. Significance of rheology for pharmaceutics

When a polymer and a drug form a single phase at the processing temperature, not only can a more uniform product can be obtained, it may also lead to other desirable product properties such as faster drug dissolution rate. Having rheological data can minimise the time for trial and error experiments and help to understand a drug's physical state during a hot melt extrusion (HME) process. Hence, for HME, the study of rheology is of great importance since it affects the processing conditions and end properties of the pharmaceutical products (Coates, 1995). Oscillatory tests are used to examine all kinds of viscoelastic materials, from low viscosity liquids to polymer solutions and melts, pastes, gels, elastomers and even rigid solids. This final mode of testing is referred to as dynamic mechanical analysis (DMA) (Mezger, 2006).

Viscosity is termed as the ratio of applied shear stress and shear rate.

$$\text{Shear stress} = \text{Applied force (F)} \div \text{Area}$$

$$\text{Viscosity} = \text{Shear rate} \div \text{Shear stress}$$

Further terms are used in discussions of the rheology of complex viscoelastic materials and brief explanations of these are given below:

The elastic (storage) modulus (G') is a measure of elasticity of material which describes the ability of the material to store energy. In contrast the viscous (loss) modulus (G") describes the ability of the material to dissipate energy.

In addition, the ratio of these moduli is known as the damping factor and is denoted as the tangent of the phase angle (Tan δ) (Breitkreutz et al., 2003).

$$\text{Tan}\delta = \text{G}'' \div \text{G}'$$

3.2.4. Plasticisation effect

The role of plasticisers is to improve the processability of polymers by lowering the glass transition temperature and the viscosity of the formulation (Rosen, 1993).

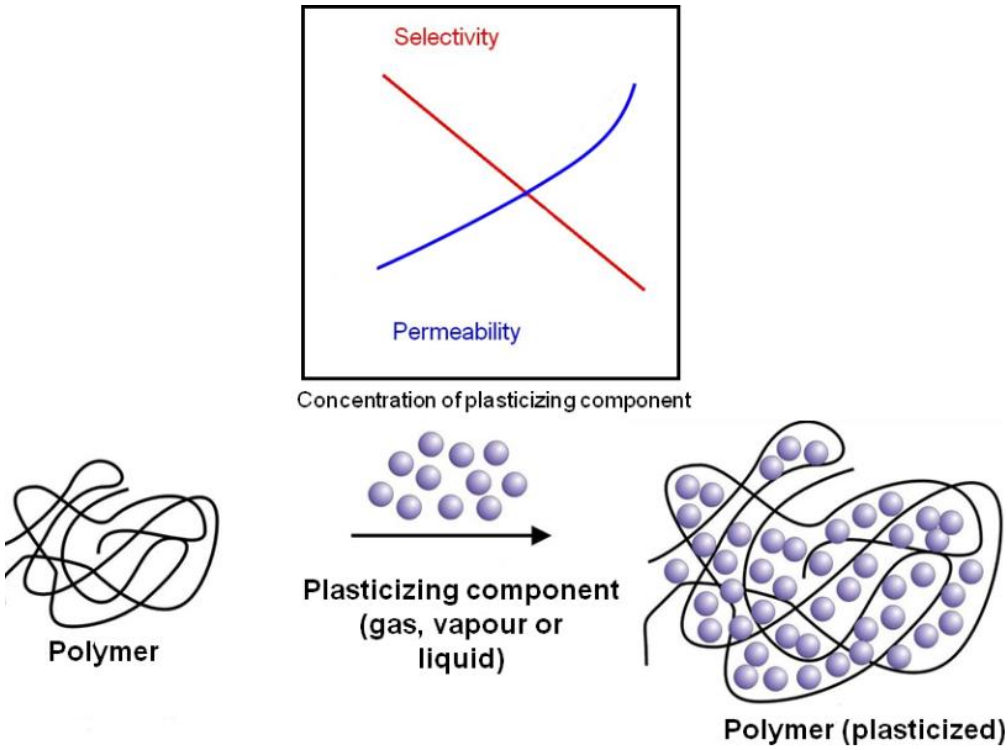

Fig. 3.8. Plasticisation effect (Schmeling et al., 2010).

Fig.3.8. shows plasticization effect in polymers. Different plasticisers can be used for pharmaceutical formulations dependent on solubility and glass transition temperature. Pharmaceutically used plasticisers are classified as hydrophilic or hydrophobic - typical materials being included in Table 3.1. In this project Triethyl Citrate has been used as a plasticizer in the preparation of solid dispersions of CBZ - Kollidon VA64.

Hydrophilic	**Hydrophobic**
Glycerin	Acetyl Tributyl Citrate
Polyethylene Glycols	Acetyl Triethyl Citrate
Polyethylene Glycol Monomethyl Ether	Castor Oil
Propylene Glycol	Phthalate Triacetin
Sorbitol Sorbitan Solution	Triethyl Citrate

Table 3.1. List of plasticisers (USP).

It should be noted that a lot of APIs also can cause plasticisation when compounded with pharmaceutical polymers leading to a beneficial reduction in the viscosity of the formulation during processing.

In this project rheological measurements have been used for preliminary thermal stability testing including effect of temperature and shear on the materials to be used. Rheological study of polymers - Kollidon VA64, Kollidon SR and Soluplus for confirmation of their suitability to be used for hot melt extrusion for the preparation of solid dispersions has been carried out. Along with these tests, rheological testing of CBZ has been carried out by making its 5%, 10%, 20% and 30% physical mixtures with Kollidon VA64 (after finding suitability of Kollidon VA64 over Kollidon SR) to find out impact of drug loading on the formulations to understand and confirm plasticization effect of API in a formulation.

3.3. X-ray diffraction (XRD)

XRD is a non - destructive technique for the qualitative and quantitative analysis of crystalline or semi-crystalline materials, in either powder or solid forms. A characteristic fingerprint region in the diffraction pattern of the material stands for crystallinity property. To detect amorphous and crystalline forms of solid dispersions XRD can be used, but there is a limitation to XRD detection in terms of absolute crystallinity.

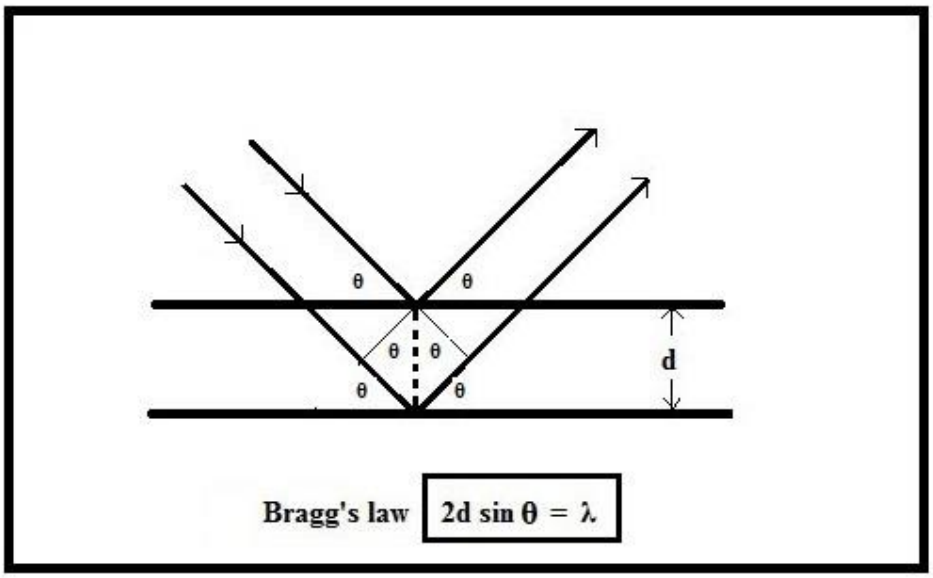

Fig. 3.9. Bragg's Law

XRD is obtained as the "reflection" of an X - ray beam from a family of parallel and equally spaced atomic planes, following Bragg's law (fig.3.9.). When a monochromatic X - ray beam with wavelength λ is incident on lattice planes with an angle θ, diffraction occurs if the path of rays reflected by successive planes (with distance d) is a multiple of the wavelength (GNR, 2013), i.e.:

$$2dsin\theta = \lambda$$

In this project PXRD has been utilised for determination of crystallinity of CBZ in the solid dispersions of CBZ + Kollidon VA64 and CBZ + Soluplus. Purity of co - crystals of IBU - NA and determination of purity of ibuprofen in dilutions of IBU-Na co-crystals with ibuprofen has been studied using PXRD.

3.4. Hot Stage Microscopy (HSM)

Hot stage microscopy is an analytical technique which involves microscopy and thermal analysis to characterise physical properties of materials with

temperature. In the pharmaceutical field, hot stage microscopy is used to characterise solid-state of pharmaceuticals crystal forms and hydrates as well as other physical properties (Vitez et al., 1998).

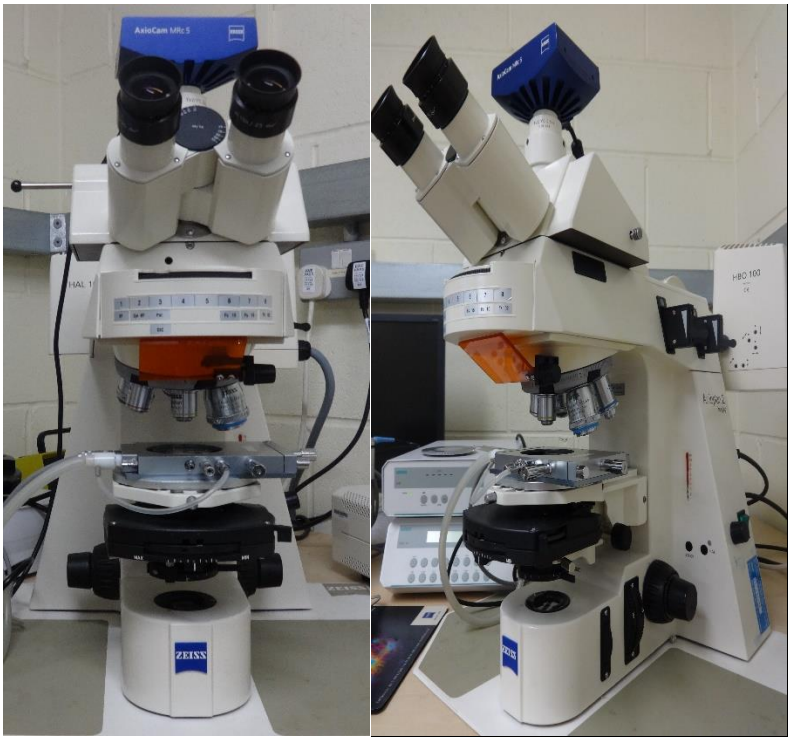

Fig.3.10. Hot Stage Microscope (Axiovision)

In this project HSM has been used for understanding thermal behaviour (melting, degradation due to temperature) of CBZ and its polymorphic form transformation as well as for studying thermal stability of Soluplus prior to its use for hot melt extrusion.

3.5. High performance liquid chromatography (HPLC)

In chromatography, separation of components of a mixture between two phases by allowing distribution of components is carried out. High Performance Liquid Chromatography (HPLC) is an important analytical technique for separation of components and can be used to determine impurities in pharmaceutical formulations.

In HPLC a liquid mobile phase is used to transport the analytes (samples to be analysed) through column packed with stationary phase) (Sabir et al., 2013). The stationary phase consists of materials with different hydrophobicity chemically bonded to a solid support. It is a highly selective technique since the analyte has the ability to interact with the mobile and stationary phases.

Fig. 3.11. Waters Alliance e 2695 HPLC system

During HPLC process, a mobile phase at fixed flow rate is pumped through the system by the aid of pump. Samples to be analysed are injected into the mobile phase without introducing air. The component mixture is carried to the top of the column in a narrow band.

During this project HPLC has been used for simultaneous estimation of CBZ and Iminostilbene.

3.6. Microwave assisted synthesis

Fig. 3.12. Monowave 300 synthesis reactor (Anton Paar, 2015).

Microwave synthesis has been used in pharmaceutical industry and it is one of the efficient and time - saving techniques over the conventional synthesis methods. Due to the microwave radiations used, it reduces time of chemical reactions. An optional immersing ruby thermometer for precise control of reaction temperature is an important feature of this reactor. Heating with holding time and cooling of the samples can be carried out using this reactor which helps in changing parameters for studying effect of change in temperature and holding time on the samples.

During this project the microwave reactor has been used for preparation of batches of IBU - NA co - crystals using various parameters such as temperature, holding and cooling time for getting pure co - crystals.

3.7 Fourier Transform Infrared (FTIR) spectroscopy

Fourier Transform Infrared (FTIR) spectroscopy is non - destructive analytical technique used to study various kinds of molecules (Glassford, 2013).

Region	Wavelength (λ) (μm)	Wavenumbers (cm^{-1})
Near	0.78 to 2.5	12800 to 4000
Middle	2.5 to 50	4000 to 200
Far	50 to 1000	200 to 10

Table 3.2. IR spectral regions table (Skoog et al., 2007).

Infrared spectroscopy is often described by the wavelength of the excitation light and is commonly denoted as Near, Mid and Far infrared spectroscopies according to the approximate table given in Table 3.2.

FTIR has been widely used in the polymer and pharmaceutical industrial research owing to its ability to characterize materials based on functional groups present in their chemical structures. It is a structure elucidation analytical technique which generates spectra of absorption frequencies which stand for particular functional groups in the molecules under examination. Its operational mechanism involves dipole moment changes during vibrations and rotations of molecules. For absorption of IR radiation, a molecule needs to undergo a net change in dipole moment during its complete vibration or rotation. Because of this only, interaction of molecule with alternating electric field of the radiation can occur. On vibration of homonuclear species such as O_2, N_2 or Cl_2 no net change takes place in dipole moment due to which these types of compounds are unable to absorb IR radiations. All other molecules can absorb IR radiation except these compounds (Skoog et al., 2007).

FTIR is a vibrational molecular spectroscopy which involves absorption of light and based on the difference in functional groups of chemical structures of the molecules, peaks at different absorption frequencies appear in the spectra. Two main types of vibrations occur between the molecules as follows:

Stretching vibrations: These involve continuous change in the interatomic distance along the axis of bond between two atoms.

Bending vibrations: These vibrations exhibit change in the angle between two bonds and are of four types (Fig. 3.13).

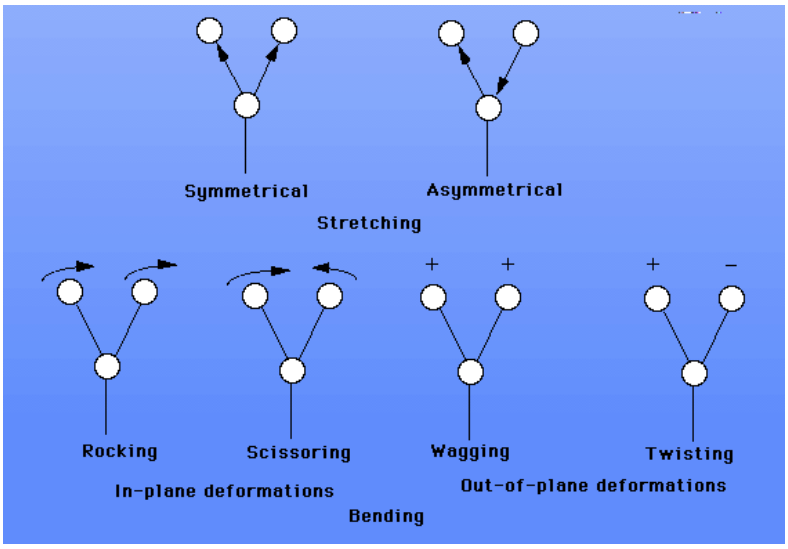

Fig. 3.13. Stretching and Bending vibrations (Shodor, 2015).

Dispersive spectrophotometers have a grating monochromator whereas Fourier transform spectrometers have an interferometer. Dispersive spectrophotometers were used widely until the 1980s, but these have been displaced by Fourier transform spectrometers for mid and far IR analysis due to their higher speeds, reliability and signal to noise advantage since more energy throughput is provided by the optics in FT instruments than that of dispersive ones Non - dispersive photometers using a filter or an absorbing

gas are used for analysis of atmospheric gases at specific wavelengths (Skoog et al., 2007).

Fig. 3.14. Nicolet iS50 FTIR by Thermo Scientific (Thermoscientific).

Fourier Transform Infrared (FTIR) spectroscopy is a vibrational spectroscopic technique which involves measurement of wavelength and intensity of the absorption of infrared radiations by a sample. The Nicolet iS50 FTIR used in the current project can work in a number of modes however for the work reported in this thesis it was run in Attenuated Total Reflection (ATR) mode.

In this project FTIR has been used for characterization of SDs of CBZ - VA64. From the FTIR spectra of IBU - NA co-crystals and that of CBZ - NA Calibration curves have been generated for quantitative analysis.

3.8. Raman Spectroscopy

As discussed in chapter 1 Raman spectroscopy is a technique which involves molecular vibrations based on inelastic scattering of light by

molecules. Raman effect is the basic principle behind this technique which can be illustrated with the example from nature and reason behind blue colour of the sky.

Fig.3.15. The Blue mystery and Raman effect (Barman, 2013).

When water molecules in sea use white Sun - light and scatter it into the wavelength which falls in region which is blue in colour due to which Sky look blue and as its reflection sea also appear blue in colour (Fig.3.15).

The rationale behind this effect can be understood by the fact that Rayleigh scattering is an elastic scattering, in which light just get deflected after confronting a molecule without changing its wavelength while because of vibrational modes of a molecules there could be inelastic scattering processes in case of Raman spectroscopy.

Some terms related with Raman spectroscopy are defined below:

Stokes and anti - Stokes scattering: When the scattered radiation's frequency is lower than that of the excitation radiation, it is known as Stokes scattering while when frequency of scattered radiation is higher than the source radiation, it is known as anti - Stokes scattering.

Rayleigh scattering: When the frequency of scattered radiation and source radiation is equal it is termed as Rayleigh scattering (Skoog et al., 2007).

3.8.1. Raman spectrophotometer instrument calibration (using universal platform)

Wavelength (780nm full range grating), Neon lamp, Laser and white light have been calibrated during Raman spectrophotometer instrument calibration.

Fluorescence reduction

To get Raman spectra of good quality without noise various parameters such as Laser power, baseline correction, change in aperture slit size, exposure time has been carried out. Various parameters in experimental set up have been tried to get fine Raman spectra and to reduce fluorescence.

1. Laser power: Laser power of 10mW, 25mW, 40mW, 50mW, 60mW, 70mW, 80mW and 100mW have been tried to find out the difference in noise and quality of Raman spectra. Better spectra were obtained with 80mW and 100mW compared to less laser powers.

2. Baseline: Correction in fluorescence was found to give clear baselines.

3. Aperture size: With 25µm slit aperture less noisy spectra were obtained than that of pinhole aperture.

4. Containers: Transparent containers (plastic self-sealing pouches) have no role in showing fluorescence while glass containers were found to fluorescent.

5. Exposure time: Raman spectra were obtained with various exposure times (10s, 20s, 30s, 40s, 60s, and 120s). It has been observed that increase in exposure time tends to show CCD overflow, increase in fluorescence and sample heating in some cases.

6. Photo bleaching time: Photo bleaching time of 0.5 to 5 min has been tried which did not reduce the fluorescence. Along with fluorescence, these Raman spectra were found to show signs of photo bleaching.

Raman spectroscopic analysis of Carbamazepine with calibrated instrument has been carried out. At 80mW laser power it has shown fine spectra. In case of solid dispersions, Raman spectra of 5% and 10% solid dispersions did not show fluorescence while that of 20% and 30% solid dispersions have shown presence of fluorescence which may indicate impact of more concentration of drug on fluorescence. With calibrated universal platform fine Polystyrene spectrum has been obtained (Fig.3.16.) which shown resemblance with that of standard Polystyrene spectrum by McCreery Research Group (McCreery, 2000). Raman shift values have been listed in Table 3.3.

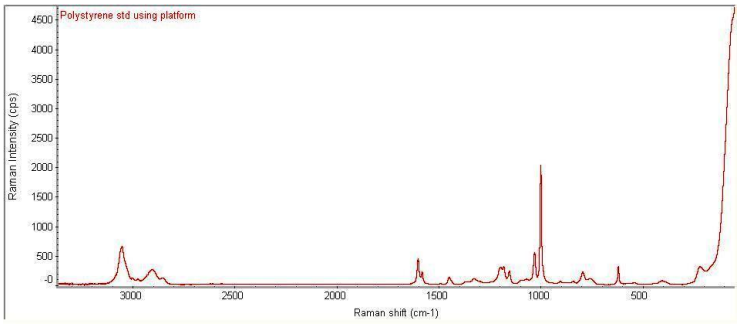

Fig. 3.16. Raman spectrum of Polystyrene

Raman shift (cm^{-1})	Intensity
620.38	298.810
795.52	211.018
1001.25	2026.643
1031.20	539.725
1155.03	220.788
1182.21	300.972

Table no. 3.3. Raman shift values in the Raman spectrum of Polystyrene

3.8.2. Raman Spectroscopy - Instrumentation (off - line) Universal platform (ups) of DXR smart Raman spectrophotometer has been used for off - line Raman spectroscopy by placing samples in transparent container on the platform which covers the area where laser spot is located for laser radiation after placing the sample.

Fig. 3.17. DXR smart Raman spectrophotometer (ups)

Specifications of DXR Raman spectrophotometer:

Laser: Visible/Invisible laser radiation Max laser o/p 300mW, 25mW, 35mW

Wavelength: 785nm, 532nm and 633nm

Class 3B laser product**.**

3.8.3. Raman spectroscopy - Instrumentation (in - line)

A schematic of Process Raman probe used for In-line monitoring by Inphotonics can be seen in Fig. 3.18.

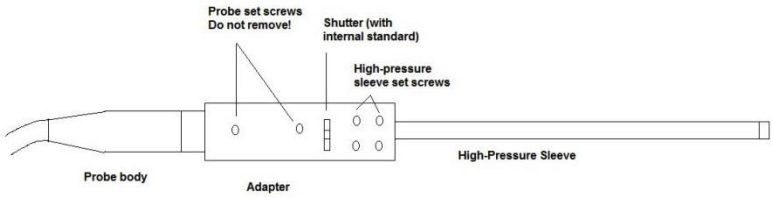

Fig. 3.18. Schematic of Process Raman probe used for In-line monitoring - Inphotonics

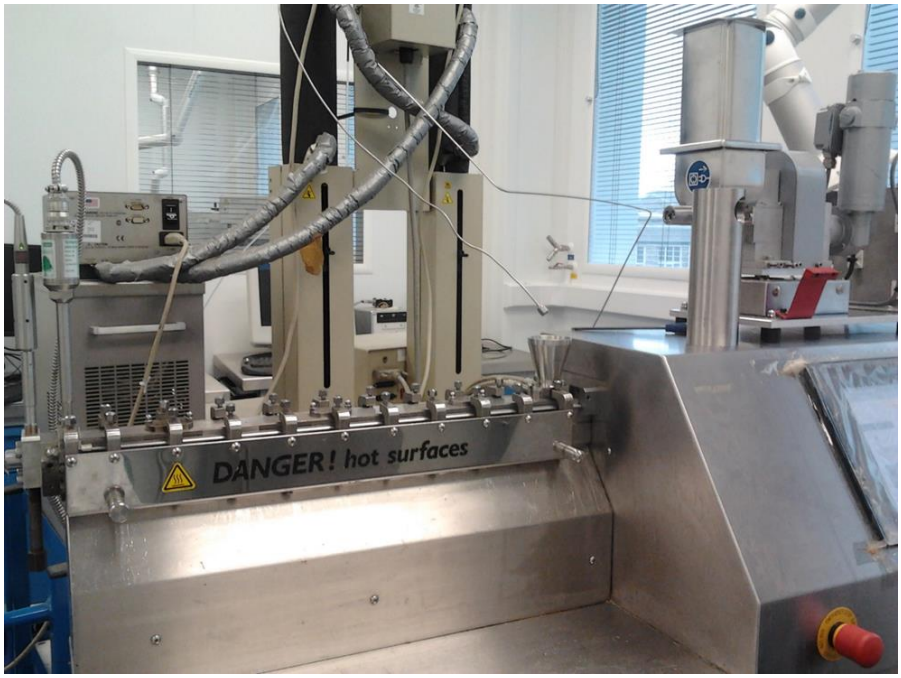

(a)

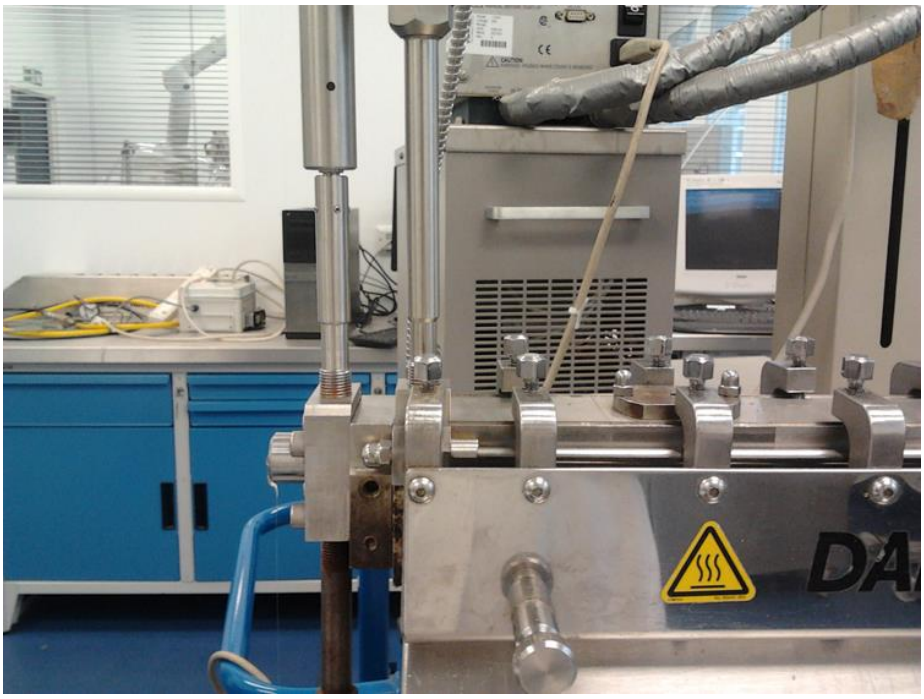

(b)

Fig. 3.19.a) In- line Raman spectroscopic monitoring during pharmaceutical HME b) Process Raman probe connected to the extruder die

Fig.3.19.a. and Fig.3.19.b show in-line Raman process Raman probe arrangement with hot melt extruder used in the present work during monitoring preparation of solid dispersions.

Specifications of Process Raman probe:

Excitation wavelength: 785nm

Excitation fibres: 100µm core with SMA connector

Collection fibres: 200µm with SMA connector

Sleeve material: 326 Stainless steel with Dynisco fitting

Window type: Sapphire (flat)

Pressure rating: 3000psi

Temperature rating: 204°C

Fig. 3.20. Process Raman Probe – Inphotonics

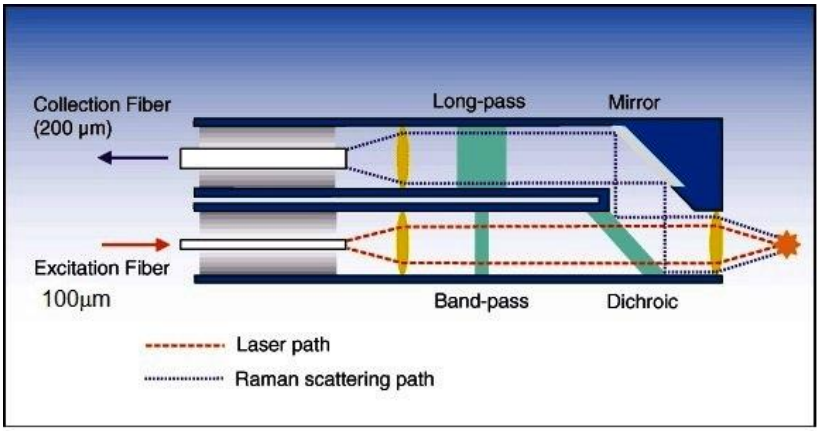

Fig.3.21. Process Raman probe fibers arrangement

Inphotonics Process Raman probe (Model number - RPP785/12-5, Serial number - 332614) showed in Fig. 3.20. has been used in this project for in - line monitoring of solid dispersions of CBZ + Soluplus. Arrangement of fibers used in connecting Process Raman probe with the laser path (to DXR smart Raman spectrophotometer) and Raman scattering path can be seen in Fig. 3.21. Details of the methods and results are discussed in Chapter 4 and 5.

Chapter 4 - Materials and Methods

4.1. Introduction

This thesis consists of four parts of research work and materials and methods for each part are covered individually prior to the results and discussion for each being provided in chapter 5. These parts have been divided as follows:

4.2.1 Preparation and characterisation of solid dispersions of Carbamazepine (CBZ) and Kollidon VA64

4.2.2. Preparation and characterisation of solid dispersions of Carbamazepine and Soluplus

4.2.3. Preparation and characterization of co-crystals of Ibuprofen (IBU) and Nicotinamide (NA)

4.2.4. Preparation and characterization of co-crystals of Carbamazepine (CBZ) and Nicotinamide (NA)

4.2.1. Preparation and characterisation of solid dispersions of Carbamazepine (CBZ) and Kollidon VA64

Materials

A variety of polymers, excipients and Active Pharmaceutical Ingredients (APIs) have been utilised throughout the project. This section briefly describes their chemistry and key physical properties.

Active Pharmaceutical Ingredients

Carbamazepine (CBZ) (DrugBank, 2005) – CBZ in polymorphic form III (*p*-monoclinic) purchased from Jay Radhe Sales, Ahmadabad, India.

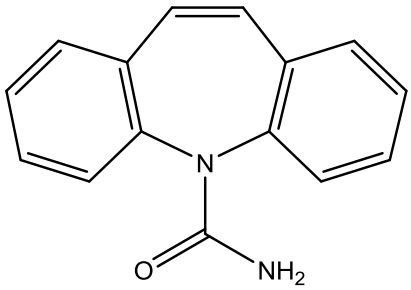

Fig. 4.1. Chemical structure of CBZ (Chem draw).

Chemical name: (5H-dibenz (b, f) azepine-5-carboxamide (Strachan et al., 2004).

Chemical class: Dibenzazepine (with two benzene rings fused to an azepine group - unsaturated heterocycles of seven atoms, with a nitrogen replacing a carbon at one position.

Therapeutic class: Anticonvulsant

Physical characteristics: White to off-white, practically insoluble in water and soluble in alcohol and in acetone. Its molecular weight is 236.27g/mol. and its melting point is reported as being between 190 - 193°C.

Polymorphism: CBZ is known to exist in four anhydrous polymorph forms: Triclinic (Form I), Trigonal (Form II), *P*-monoclinic (Form III) and *C*-monoclinic (Form IV) as well as a dihydrate. A primitive monoclinic polymorph was the first to be structurally defined by x-ray analysis. A triclinic polymorph has also been characterized (Ceolin et al., 1997). The nomenclature of these polymorphs has varied between papers. Designation of the characterized *p*-monoclinic polymorph as form III and the triclinic polymorph as form I appear to be the most common system. Form III is stable at ambient temperature. The polymorphs and hydrate of CBZ have been shown to exhibit different dissolution rates and bioavailabilities (Kobayashi et al., 2000) and different commercial brands of CBZ tablets

have a history of bioinequivalence and clinical failure which may be due to polymorphism (Meyer et al., 1992). Hence CBZ is one example of a drug that illustrates the necessity to identify, monitor and understand pharmaceutical polymorphs as fully as possible.

Order of stability: form III > form I > form IV > form II

Form III is the commercial form. Form I is obtained by heating Form III and Form II, is crystallised from ethanolic solution (DrugBank, 2005).

Polymers

Kollidon SR

This material was provided by BASF, Germany as a gift sample.

BASF's Kollidon SR (BASF, 2011) is polyvinyl acetate and povidone based matrix retarding agent. It contains 80% polyvinyl acetate and 19% povidone Ph. Eur./ USP (Kollidon 30) in a physical mixture.

Solubility: Insoluble in water (The povidone part is soluble but the polyvinyl acetate part is insoluble).

Molecular weight: (Average) of polyvinyl acetate part: 4,50,000 Da.

One of the povidone K30 part: 50,000 Da.

Glass transition temperature (Tg): 39°C/ 152 °C.

Kollidon VA64 (Vinylpyrrolidon-vinylacetate copolymer)

This material was provided by BASF, Germany as a gift sample.

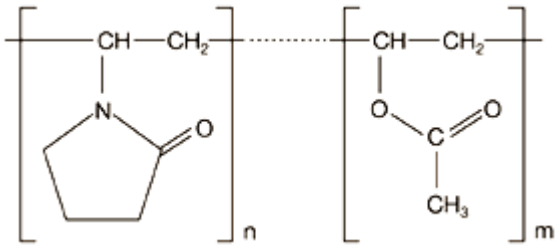

Fig. 4.2. Chemical structure of Kollidon VA64 (BASF)

BASF's Kollidon VA64 (BASF, 2011)_is a mixture of 6 parts of N-vinyl pyrrolidone and 4 parts of vinyl acetate.

Solubility: Vinyl pyrrolidone is a hydrophilic, water soluble monomer whereas vinyl acetate is lipophilic and water insoluble. The ratio of both monomers is balanced in such way that the polymer is still freely water soluble. Due to solubility in all hydrophilic media, the release profile is mostly instant.

Molecular weight: 45,000 -70,000 Da.

Glass transition temperature (Tg): 107°C.

Thermal stability: Up to 150°C.

Sample preparation: Physical mixtures of accurately weighed drug and polymer were prepared by mixing the drug and polymer using a glass mortar and pestle in various concentrations of 5%, 10%, 20% and 30% w/w CBZ.

TGA studies: 2 - 5mg of solid dispersions of the various concentrations were ground using a mortar and pestle. Samples were transferred to platinum crucubles for analysis. Taring of balance has been carried out prior to running the tests. TGA results were obtained in the range of 40 - 250°C using TA Instruments Universal Analysis 2000 software coupled to a TA Instruments Q500 Analyser.

DSC studies: Thermal profiles were generated in the range of 40 - 250°C with the heating rate of 10°C / minute using a Q2000 calorimeter from TA Instruments. Temperature calibration was performed using an indium metal standard supplied with the instrument at the respective heating rate. Accurately weighed samples (3 - 5mg) were placed in aluminium pans using similar empty pans as a reference. Measurements were carried out in an inert atmosphere by purging nitrogen gas at the flow rate of 50 mL/min. The

acquired thermograms were analysed with TA Instruments Universal Analysis 2000 software.

Rheological studies: Rheological characterisation of all samples were conducted using an Anton-Paar MCR 301 rheometer with plate-plate geometry with the diameter of the plate being 25 mm and a gap size of 1 mm. Calibration for zero gap and normal force were performed prior to its operation in the oscillatory mode. Preliminary analysis of results was performed using RheoPlus software (Anton-Paar).

Amplitude sweep: In order to establish the extent of the linear visco-elastic region (LVR) an oscillatory amplitude sweep was conducted over the strain range of 0.01 to 100 % at a constant angular frequency of 10 rad/s. The effect of stress on the elastic (G') and viscous moduli (G'') were monitored and a suitable value of the strain for the frequency sweeps was determined.

Frequency sweep: Samples were exposed to angular frequencies in the range 0.1 to 100 rad/s at a constant strain of 3%, this value having been determined as being suitable by the preceding amplitude sweep. The effect of shear rate on elastic (G') and viscous moduli (G'') and complex viscosity was determined at temperatures of 145,150 and 155°C.

Raman spectroscopic studies: Off-line Raman analysis of CBZ, Kollidon VA64 and physical mixtures of CBZ and Kollidon VA64 was carried out by placing samples in transparent containers on the Universal Platform of the Thermo Scientific DXR Smart Raman spectrophotometer after calibration and background corrections in the wavenumber range of 200 - 3500cm^{-1}. Raman spectra were converted into Grams format for interpretation using Grams 9.1 spectroscopy software (Thermo Fisher Scientific Inc.). The 785

nm laser power was set at 80mW with a warm up time of 5 minutes. 32 scans of 10 seconds duration were taken for each sample. For each scan approximately 11.25 seconds was required.

Hot melt extrusion: Solid dispersions were prepared by the hot melt extrusion method using physical mixtures of various concentrations as 5%, 10%, 20%, 30% and 40%. Prior to extrusion, CBZ and Kollidon VA64 were ground properly using mortar and pestle in predefined weight ratios. The powder blends were fed from a gravimetric twin screw feeder (Brabender, Germany) into the Pharmalab 16 Twin screw Extruder (Thermo Scientific, UK) using a calibrated feed rate of 0.25 kg/hr and the extruder was continuously run at a set screw speed of 25rpm. The extruder is a 16mm diameter co-rotating twin screw extruder with screw length to diameter ratio of 40.The temperature profile maintained along the length of the barrel is shown in Table 4.1 and the modular screw design is summarised in Table 4.2.

	Zone									
T (°C)	**Die**	**10**	**9**	**8**	**7**	**6**	**5**	**4**	**3**	**2**
A-1	140	140	140	130	120	110	110	100	90	50

Table 4.1. Temperature profile (°C) along extruder barrel

Pharma 4 screw configuration used for HME	
No. of elements	**Type of element**
28	Forward conveying

9	30^{o} forward mixing
5	60^{o} forward mixing
4	90^{o} mixing
6	Forward conveying
1	Discharge

Table 4.2. **Pharma 4 screw configuration used for HME**

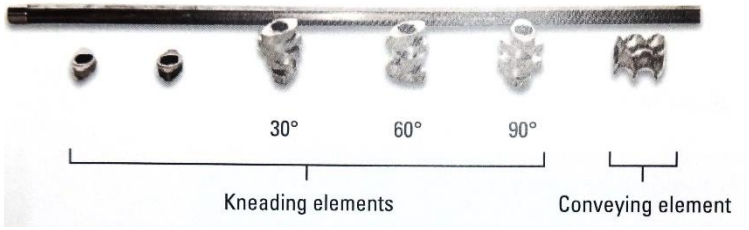

Fig. 4.3. Types of screw elements used for HME

The prepared solid dispersions were subjected to off-line Raman analysis at the same settings discussed above for the physical mixtures of CBZ and Kollidon VA64.

XRD analysis: The crystal structure of the solid dispersions was determined by X-ray powder diffraction using a Bruker D8 diffractometer (wavelength of X-rays 0.154 nm from a Cu source, voltage 40 keV, and filament emission 40 mA). Samples were scanned in the range of 2 to 40° (2θ) using a 0.01° step width and a 1 second time count. The receiving slit was set to 1° and the scatter slit to 0.2°.

FTIR studies: FTIR studies of CBZ, Kollidon VA64 and SDs in the various concentrations (5%, 10%, 20%, and 30%) were carried out by using a Digilab

FTIR microscope. Backgrounds were collected before the actual spectra with 16 scans each. FTIR spectra were obtained using Digilab Merlin software.

4.2.2. Preparation and characterisation of solid dispersions of Carbamazepine and Soluplus

Materials

Soluplus

This polymer was provided by BASF, Germany as a gift sample. Soluplus (BASF, 2011) is a polyvinyl caprolactam - polyvinyl acetate - polyethylene glycol graft copolymer. It is a polymeric solubiliser with amphiphilic chemical structure. Since it is bifunctional in nature, it can be used as a matrix polymer for solid solutions as well as an aid for solubilising poorly soluble drugs in aqueous media.

It is a free flowing white to slightly yellowish granule without taste. It can increase solubility and bioavailability of poorly soluble drugs. For hot melt extrusion, it has been found as an ideal candidate due to its excellent extrudability and easy processing.

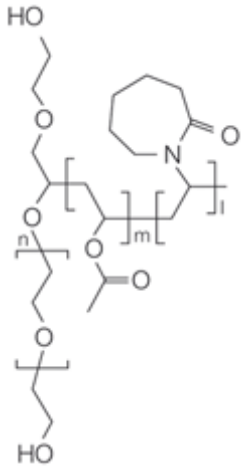

Fig. 4.4. Chemical structure of Soluplus (BASF)

Glass transition temperature (Tg): Approximately 70˚C

Solubility: Soluble in water, soluble in acetone (up to 50%), methanol (up to 45%), ethanol (up to 25%) and dimethylformamide (up to 50%)

Molecular weight: 90,000-1, 40,000 g/mol.

Extrusion recommendations: Pure polymer can be extruded on a 16mm twin screw extruder at temperatures starting around 120˚C to 180˚C depending upon the applied screw configuration. The polymer shows no chemical degradation even after extrusion at 180˚C. Incorporation of a drug can lead to lower temperatures than 120˚C in dependence on the drug melting point.

Solid dispersions of Carbamazepine (CBZ) (5*H*-dibenzo [*b*, *f*] azepine-5-carboxamide) and Soluplus were prepared by a hot melt extrusion process using a twin screw extruder at a screw speed of 30rpm and at temperatures in the range of 120 to 170˚C using two temperature profiles T1 and T2 and a feed rate of 0.18 kg/hr.(Table 4.3). A comparative study of Raman spectra of extrudates with that of metabolite of carbamazepine, 5H-Dibenz (b, f) azepine (Iminostilbene) was carried out. In-line Raman spectroscopic analysis of Carbamazepine, Soluplus and solid dispersions of Carbamazepine-Soluplus (5, 10, 20, and 30%) has been carried out using Inphotonics Raman probe with 80mW laser power and 2 scans of 60s acquisition. A series of spectra was collected using with OMNIC software. Spectra were converted into Grams format using Grams 9.1 by ThermoScientific.

	Zone									
	Die	**10**	**9**	**8**	**7**	**6**	**5**	**4**	**3**	**2**
T1 (°C)	170	170	170	150	150	150	140	140	140	130

T2 °C)	170	160	160	160	150	140	120	120	120	120

Table 4.3. Temperature profiles used during hot melt extrusion

DSC analysis of CBZ, Soluplus and CBZ-Soluplus physical mixtures was carried out using a similar method to that described in section 4.2.1. Physical mixtures were prepared by using mortar and pestle in concentrations 5, 10, 20 and 30%w/w. Thermal profiles were generated in the range of 20°C - 220°C at a heating rate of 10°C per minute.

XRD and off-line Raman analyses of base materials, physical mixtures and solid dispersions were carried out using the same methods as for section 4.2.1. Two scans of 120 seconds were taken for the off-line Raman using 80mW laser power.

Additionally samples were subjected to hot stage microscopic analysis (HSM) utilizing Axiovision software connected to Linksys 32 software with a Linkam hot stage attached to a microscope.

Small amount of samples (2-3mg) were placed on open glass slides fixed onto the hot stage with 10x/0.20 magnification with bifocal light and heated form 30°C to 220°C at 10°C per minute.

4.2.3. Preparation and characterization of co-crystals of Ibuprofen (IBU) and Nicotinamide (NA)

Materials:

Ibuprofen (Wishart DS et al., 2006).

This material was purchased from Albemarle, USA.

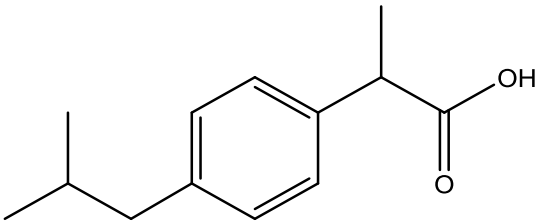

Fig. 4.5. Chemical structure of Ibuprofen (Chem draw)

IUPAC name: (*RS*)-2-(4-(2-methylpropyl) phenyl) propanoic acid

Therapeutic class: nonsteroidal anti-inflammatory drug (NSAID)

Molecular formula: $C_{13}H_{18}O_2$

Molecular mass: 206.29g/mol

Density: 1.03g/ml/ g/cm^3

Melting point: 75 to 78°C

Nicotinamide (Wishart DS et al., 2006).

This material was purchased from Fluka analytical - SIGMA - ALDRICH - GmbH, Steinheim.

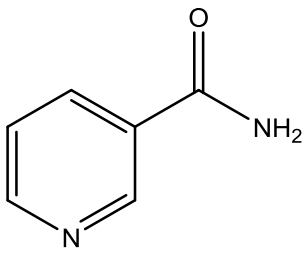

Fig.4.6. Chemical structure of Nicotinamide (Chem draw)

IUPAC name: pyridine-3-carboxamide

Therapeutic class: a water-soluble vitamin and is part of the vitamin B group.

Molecular formula: $C_6H_6N_2O$

Molecular mass: 122.12g/mol

Density: 1.4463g/cm^3

Melting point: 129.5°C

Two methods of preparation of Ibuprofen-Nicotinamide co - crystals were investigated in this study:

a) Preparation by solvent evaporation using a method reported in the recent literature (Soares and Carneiro, 2013) and,

b) Preparation by solvent mediated co - crystallisation using a microwave reactor.

a) Preparation of IBU - NA co - crystals by solvent evaporation:

3 mmol of ibuprofen (618.8 mg) and 3 mmol of nicotinamide (366.4 mg) were placed in a beaker and dissolved in 3 ml of methanol. After 10 - 12 hours, co-crystals were obtained on complete evaporation of the solvent. For complete removal of residual moisture, the resultant co-crystals were heated in an oven at 40°C for more than 12 hours. The purity of the produced co-crystals was established using DSC and XRD techniques. Preparation of physical mixtures of pure Ibuprofen and co-crystals of Ibuprofen and Nicotinamide in various concentrations (Table 4.4.) was carried out.

Sample name	% of pure Ibuprofen	% of IBU-NA co-crystals
CC1	10	90
CC2	20	80
CC3	30	70
CC4	40	60
CC5	50	50
CC6	60	40
CC7	70	30
CC8	80	20
CC9	90	10

Table 4.4. Concentrations of physical mixtures of Ibuprofen and co-crystals of Ibuprofen and Nicotinamide

Crystallinity of co - crystals along with pure Ibuprofen and Nicotinamide was determined by powder X - ray powder diffraction using the same methods for solid dispersions described earlier (under section 4.2.1. methods).

b) Preparation of IBU - NA co-crystals by microwave - reactor method:

Ibuprofen and Nicotinamide in molar ratio (1:1) were mixed with 82µL of distilled water and added in 30 mL capacity glass tube. The initial temperature chosen was 70°C and samples were subjected to microwave irradiation with the holding time of 1 minute and cooled at 40°C for 1 minute. Various batches of co-crystals were prepared to get pure co-crystals with

different holding times and temperatures during microwave preparation as mentioned in the table 4.5. The obtained IBU-NA co-crystals were analysed by DSC and XRD.

Batch name	Heating temperature △(°C)	Holding time ▷ (min)	Cooling temperature ▽ (°C)
C1	70	1	40
C2	70	2	40
C3	70	3	40
C4	75	1	40
C5	75	2	40
C6	75	3	40
C7	80	1	40
C8	80	2	40
C9	80	3	40
C10	70	5	40
C11	75	5	40
C12	80	5	40
C13	70	5	40
C14	75	5	0
C15	80	5	40
A,B,C,D,E	80	5	40

Table 4.5. Microwave preparation parameters during preparation Ibuprofen-Nicotinamide co-crystals.

Thermal profiles from DSC were generated in the range of 40 – 170°C using a Q2000 calorimeter from TA Instruments. Accurately weighed samples (3-5mg) were placed in aluminium pans using similar empty pans as a reference. A heating rate of 10°C per minute was employed.

The diffractograms of co-crystals along with pure Ibuprofen and Nicotinamide has been determined by X-ray powder diffraction using the techniques described above.

Offline Raman spectroscopic analysis of all physical mixtures (CC1 to CC9) along with %age co-crystals (Ibuprofen-Nicotinamide physical mixture 1:1) and 100% pure co-crystals was carried out using the Thermo Scientific DXR Smart Raman spectrometer with universal platform accessory.

All spectra were collected using 80 mW laser power, 25 µm slit with 780 nm laser with estimated spot size of 3.1µm and estimated resolution of 5.0 to 9.2cm^{-1}. 2 scans of 60s acquisition each were collected. A new chemometric method was created for preparing calibration curve for prediction of concentration of Ibuprofen and co-crystals of Ibuprofen and Nicotinamide using the software TQ Analyst 8 by Thermoscientific. A Partial Least Squares (PLS) method was selected with standard normal variate and second derivative spectra were selected for the study.

In addition, FTIR analysis of Ibuprofen-Nicotinamide (IBU - NA) co-crystal dilutions with Ibuprofen (10-100%) was carried out using Nicolet is50 ATR FTIR by Thermoscientific. Samples were analysed at 32 scans with 4cm^{-1} resolution and calibration curves generated from FTIR spectra using the software TQ Analyst and Microsoft excel.

4.2.4. Preparation and characterization of co-crystals of Carbamazepine (CBZ) and Nicotinamide (NA)

A 1:1 physical mixture of Carbamazepine (2.363 g, 0.01mol) and Nicotinamide (1.221 g, 0.01 mol) was dissolved in 20 ml of absolute ethanol, heated and stirred for 30 minutes. The mixture was then left to evaporate at 303.2 K for 72 hours for evaporation (Ali et al., 2014). Co-crystals obtained were dried using filter paper and characterised by DSC.

DSC analysis of co-crystals of CBZ-Na was carried out using a Discovery DSC by TA Instruments. Thermal profiles were generated by using a heating ramp of 5°C/min in the range of 40 to 220°C. Accurately weighed samples (3-5mg) were placed in aluminium pans using similar empty pans as a reference. Measurements were carried out in an inert atmosphere by purging nitrogen gas at the flow rate of 50 mL/min.

DSC profiles obtained in Trios format were exported in Microsoft excel for generation of a calibration curve using enthalpy values. A calibration curve was generated by plotting a graph of actual concentration of dilution co-crystals with CBZ versus measured concentration of dilutions co-crystals with CBZ from DSC enthalpy data.

Dilutions of co-crystals of CBZ-NA (Table 4.6.) with CBZ have been prepared by making physical mixtures using mortar and pestle. Off-line Raman spectroscopic analysis of these dilutions along with physical mixture of Carbamazepine and Nicotinamide (1:1) and co-crystals has been carried out using DXR Smart Raman spectrophotometer by Thermo Scientific. All spectra were collected using 80mW laser power, 25µm slit at 780nm with 2 scans of 10 seconds acquisition each.

A new chemometric method was created for generating calibration curve for prediction of concentration of Carbamazepine and co-crystals of CBZ and Na using TQ Analyst 8. Partial least squares (PLS) method was selected with standard normal variate and second derivative spectra were selected for the study. Spectral data normalisation was carried out by using the mean centering technique.

Sample name	% co-crystals of CBZ-Na	% of pure CBZ
CNA1	90	10
CNA2	80	20
CNA3	70	30
CNA4	60	40
CNA5	50	50
CNA6	40	60
CNA7	30	70
CNA8	20	80
CNA9	10	90

Table 4.6. Dilutions of physical mixtures of co-crystals of CBZ and NA with CBZ.

FTIR analysis of Carbamazepine-Nicotinamide (CBZ - NA) co-crystal dilutions with Ibuprofen (10-100%) has been carried out using Nicolet is50 ATR FTIR by Thermoscientific. Samples have been analysed at 32 scans with 4cm^{-1} resolution. Calibration curves have been generated from FTIR spectra using the software TQ Analyst and Microsoft excel.

Chapter 5 - Results and discussion

5.1. Introduction

For improving solubility of pharmaceutical active ingredients and to get better formulations as a result, preparation of solid dispersions is a great approach. Carbamazepine has been selected based on its polymorphic nature to study its various forms and degradation due to temperature as well as impact of shear on it. After carrying out some literature and basic thermal characterization Kollidon VA64 and Soluplus have been selected as polymers to be used in the preparation of solid dispersions. Ibuprofen-Nicotinamide has been used widely as a model co-crystal system which has been selected to be studied using Raman spectroscopy. Also in the present work, preparation of Ibuprofen-Nicotinamide co-crystals has been carried out by microwave and solvent evaporation method as well as of carbamazepine-nicotinamide co-crystals by solvent evaporation and hot melt extrusion method. This chapter focusses on pharmaceutical systems used for proposed study including solid dispersions of Carbamazepine - Kollidon VA64, Carbamazepine - Soluplus and co-crystals of Ibuprofen - Nicotinamide and Carbamazepine- Nicotinamide. After preliminary characterization by DSC, TGA and PXRD, analysis of all these systems has been carried out by off-line and in-line methods. As mentioned in chapter 4 results and discussion have been described in four parts of present research work. A flow chart explaining contents in this chapter in precise manner is shown in Fig.5.1.

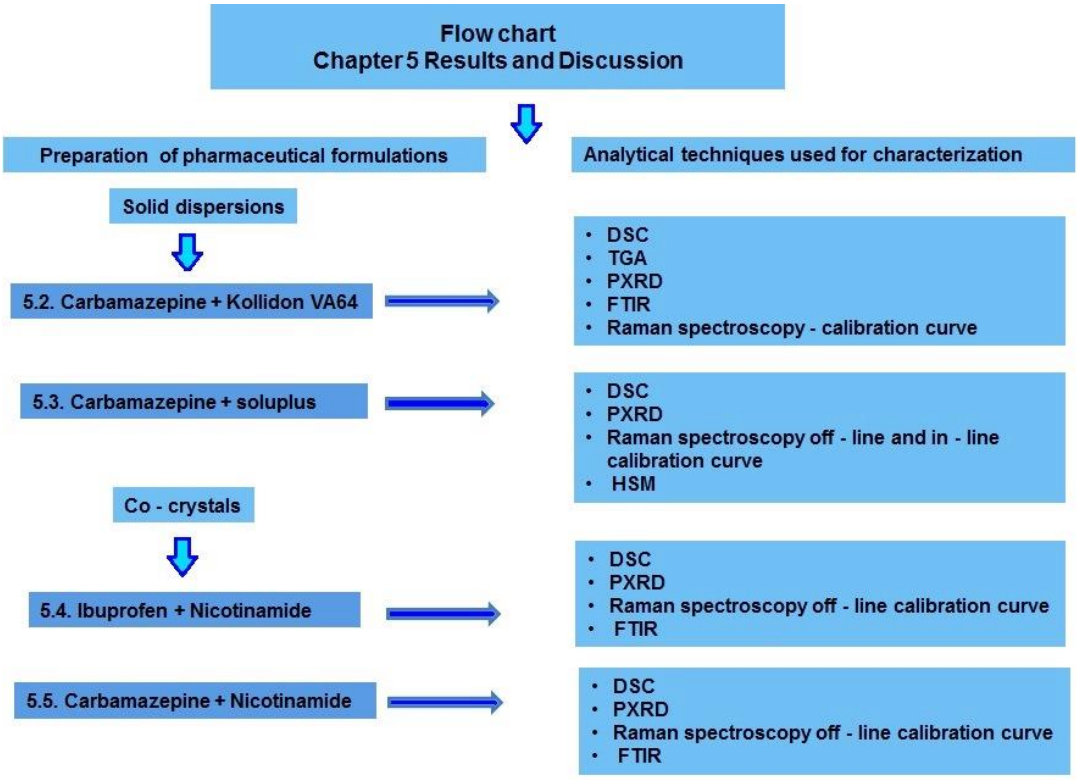

Fig.5.1. Flow chart showing contents of chapter 5

5.2. Preparation and characterisation of solid dispersions of Carbamazepine (CBZ) and Kollidon VA64

5.2.1. DSC results

CBZ and Kollidon VA64 were analysed by DSC using TA Instruments Q2000 to study their thermal properties for further processing. Solid dispersions of different concentrations of CBZ (5%, 10%, 20%, and 30%) and pure Kollidon VA64 were prepared by HME. DSC thermo grams of these solid dispersions were obtained by the same method and difference between thermal properties of API, polymer and solid dispersions was studied.

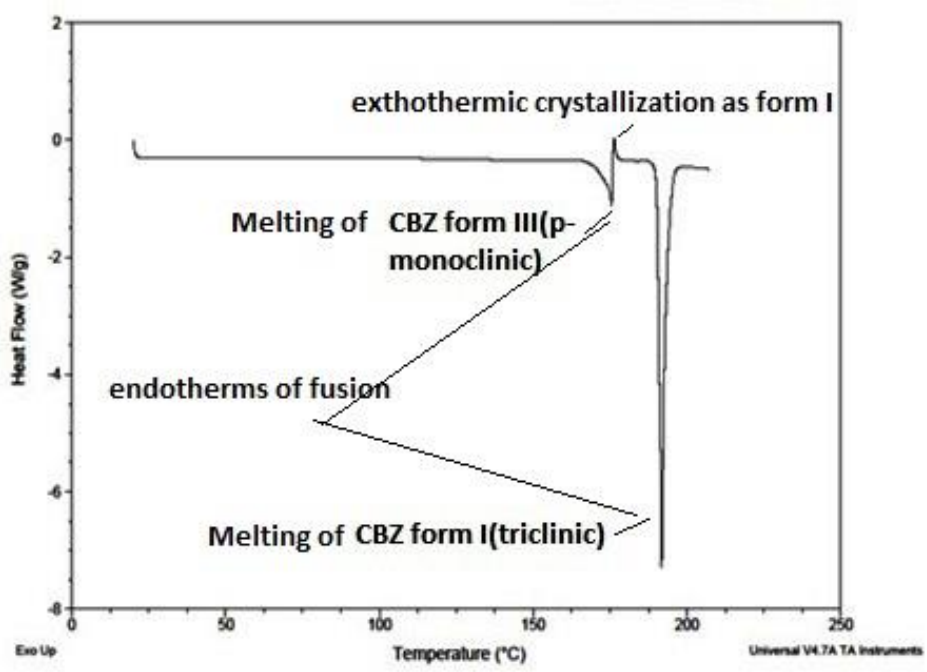

Fig.5.2. DSC profile of CBZ

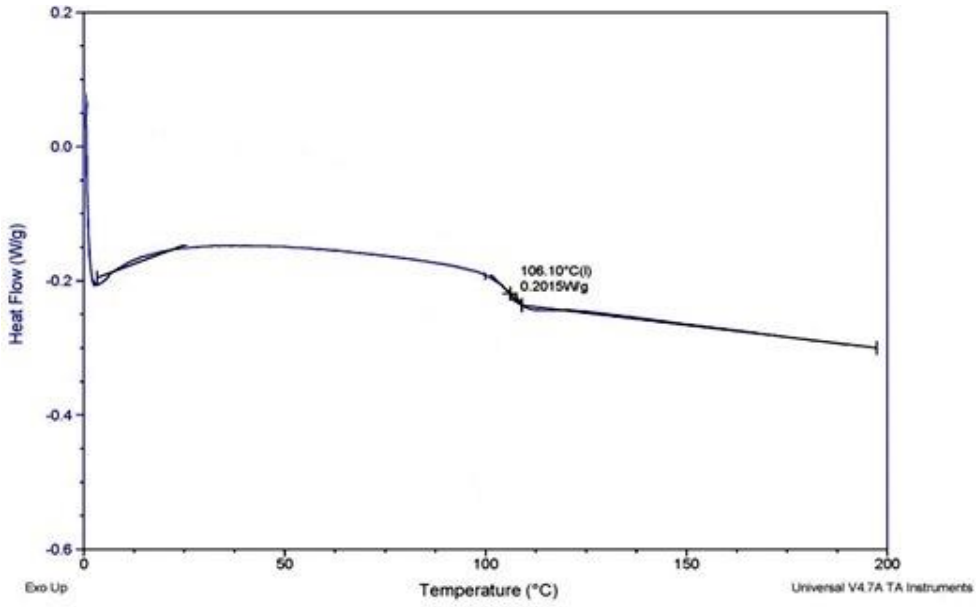

Fig.5.3. DSC profile of Kollidon VA64

In the DSC profile of CBZ- commercial form two endotherms of fusion were observed. Melting of CBZ - III (*p*-monoclinic) can be seen at 177˚C (Fig. 5.2.). An exothermic peak showing crystallization as form - I (triclinic) and its melting can be seen as an endothermic peak at 193˚C. DSC profile of Kollidon VA64 shows Tg value of 106˚C (Fig. 5.3).

5.2.2. MDSC results

Modulated DSC determines heat capacity and aids in separating heat flow due to reversible and non-reversible events. Refer back to chapter 3 - Experimental techniques for details describing the linear heating rate and amplitude and frequency of modulation.

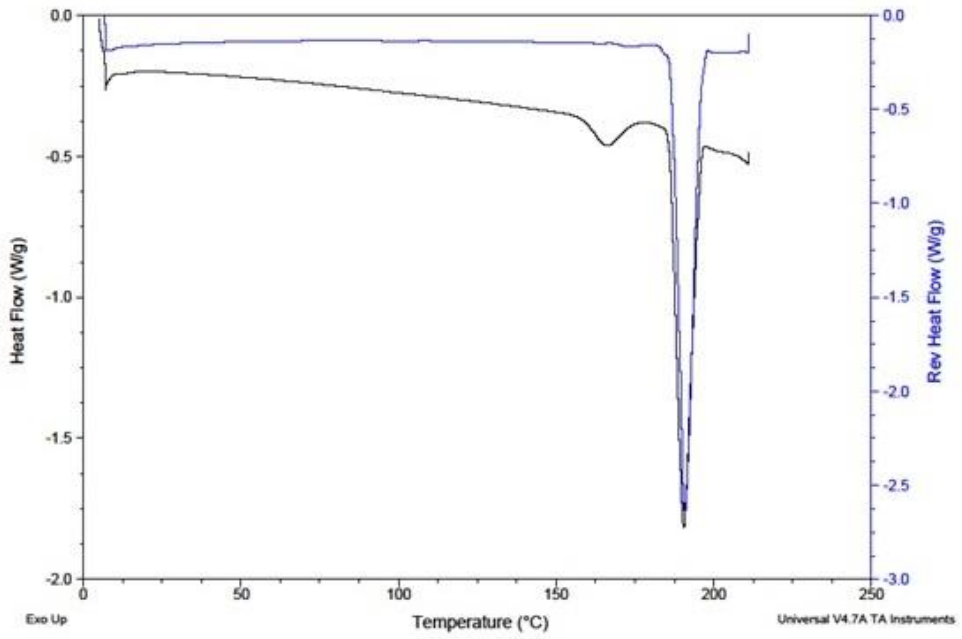

Fig.5.4. MDSC profile of CBZ: Reversible heat flow

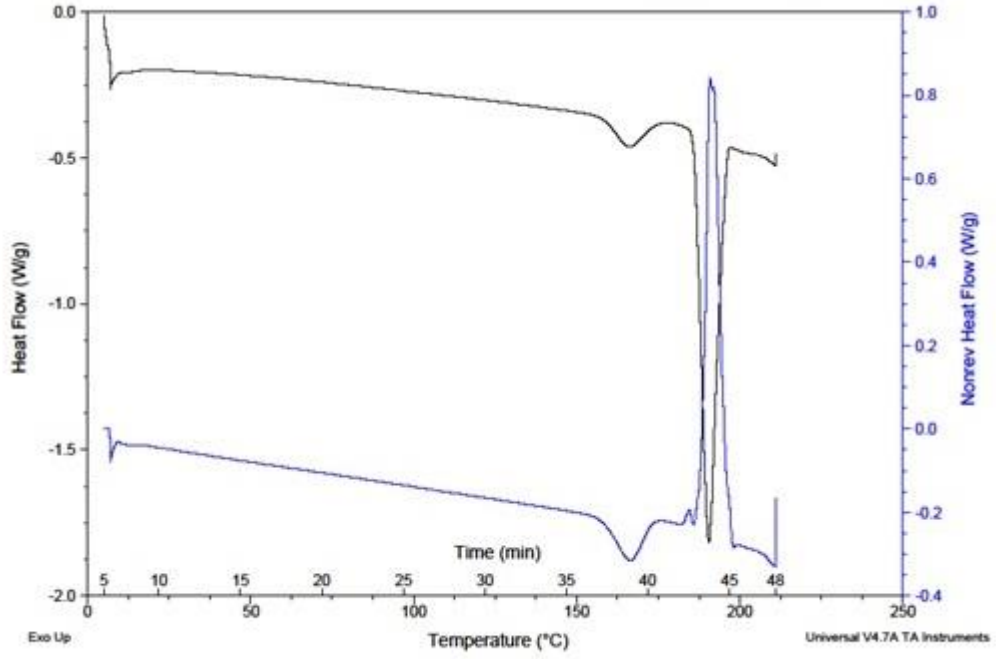

Fig.5.5. MDSC profile of CBZ: Non-reversible heat flow

MDSC analysis of Carbamazepine was carried out with heating rate of 5˚C/min, amplitude of +/- 1 ˚C and modulation period of 60sec. From Fig.5.4.

and 5.5., it was observed that form 1 started melting first, and then the molten form got recrystallized which indicate conversion into form III.

DSC studies of solid dispersions of various concentrations of CBZ in Kollidon VA64 were carried out. Results obtained from these studies indicate that an increase in the concentration of active pharmaceutical ingredient - Carbamazepine decreases the glass transition temperature of the solid dispersion.

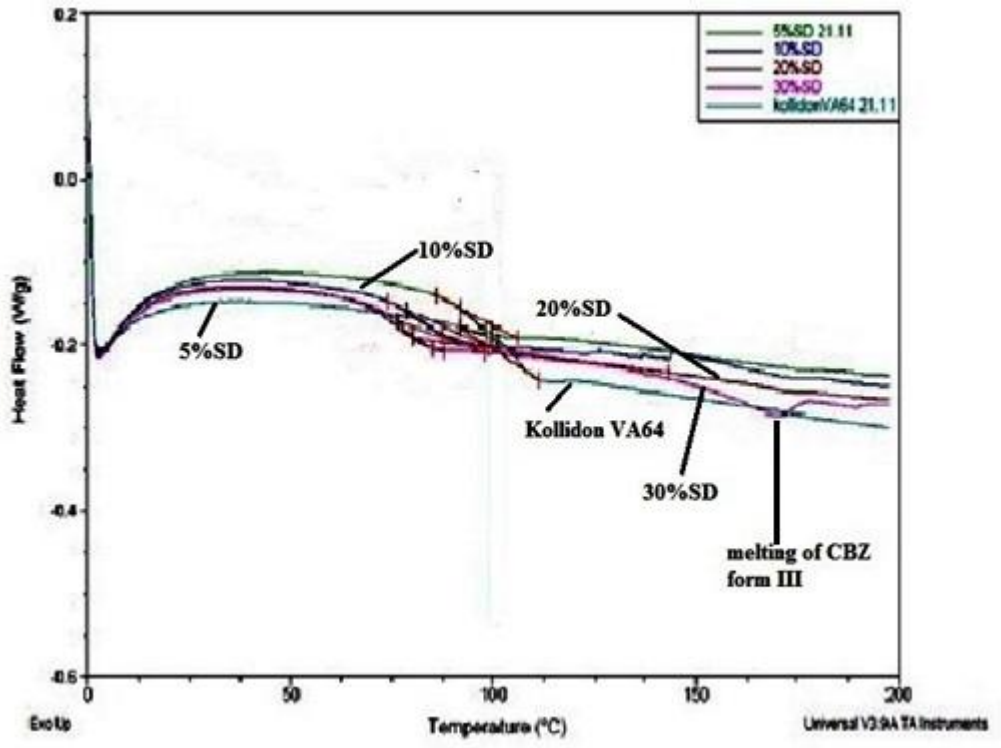

Fig.5.6. DSC profiles of CBZ - Kollidon VA64 SDs

A melting peak can be seen in Fig. 5.6. at 170°C which can be because of melting of CBZ form III (*p*-monoclinic).

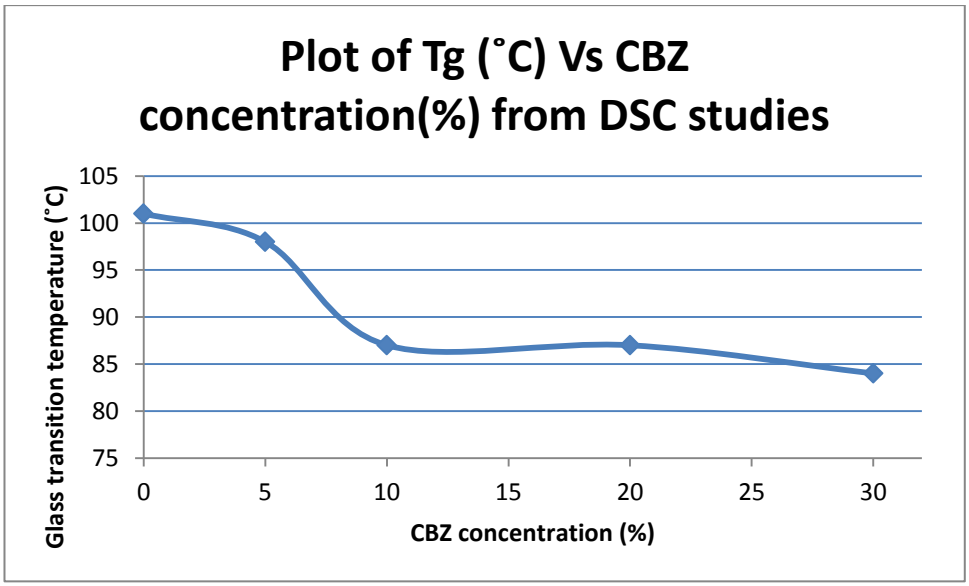

Fig.5.7. Plot of glass transition temperature Tg (˚C) Vs CBZ concentration (%) from DSC studies

From Fig 5.7., it is observed that there is decrease in Tg value of solid dispersion as per increase in CBZ concentration.

5.2.3. TGA results

TGA was used to observe the decomposition temperature of the samples and to determine the moisture content of solid dispersions. The sample of pure CBZ was allowed to heat from 40°C to 200°C at the rate of 10°C/min.

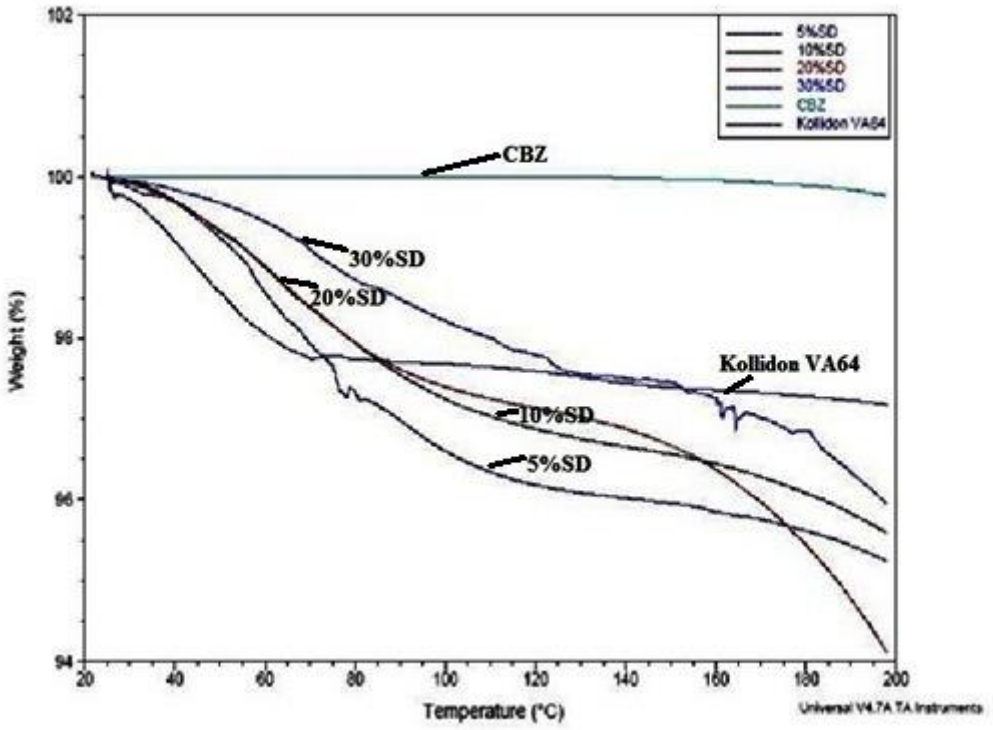

Fig.5.8.TGA profiles of CBZ, Kollidon VA64, and SDs (5, 10, 20 and 30%)

TGA profile of Kollidon VA64 indicates presence of moisture which can be because of its hygroscopic nature. From the TGA profiles of solid dispersions (Fig. 5.8.) it can be seen that there is loss of moisture in 5% SD which is more than that of in 10%, 20% and 30%SDs.

5.2.4. Preparation of different forms of Carbamazepine and characterization by DSC

Carbamazepine was selected for the present study as mentioned before based on its polymorphic nature and after its preliminary analysis. Form I and dihydrate of carbamazepine have been prepared and analysed along with carbamazepine by DSC to find out the difference between all forms.

5.2.5. Preparation of Carbamazepine form I (triclinic) from form III (*p*-monoclinic)

Carbamazepine form I (triclinic) was prepared by heating commercial carbamazepine form III (*p*-monoclinic) at 170°C for 2 hrs.

5.2.6. Preparation of Carbamazepine dihydrate

Carbamazepine dihydrate was prepared by dissolving commercial Carbamazepine (4g) sample in distilled water (100mL) and kept it for stirring for 24 hrs. After that it was filtered using vacuum pump and dried at ambient temperature using filter paper (O'Brien et al., 2004). DSC profile of carbamazepine dihydrate exhibits a peak at 110-120°C which is absent in the DSC profile of commercial carbamazepine (form III). This can be seen in Fig.5.9.

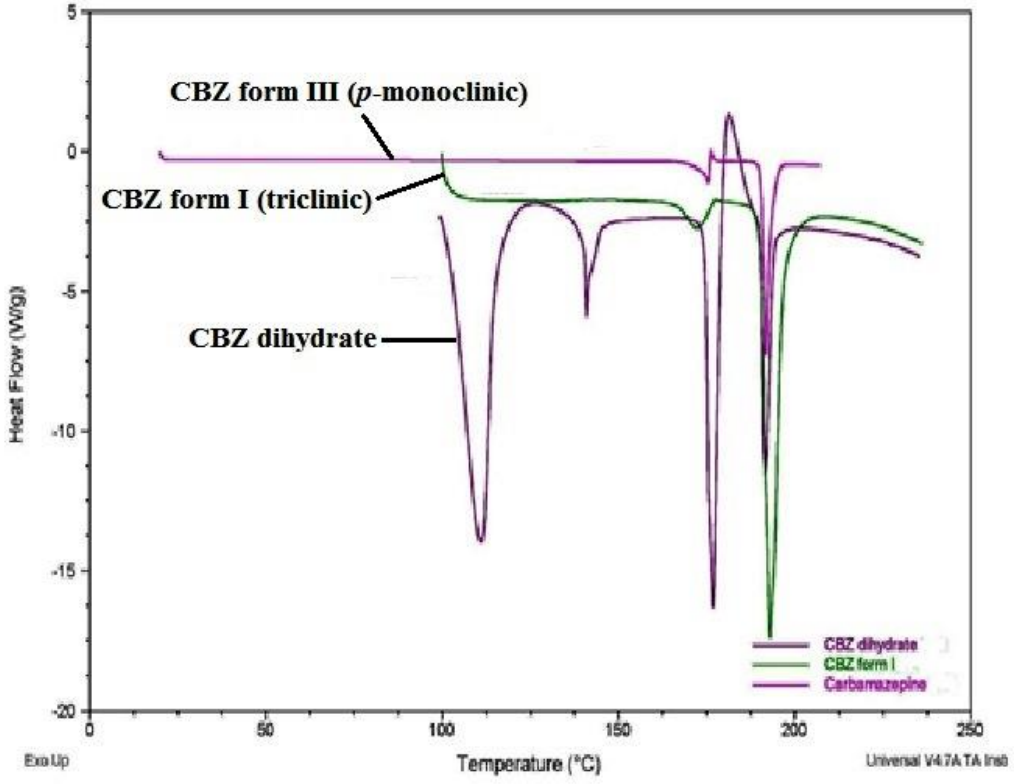

Fig.5.9. DSC profiles of CBZ form III, I and dihydrate

In the DSC of CBZ dihydrate there is a peak at 177°C which may be due to conversion into form I and its crystallization and again melting as form - I. These peaks resemble those reported in the literature (O'Brien et al., 2004).

5.2.7. Hot melt extrusion results

Hot melt extrusion of physical mixtures of various drug concentrations as 5%, 10%, 20%, and 30% was carried out. Extrusion of the 40% physical mixture was also attempted, but instead of an 'elastic' extrudate, it produced a liquid not suitable for extrusion. 5% Triethyl citrate (TEC) was used as a plasticizer using syringe pump ISCO model 100DX by Presearch with flow rate of 0.2175 ml/min.

From preliminary studies it was observed that Carbamazepine gets degraded above 140°C while rheology studies of Kollidon VA64 have shown it is stable to be up to 150°C. Based on these observations, temperature profile of 50-140°C was selected for hot melt extrusion process (Refer back to chapter 4 - Materials and methods showing whole temperature profiles).

Temperature profile :	Drug concentration in %				
50-140°C	5	10	20	30	40
Extrusion status	✓	✓	✓	✓	×
Successful – ✓ Unsuccessful - ×					

Table 5.1 HME results

5.2.8. Rheology results

Rheology studies were carried out as a preliminary analysis of APIs and polymers. Understanding of polymer stability at high temperatures along with API to further process it on hot melt extruder was essential. Based on results obtained using rheology testing, temperature ranges to be used in hot melt extrusion for preparation of solid dispersions have been selected. Along with temperature, plasticizing effect and shear thinning behavior have been indicated by rheology results.

Frequency sweeps are oscillatory tests performed at variable frequencies, with a strain amplitude of 3%, this having been found to be within the linear viscoelastic range from amplitude sweeps on the same material. Frequency sweeps have been used to investigate time-dependent shear behaviour since the frequency is the inverse of time.

5.2.9. Polymer analysis

Kollidon VA64 and Kollidon SR comparative study at 150°C

Rheological analysis of Kollidon VA64 and Kollidon SR has been carried out to find out suitability for use in the preparation of solid dispersions.

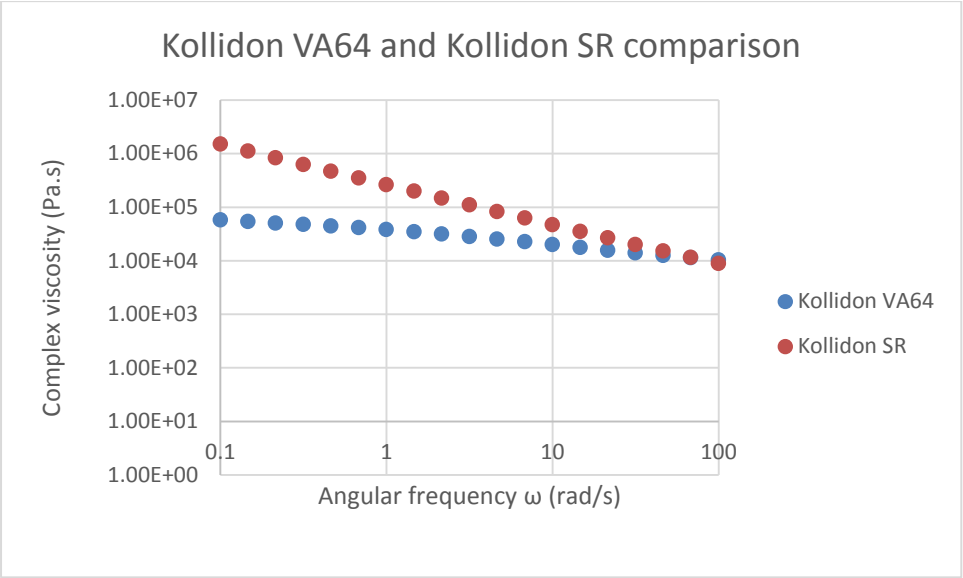

Fig.5.10. a. Complex viscosity Vs angular frequency: Kollidon VA64 SR

Kollidon VA64 exhibits much lower values of complex viscosity than Kollidon SR (Fig. 5.10.a.) allowing easier processing in the small twin screw extruder used in the present studies hence providing the rationale behind the selection of Kollidon VA64 over Kollidon SR for production of solid dispersions.

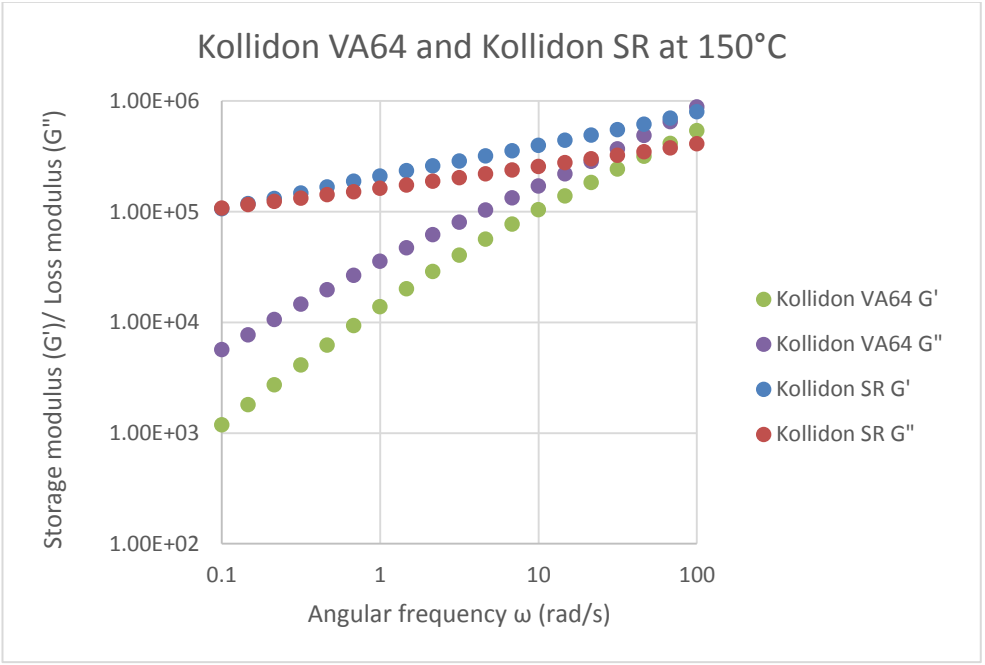

Fig. 5.10.b. G'/G" Vs angular frequency: Kollidon VA64 and Kollidon SR

From the Fig. 5.10.b. it can be clearly seen that increases in storage and loss moduli for both Kollidon VA64 and Kollidon SR with increase in angular frequency are apparent. At high shear rates the values are very similar for both polymers while at low shear rate the moduli values are much lower for Kollidon VA64.

From the results shown in Fig.5.10.a. and 5.10.b. it can said that Kollidon VA64 will be much easier to process than Kollidon SR due to its less viscous nature.

5.2.10. Rheological analysis of Kollidon VA64

Prior to formulation development, understanding of rheological properties of polymer to be used for the study was important. Rheological studies of Kollidon VA64 have been carried out to determine its thermal stability as well as to see effect of drug loading along with it which was significant information for using it on hot melt extrusions.

Time sweep test for Kollidon has been carried out. A graph of complex viscosity Vs time was plotted using Kollidon VA64 data which shows thermal stability of Kollidon VA64 (Fig. 5.11.).

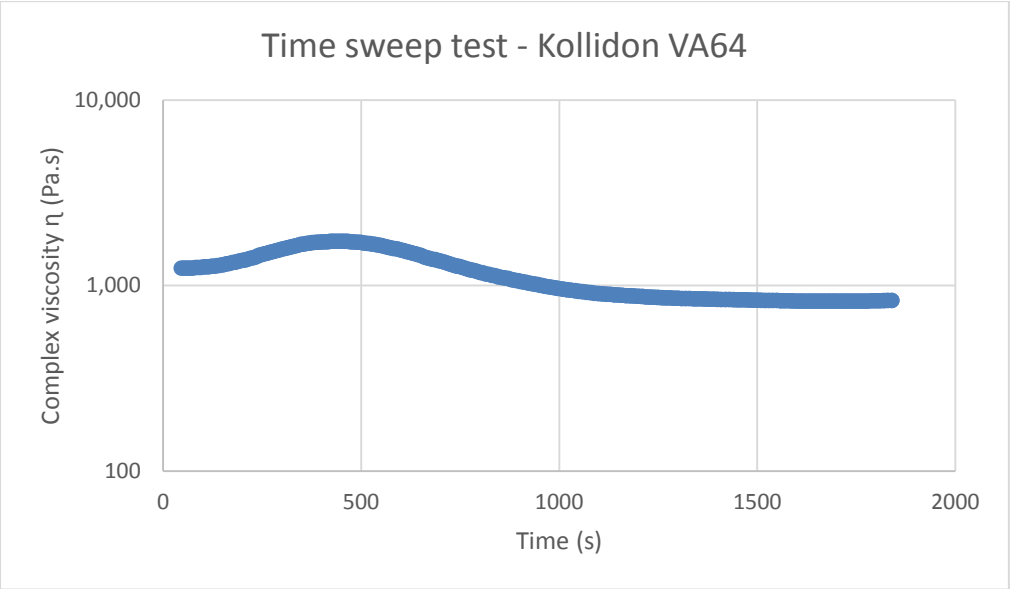

Fig.5.11. Time sweep test for Kollidon VA64

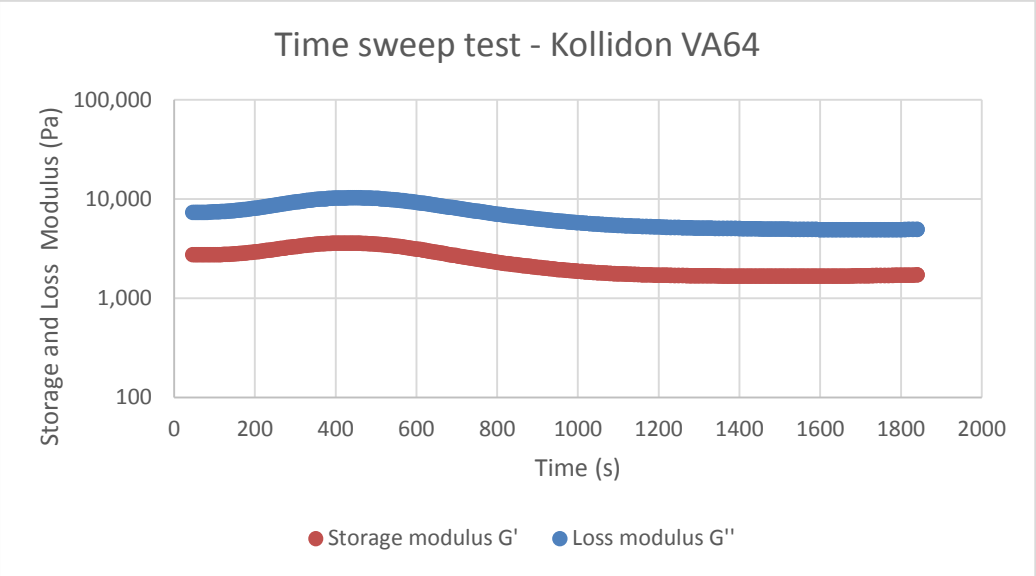

Fig. 5.12. Time sweep test (amplitude strain = 3%)

The plot shown in Fig. 5.12. is a time sweep which indicate that the material is stable in flow at this temperature even after half an hour. Since the material would stay at this temperature in the extruder for less than this time then we can say that VA64 is a stable material exhibiting little degradation.

5.2.11. Polymer and physical mixture analysis: study of effect of drug loading

Rheological analysis of 0%, 5%, 10%, 20% and 30% CBZ-VA64 physical mixtures has been carried out.

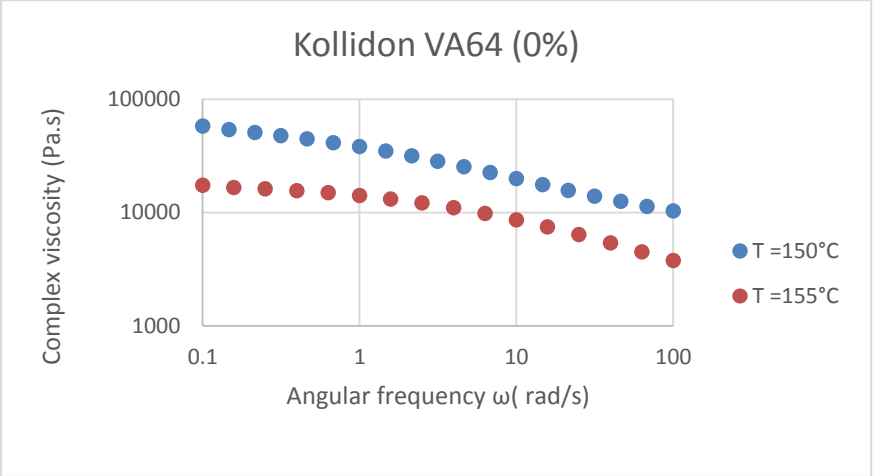

Fig. 5.13. Complex viscosity Vs angular frequency plot for pure Kollidon VA64

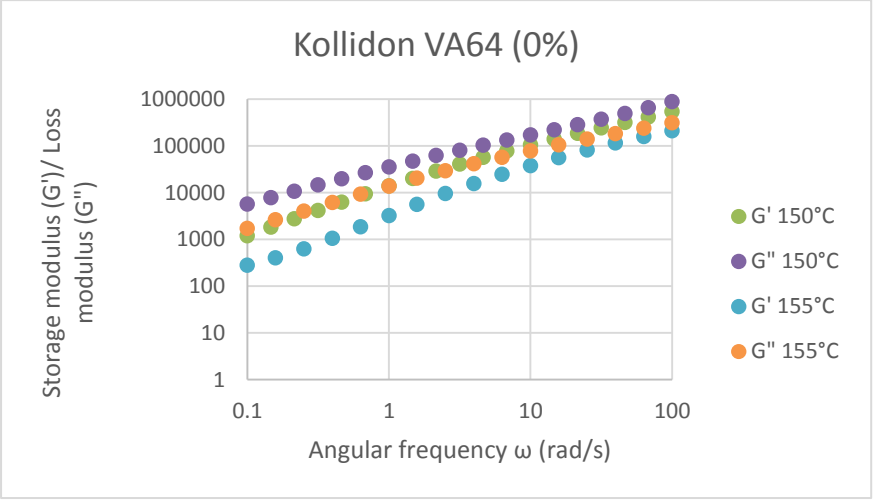

Fig. 5.14. G'/G" Vs angular frequency plot for pure Kollidon VA64

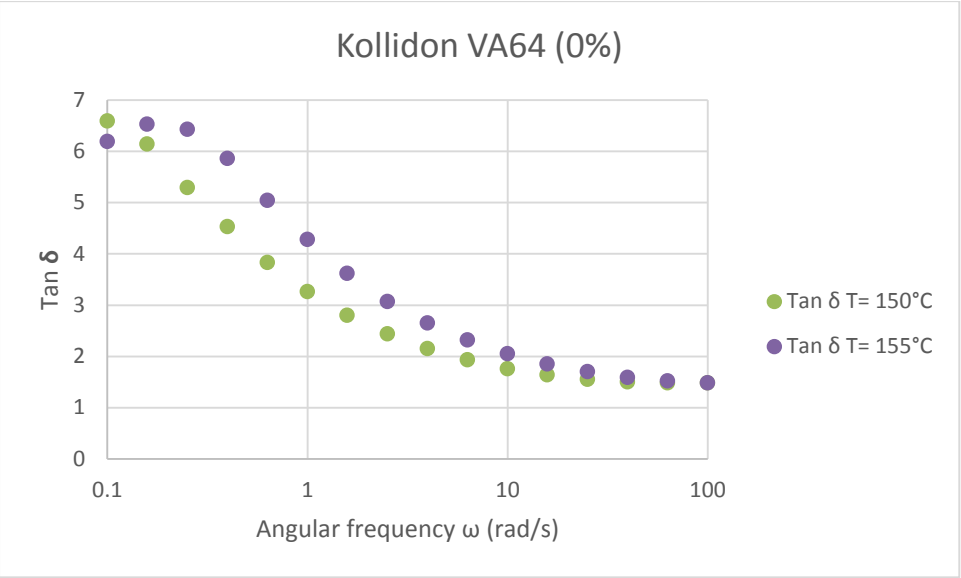

Fig. 5.15.Tan δ Vs angular frequency plot for pure Kollidon VA64

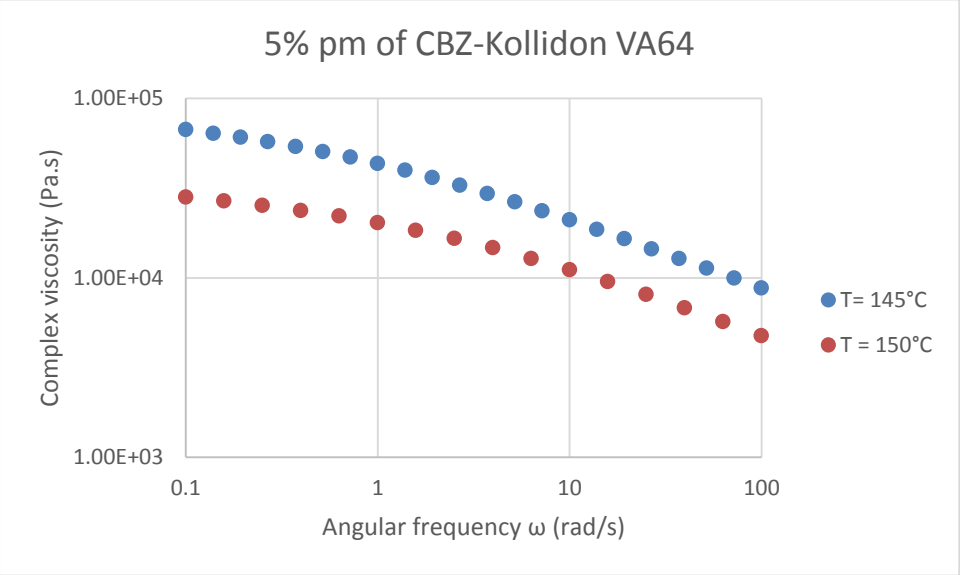

Fig. 5.16. 5% Complex viscosity Vs angular frequency

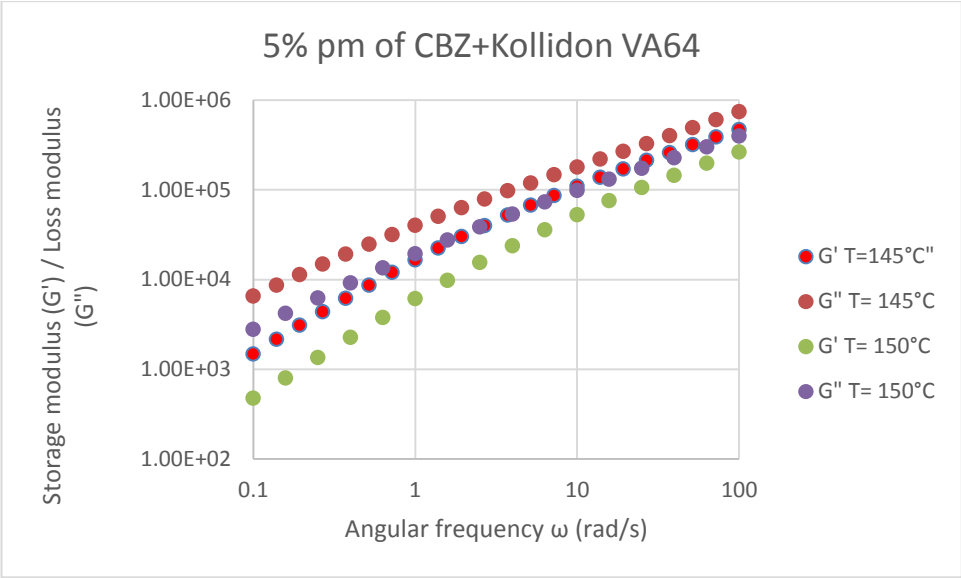

Fig. 5.17. 5% G'/G" Vs angular frequency

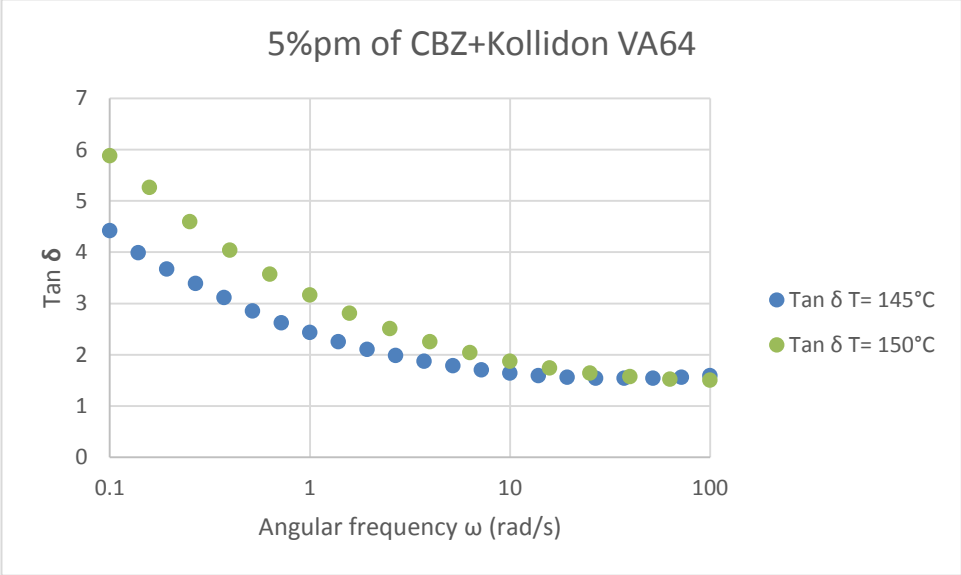

Fig. 5.18. 5% Tan δ Vs angular frequency

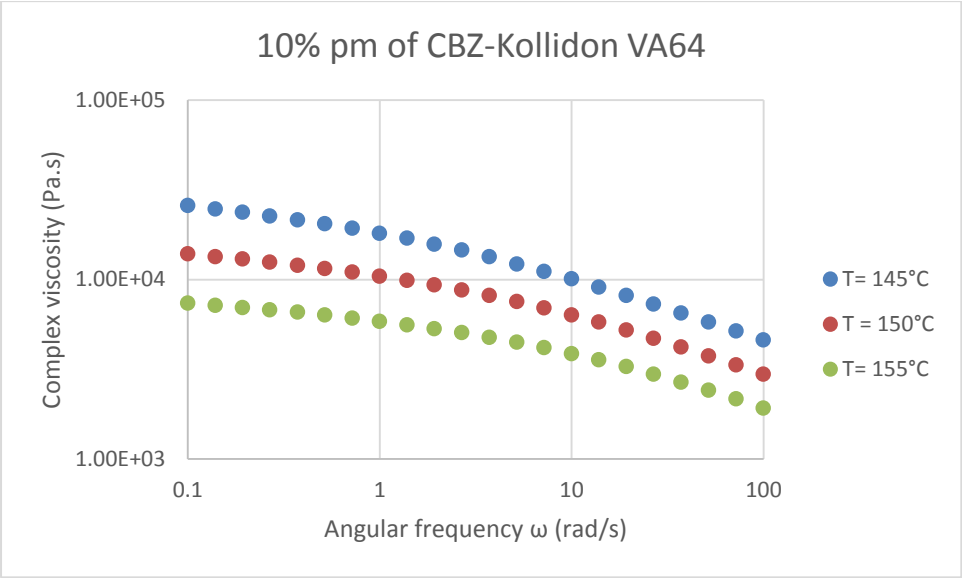

Fig. 5.19. 10% Complex viscosity Vs angular frequency

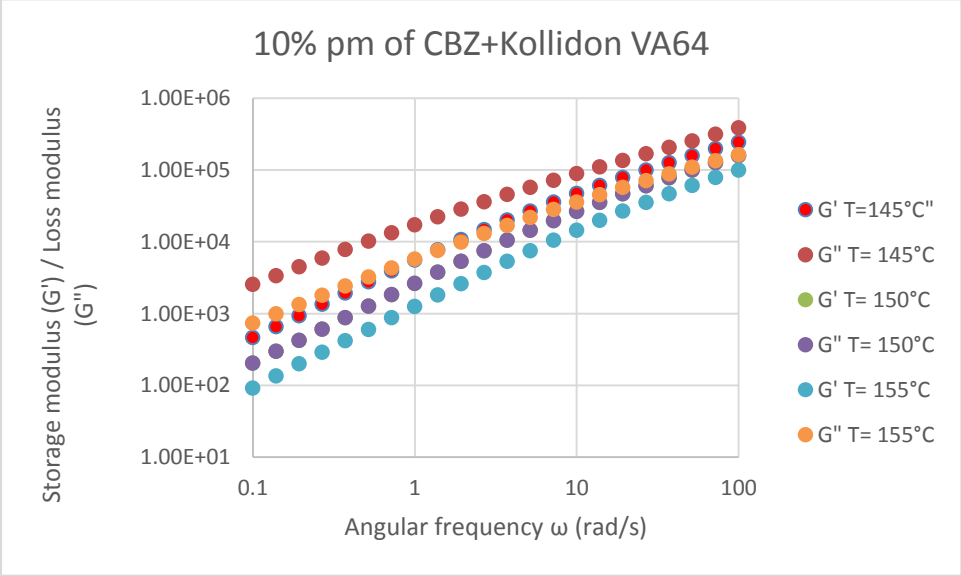

Fig. 5.20. 10% G'/G" Vs angular frequency

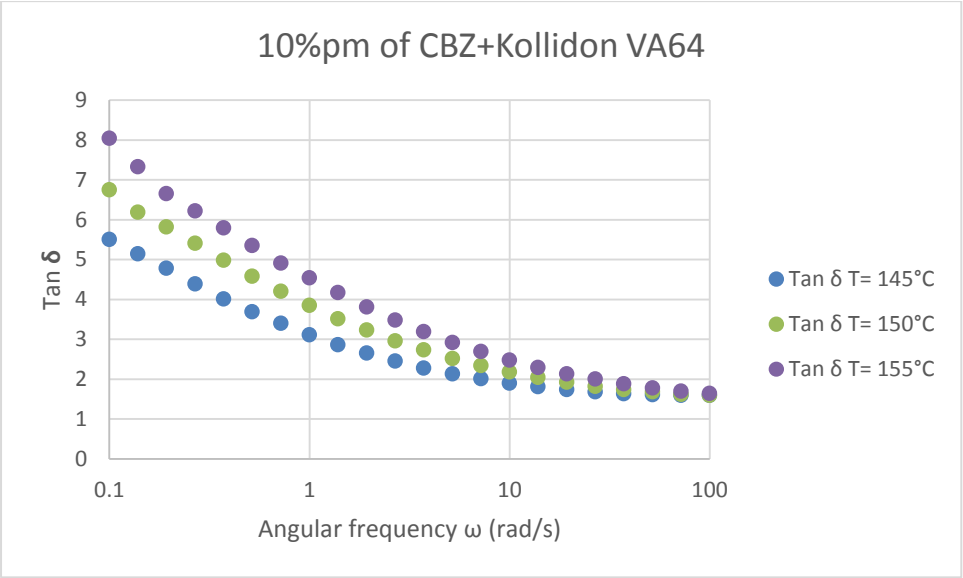

Fig.5.21. 10% Tan δ Vs angular frequency

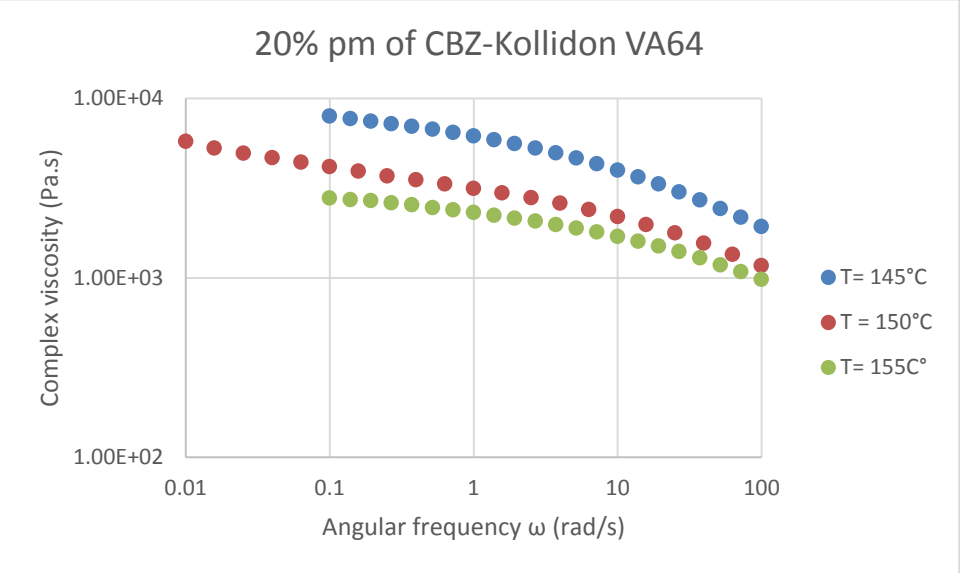

Fig. 5.22. 20% Complex viscosity Vs angular frequency

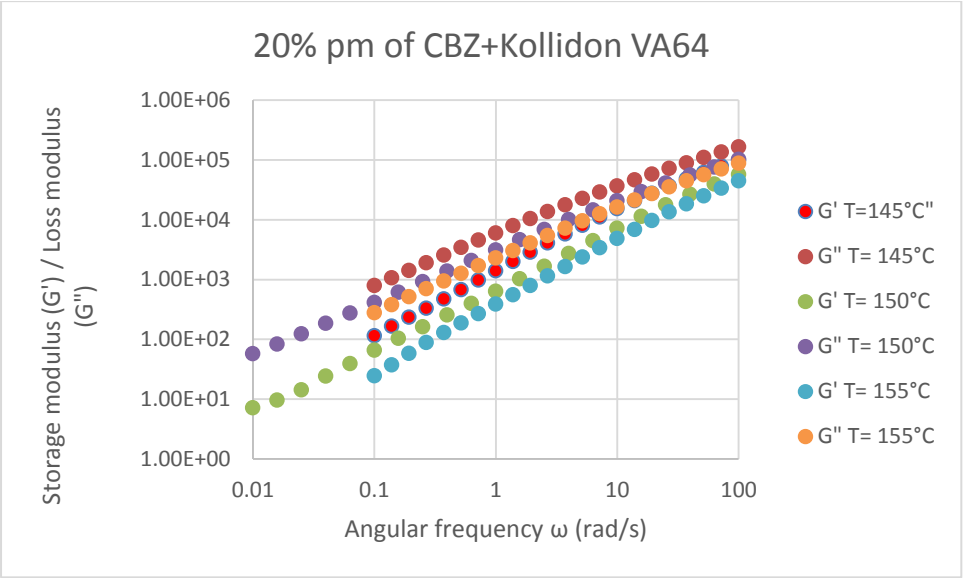

Fig. 5.23. 20% G'/G" Vs angular frequency

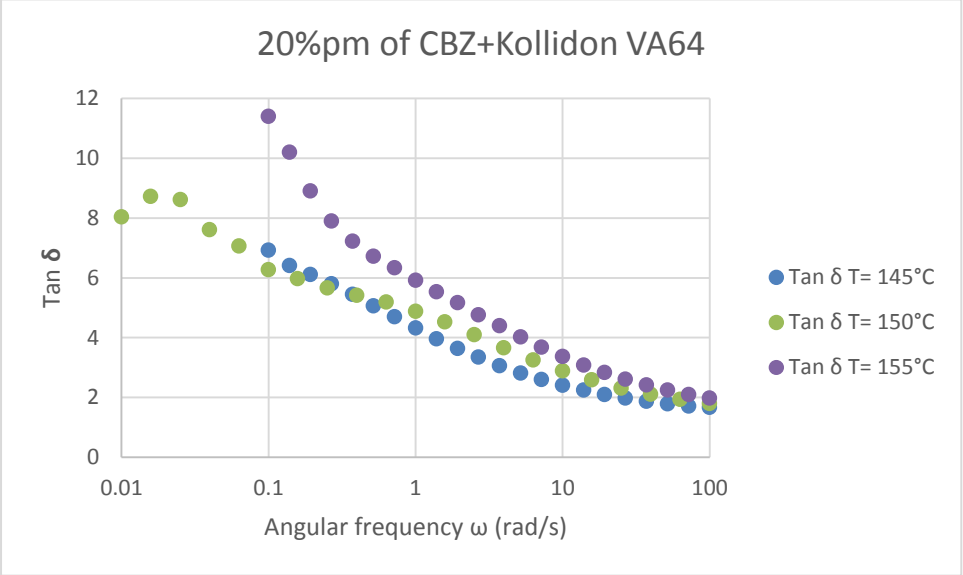

Fig.5.24. 20% Tan δ Vs angular frequency

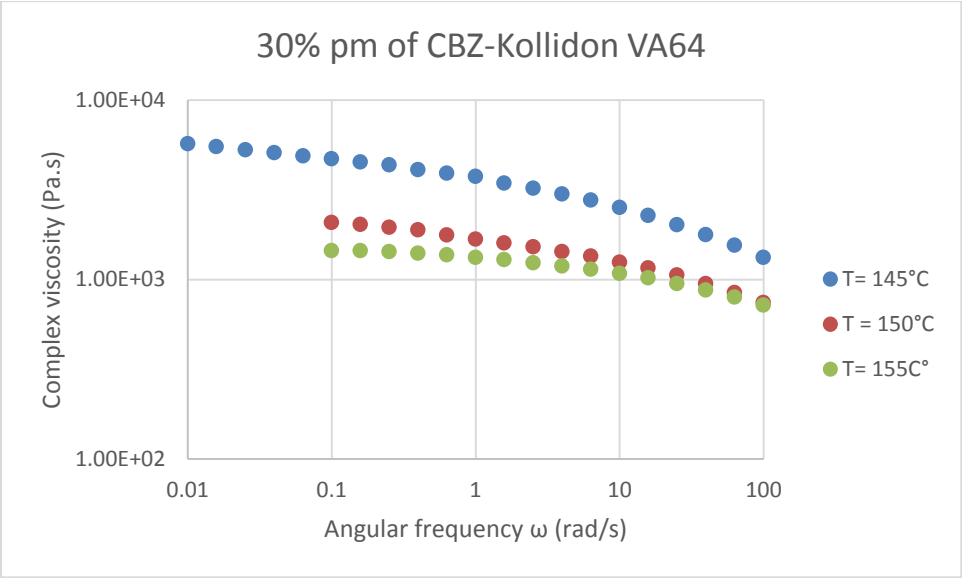

Fig.5.25. 30% Complex viscosity Vs angular frequency

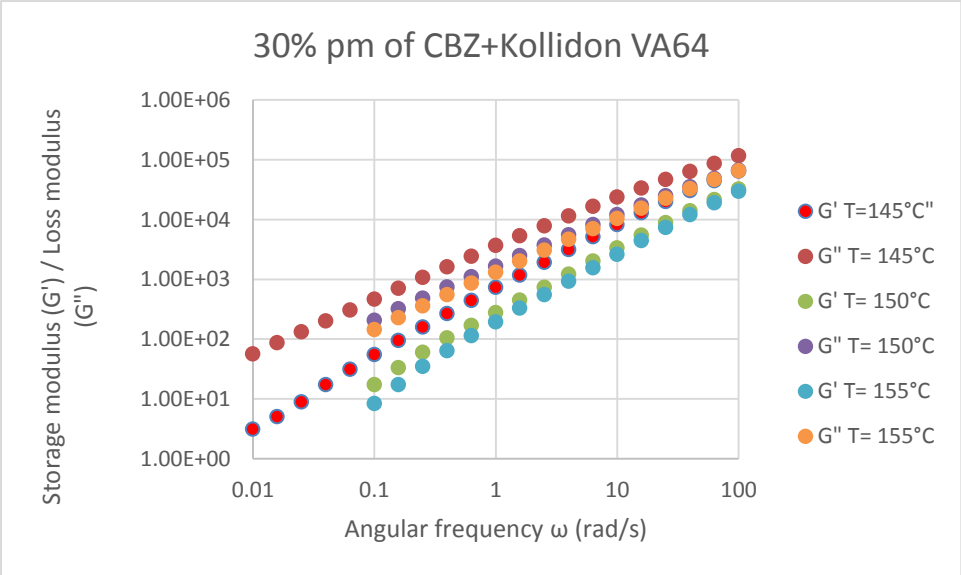

Fig.5.26. 30% G'/G" Vs angular frequency

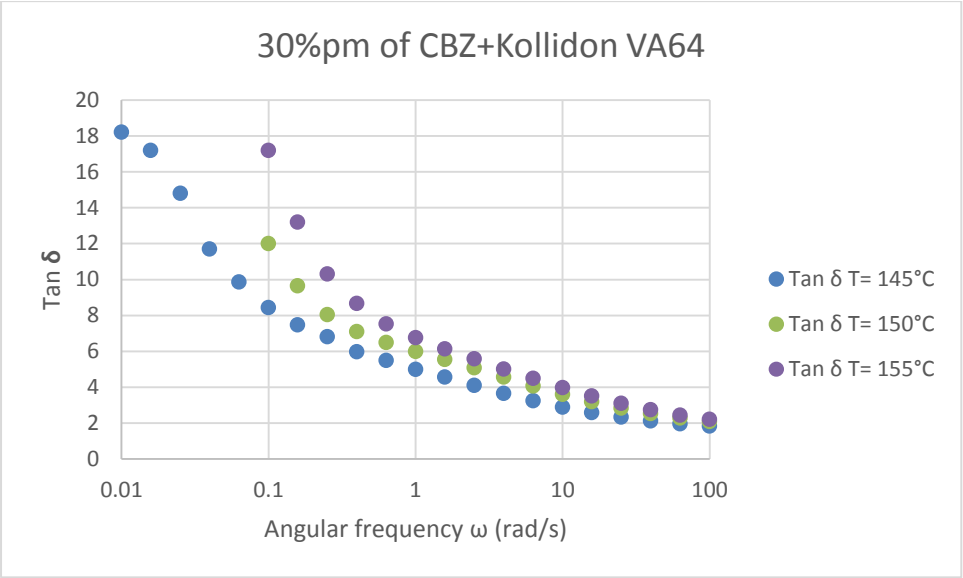

Fig.5.27. 30% Tan δ Vs angular frequency

Kollidon VA64 was found to be stable at 150°C by rheology studies. It can be seen from the plot (Fig. 5.13.) that with increase in angular frequency, there is decrease in complex viscosity. It indicates that as the shear rate goes up (increasing angular frequency) then viscosity reduces. In Fig. 5.14. it can be seen that the storage and loss moduli is comparatively high at 150°C with increase in angular frequency than for 155°C.Damping factor Tan δ has been found to be reduced with an increase in angular frequency) Fig.5.15.).

Fig. 5.16. shows reduction in complex viscosity of 5% pm of CBZ - Kollidon VA64 with increase in angular frequency and it is with faster rate at 145°C compared to 150°C while from Fig. 5.17. it can be observed that increasing angular frequency leads to increase in storage modulus and loss modulus values with higher rate at 145°C in similar way as that of with complex viscosity plot.

With increase in angular frequency damping factor was found to be reduced with a higher rate than at 145°C in case of 5% pm of CBZ - Kollidon VA64 (Fig.5.18.)

From Fig. 5.19. it can be seen that with increase in angular frequency there was decrease in complex viscosity in case of 10% pm of CBZ + Kollidon VA64 with higher rate of decrease at 145°C, 150°C and 155°C respectively. Results of G' and G" and damping factor decreasing with increase in angular frequency in case of 10%pm of CBZ+ Kollidon VA64 can be seen in Fig.5.20. and Fig.5.21. respectively.

In Fig.5.22. and 5.24. with increasing angular frequency, viscosity, storage modulus and loss modulus and damping factor were found to be reduced. Fig.5.23. shows results of storage modulus and loss modulus Vs angular frequency for 20%pm. Fig. 5.25., 5.26. and 5.27. indicate reduction in viscosity with increase in angular frequency, increase in storage and loss modulus with increasing angular frequency while tan δ has been found to decrease more rapidly with decrease in temperature as angular frequency increases. From all these results it can be said that Carbamazepine acts as a plasticizer itself.

Rheological analysis of Kollidon VA64 - CBZ blends/physical mixtures at 145°C have been carried out. Since Carbamazepine have reported to get degraded above 140°C, to study effect of drug loading and plasticizing effect along with polymer, 0 - 30% physical mixtures have been used for this analysis.

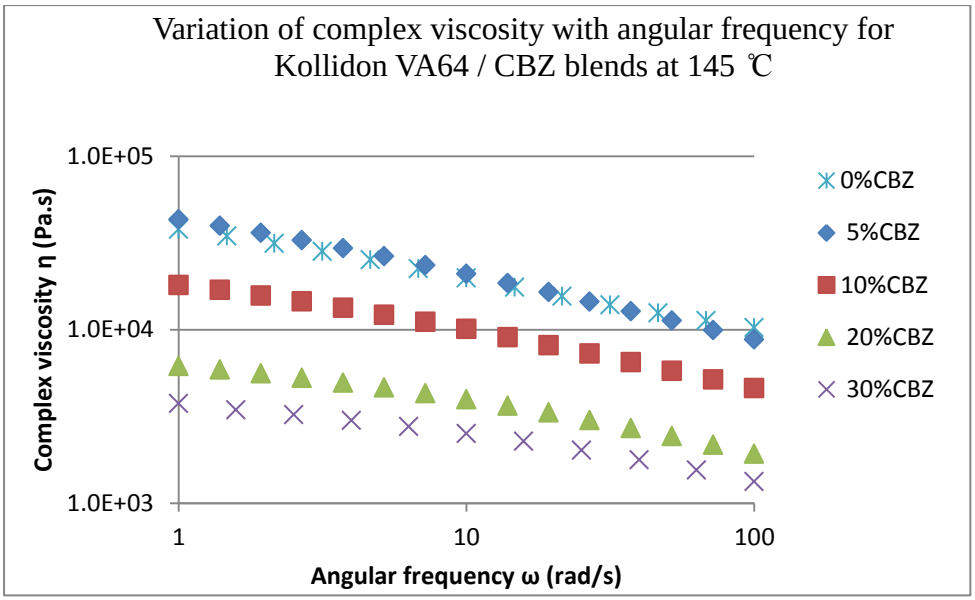

Fig. 5.28. Variation of complex viscosity with angular frequency for Kollidon VA64 / CBZ blends at 145℃

Rheology data (Fig. 5.28.) indicates that the complex viscosity decreases with increasing drug loading (5%, 10%, 20%, 30%) and with increase in angular frequency indicating a platicising effect of the drug upon the formulation as well as shear thinning behaviour.

5.2.12. Raman Spectroscopy results

The characterization of CBZ, Kollidon VA64, their physical mixtures and solid dispersions produced by HME was carried out by Raman spectroscopy using the Thermo Scientific DXR Smart Raman spectrophotometer. Raman spectra were converted into Grams format for interpretation using GRAMS 9.1 spectroscopy software (Thermo Fisher Scientific). While choosing picking parameters, peak height thresholds of 500, 30, 25, 10 and 5 were selected for CBZ, 30% SD, 20% SD, 10% SD and 5% SD respectively to get desirable peaks.

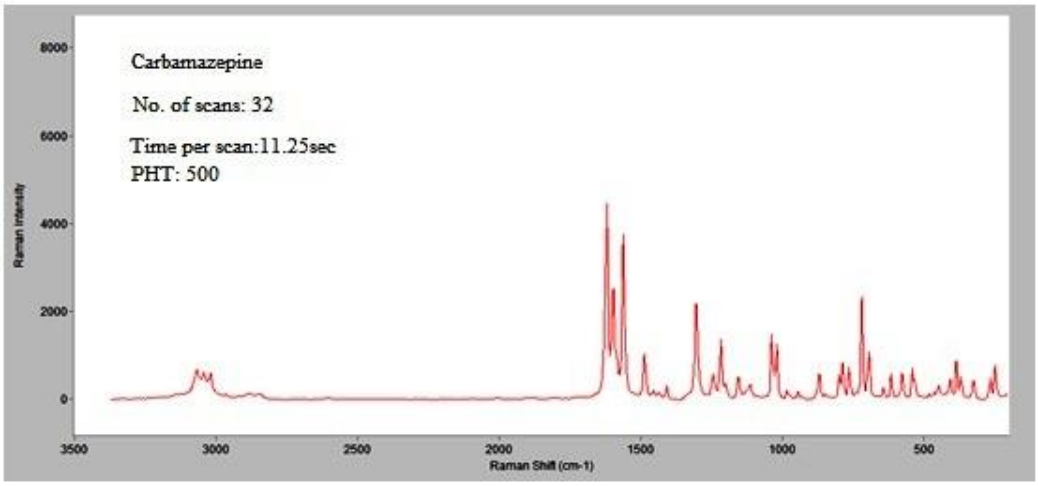

Fig 5.29. Raman spectrum of CBZ (*p*-monoclinic form)

No.	Raman shift $(cm)^{-1}$	Functional group assignment
1.	3065-3017	Aromatic v(C-H)
2.	1617	v(C=O)
3.	1559-1594	v(C-C)
4.	1483	β(C-H)
5.	1302	v(C-C)
6.	1243	β(C-H)
7.	1215	β(N-H), β(O-H) in carboxamide gr.
8.	1034, 1018	v(C-C), β(N-H) in carboxamide gr.
9.	785	β(O-H) , β(N-H), β(C-H) in carboxamide gr.
10.	716	β(N-H), β(O-H) in carboxamide gr.
11.	692	β(O-H) , β(N-H), β(C-H) in carboxamide gr.
12.	537	B(C-O) , β(N-H), β(O-H) in carboxamide gr.

Table 5. 2. Functional group assignment of Raman spectra of CBZ (*p*-monoclinic form) (v – stretching, β – bending vibrations) (Czernicki and Baranska, 2013)**.**

Raman spectrum of CBZ (Fig. 5.29.) showed prominent absorption bands of aromatic C-H stretching at 3065-3017 cm^{-1} and a sharp peak at 1617 cm^{-1} for the C=C stretching of the amide group. The C-C stretching vibrations responsible for strong peaks at 1559- 1594 cm^{-1} and weak peaks at 1035 and 1018 cm^{-1} in carboxamide group. These characteristic peaks are found to be in resemblance with those reported in the literature (Czernicki and Baranska, 2013).

Fig. 5.30. and 5.31. show comparison of Raman spectra of physical mixtures of CBZ-Kollidon VA64 and Raman spectra of CBZ-Kollidon VA64 SDs respectively. There was some shifting of wavenumber in the spectra as there might be interaction between the API and polymer. Appearance of characteristic peaks with reduced intensity indicates the decrease in crystallinity of CBZ in SDs which can be seen listed in the table 5.2.

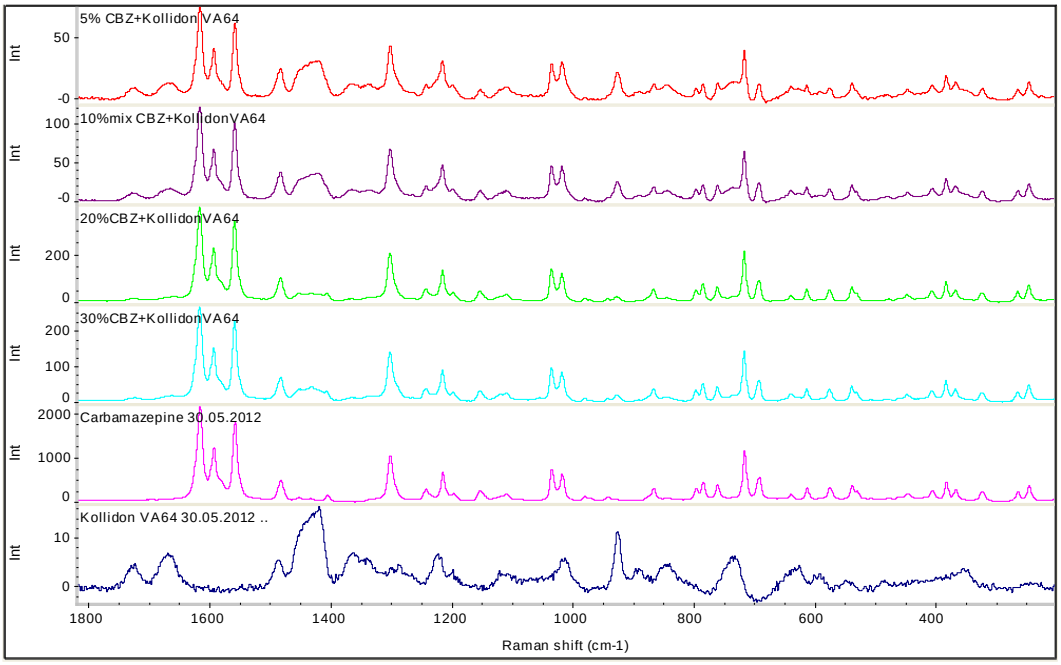

Fig 5.30. Comparison of physical mixtures of CBZ and VA64 with CBZ

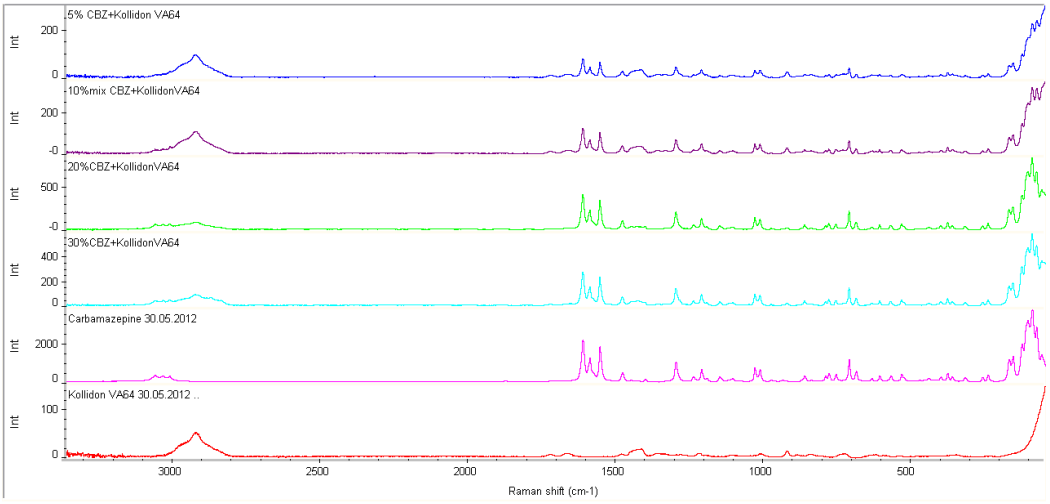

Fig. 5.31. Comparison of solid dispersions of CBZ and Kollidon VA64 with CBZ

No.	Raman shift $(cm)^{-1}$	Group	↓ indicates decrease in wavenumber							
	CBZ		5%		10 %		20%		30%	

(v – stretching, β - bending vibrations)			**PM**	**SD**	**PM**	**SD**	**PM**	**SD**	**PM**	**SD**
1.	3065-3017	Aromatic v(C-H)	2222				PM			
2.	1617	v(C=O)	1617	1613 ↓	1619	1613 ↓	1620	1613 ↓	1620	1614 ↓
3.	1559-1594	v(C-C)	1560	1555 ↓	1596	1590 ↓	1597	1590 ↓	1597	1591 ↓
4.	1483	β(C-H)	1485	1484 ↓	1486	1483 ↓	1486	1483 ↓	1486	1482 ↓
5.	1302	v(C-C)	1302	1298 ↓	1304	1298 ↓	1306	1298 ↓	1305	1299 ↓
6.	1243	β(C-H)	-	-	-	-	-	-	-	-
7.	1215	β(N-H), β(O-H) in carbo	1215	1215	1218	1211 ↓	1218	1211 ↓	1218	1212 ↓

		xamide gr.								
8.	1034, 1018	v(C-C), β(N-H) in carboxamide gr.	1017	1011↓	1036,1019	1027, 1011↓	1037,1021	1029, 1011↓	1037,1021	1030, 1013↓
9.	785	β(O-H) , β(N-H), β(C-H) in carboxamide gr.	-	-	-	-	787	782↓	788	783↓
10.	716	β(N-H), β(O-H) in carboxamide gr.	733	729↓	719	711↓	719	711	719	712

11.	692	β(O-H) , β(N-H), β(C-H) in carboxamide gr.	-	-	694	-	695	-	695	688
12.	537	β (C-O) , β(N-H), β(O-H) in carboxamide gr.	-	-	-	-	540	-	540	538

Table 5. 3. Comparison of Raman frequencies of CBZ with physical mixtures and solid dispersions

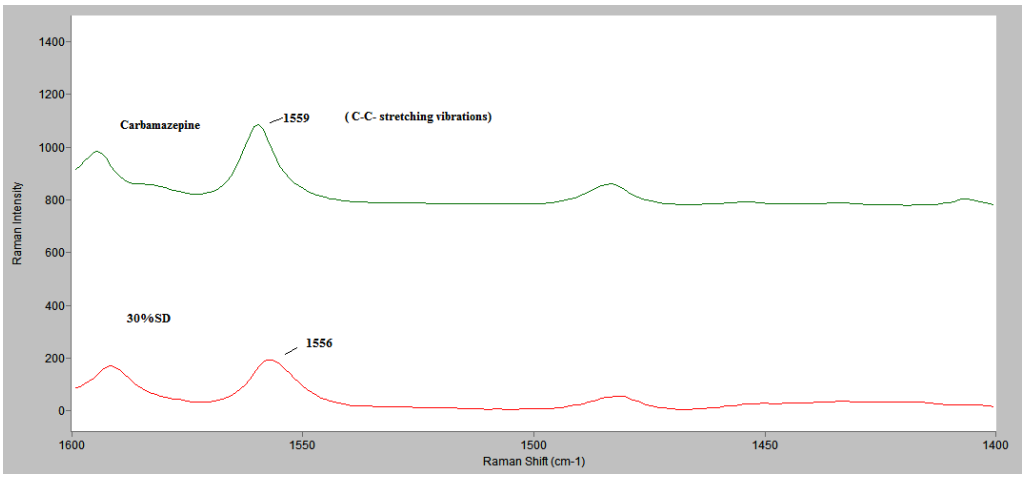

Fig. 5.32. Differentiation between CBZ and SD by Raman Spectroscopy

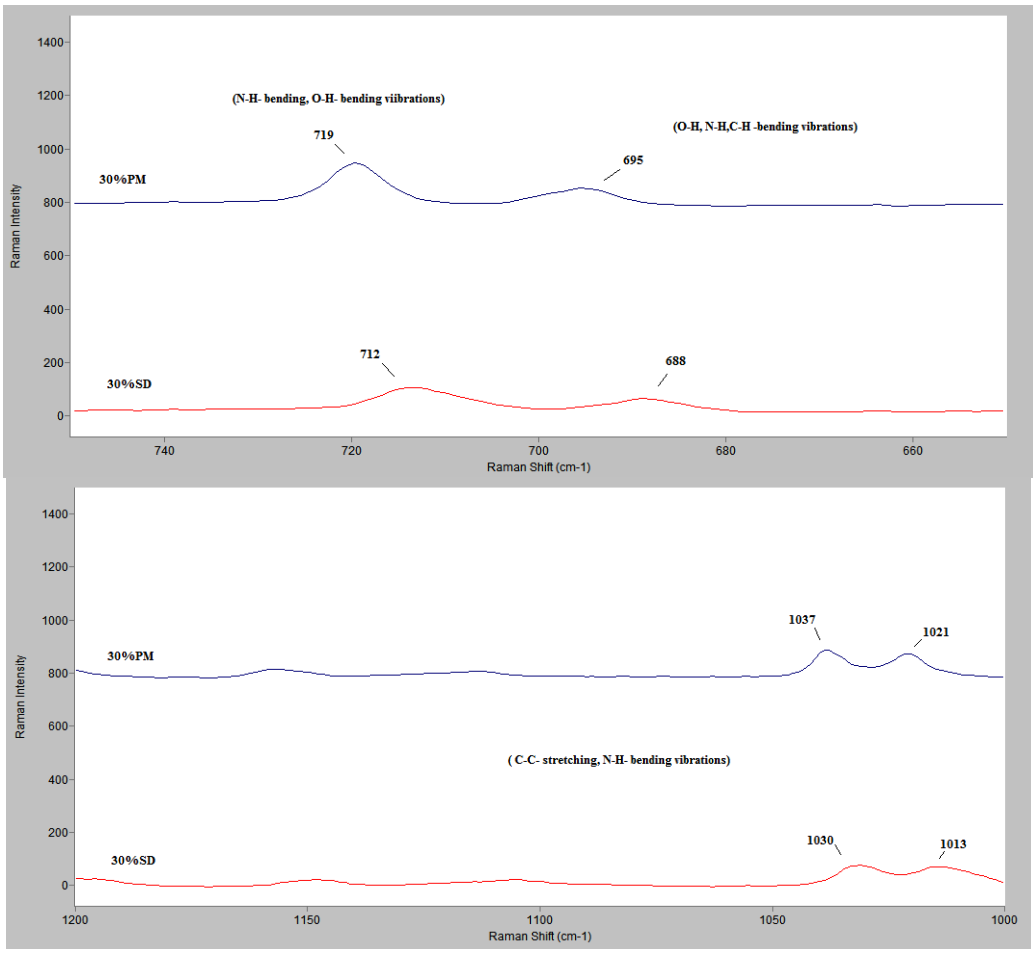

Fig. 5.33. Differentiation between PM (up) and SD (down) (30%) by Raman Spectroscopy

Fig.5.32. shows the difference between CBZ and SD (30%) where decrease in wavenumber for C-C stretching can be seen.

Fig.5.33. shows difference between peaks of C-C stretching and N-H bending in case of 30% PM and 30% SD after HME. In the Raman spectra of 5% and 10% SDs the characteristic absorption bands of CBZ were not prominent. The characteristic peak of CBZ might overlap between the absorption bands of the Kollidon VA64. While in the Raman spectra 20% and 30% SDs the characteristic peaks of CBZ with reduced intensity can be seen in the region of 1600-1000 cm^{-} which can be an indication of reduced crystallinity of CBZ tending towards amorphous form.

5.2.13. Calibration curve for Carbamazepine concentration in solid dispersions of Carbamazepine and Kollidon VA64 from Raman spectroscopic results

Calibration curve has been generated for Carbamazepine concentration in solid dispersions of Carbamazepine and Kollidon VA64 using the full range Raman spectra of 0 - 30% SDs using TQ Analyst by Thermoscientific. A partial least square method with 3 factors was found to give correlation coefficient value of 0.9844. This can be seen in Fig. 5.34.

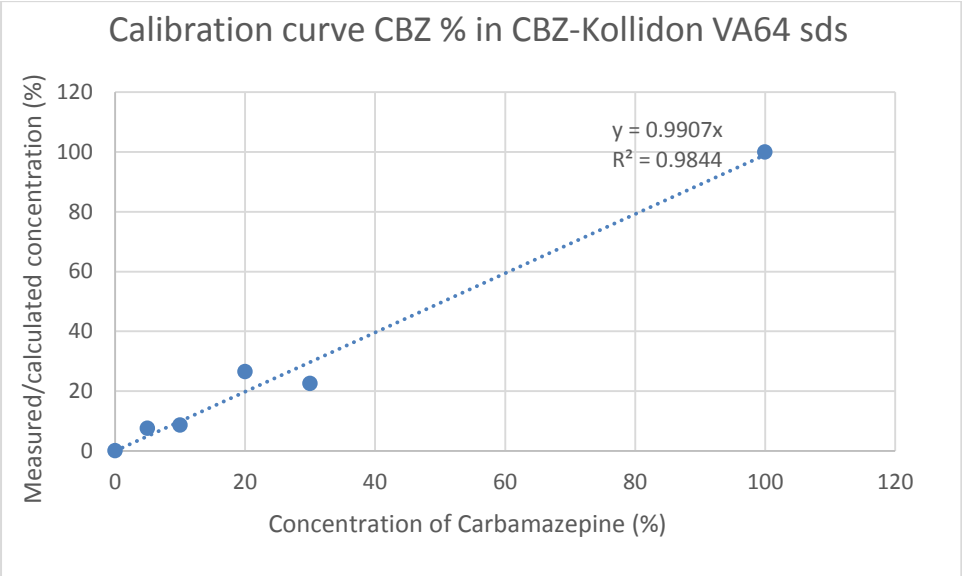

Fig. 5.34. Calibration curve - CBZ concentration in CBZ - Kollidon VA64 SDs

This clearly shows that Raman is a suitable technique for monitoring of CBZ levels in solid dispersions of CBZ- Kollidon VA64.

5.2.14. Fourier transformed infra-red spectroscopy (FTIR) results

To further understand chemical interaction between functional groups of the molecules, FTIR analysis was carried out.

Functional group assignment has been carried out based on the peaks corresponding to the functional groups as per FTIR values.

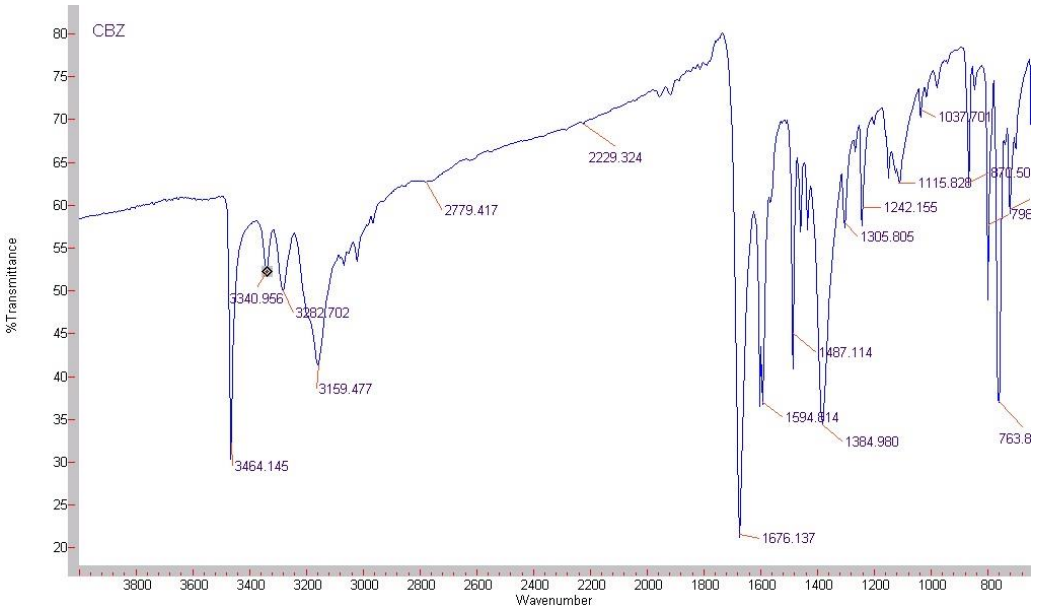

Fig.5.35. FTIR spectra of CBZ

Sr. No.	v $(cm)^{-1}$	Functional group assignment
1.	3464	-N-H stretching
2.	3340	-C-H stretching
3.	3159	Aromatic-C-H stretching
4.	1676	-C=O stretching

Table 5.4. Functional group assignment of FTIR spectra of CBZ

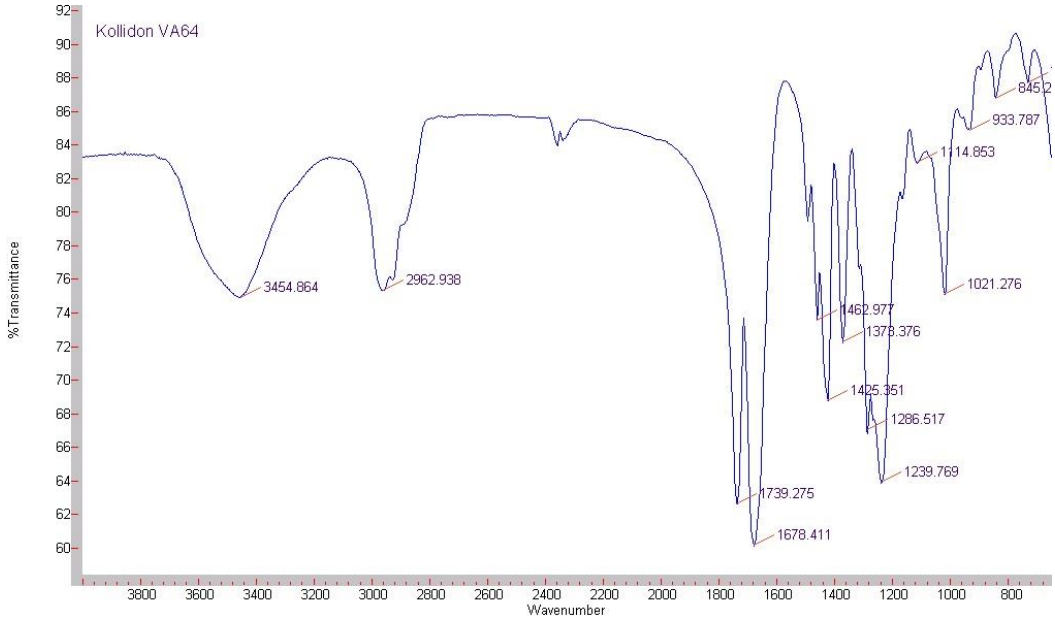

Fig.5.36. FTIR spectra of Kollidon VA64

Sr. No.	**v $(cm)^{-1}$**	**Functional group assignment**
1.	3454	Aromatic -OH stretching.
2.	2962	Aliphatic -C-H stretching
3.	1739	-C=O stretching
4.	1678	-C=O stretching

Table 5.5. Functional group assignment of FTIR spectra of Kollidon VA64

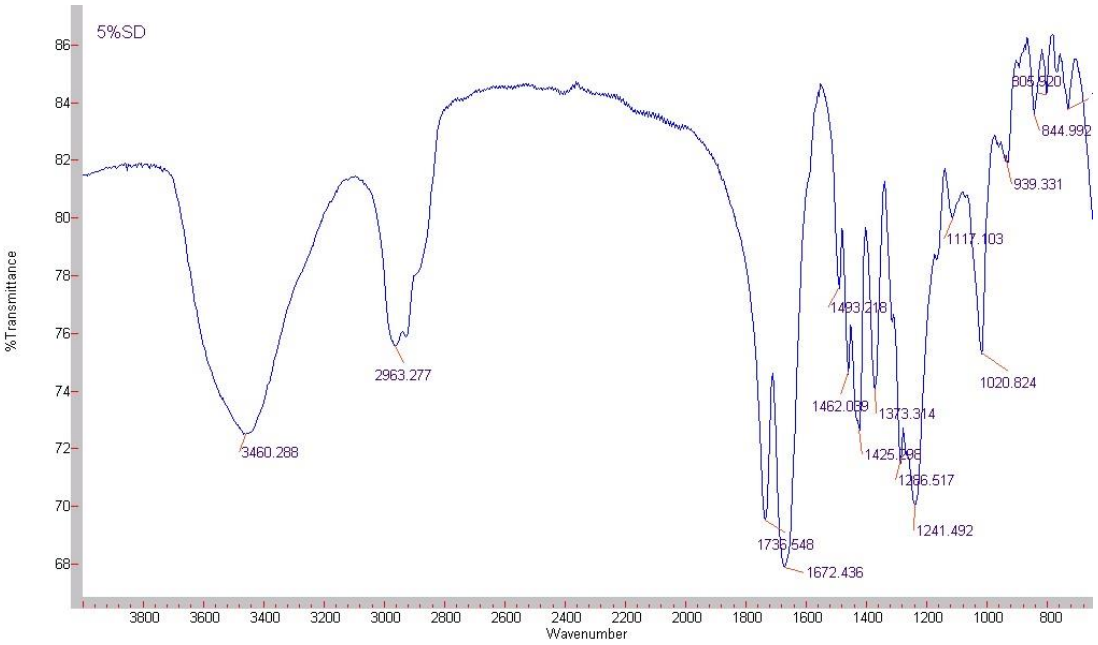

Fig.5.37. FTIR spectra of 5% SD

Sr. No.	v $(cm)^{-1}$	Functional group assignment
1.	3460	Aromatic -OH stretching.
2.	2963	Aliphatic -C-H stretching
3.	1736	Aromatic -C=O stretching

Table 5.6. Functional group assignment of FTIR spectra of 5% SD

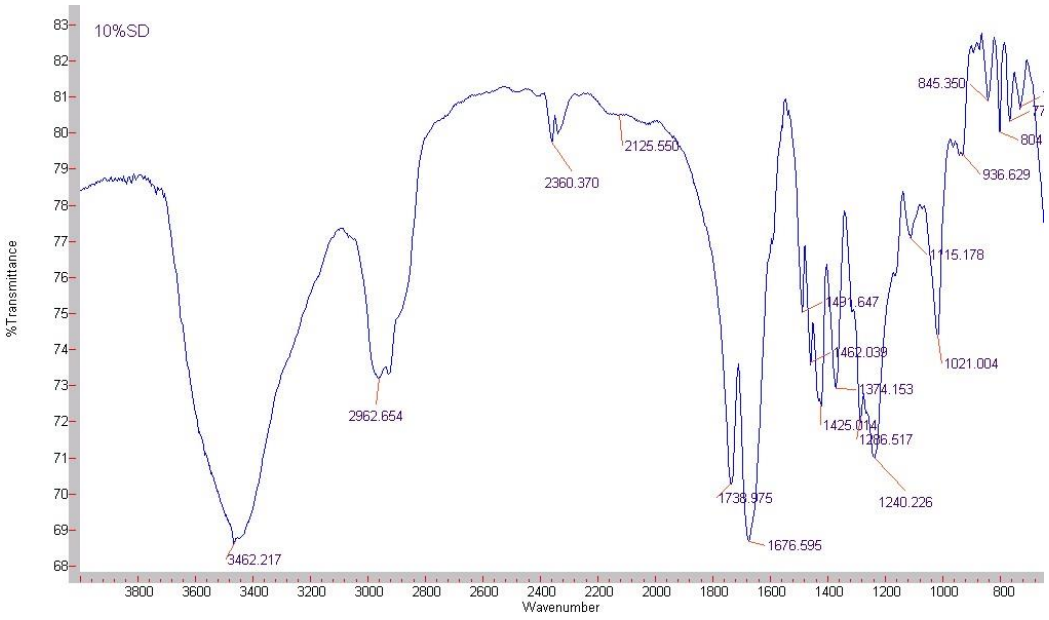

Fig.5.38. FTIR spectra of 10% SD

Sr. No.	v $(cm)^{-1}$	Functional group assignment
1.	3462	Aromatic O-H stretching
2.	2962	-CH stretching.
3.	1738	C=O stretching
4.	1676	Aromatic -C=C stretching.

Table 5.7. Functional group assignment of FTIR spectra of 10% SD

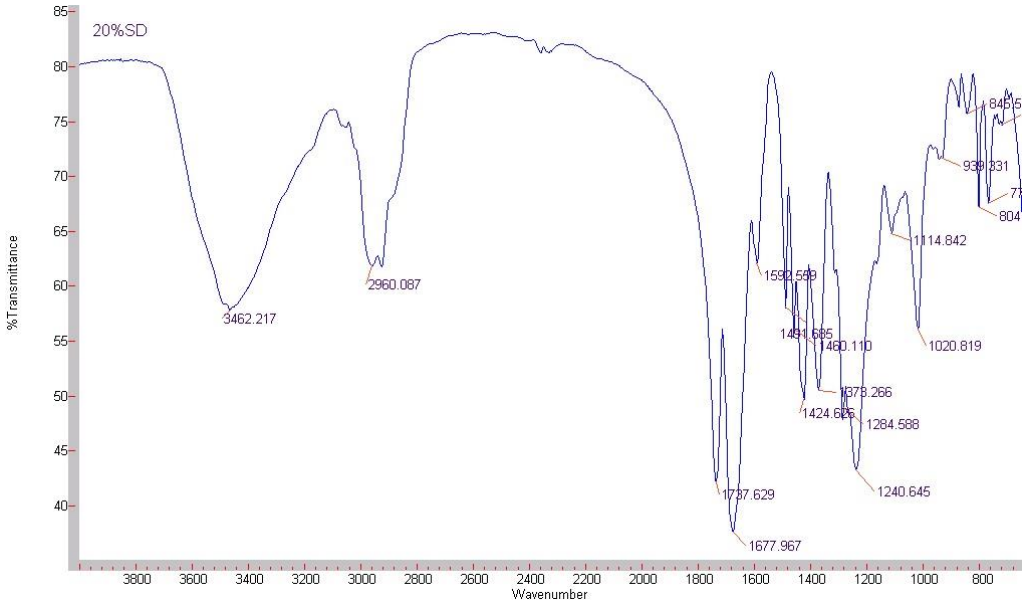

Fig.5.39. FTIR spectra of 20% SD

Sr. No.	v $(cm)^{-1}$	Functional group assignment
1.	3462	Aromatic O-H stretching.
2.	2960	Aliphatic -C-H stretching
3.	1737	C=O stretching
4.	1677	Aromatic C=C stretching

Table 5.8. Functional group assignment of FTIR spectra of 20% SD

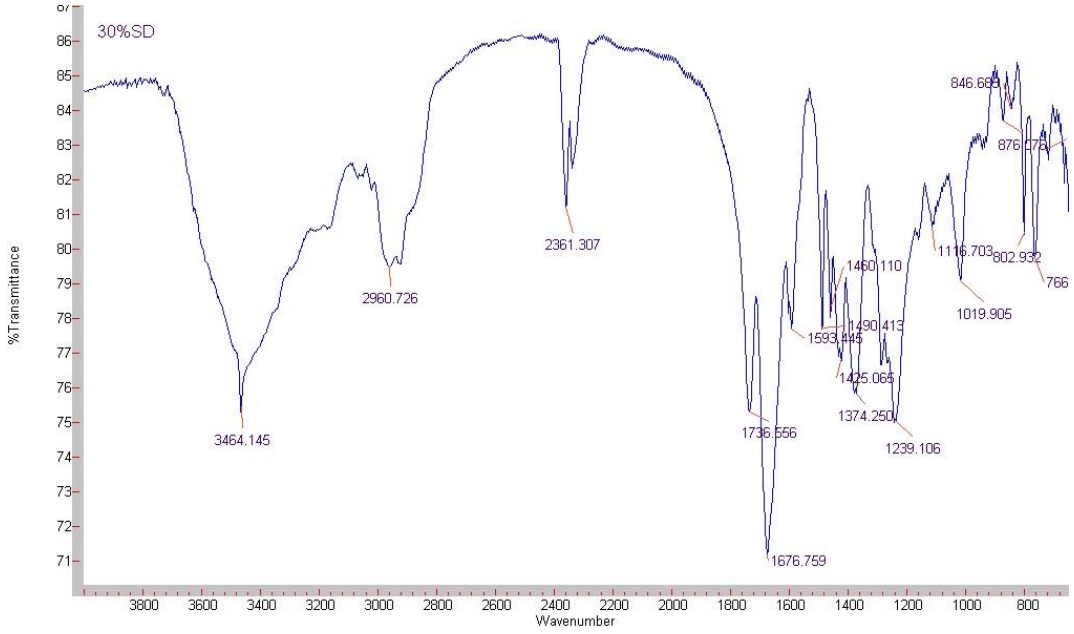

Fig.5.40. FTIR spectra of 30% SD

Sr. No.	v $(cm)^{-1}$	Functional group assignment
1.	3464	Aromatic N-H stretching.
2.	2960	Aromatic C-H stretching
3.	1736	Aromatic C=O stretching
4.	1676	Aromatic C=C stretching

Table 5.9. Functional group assignment of FTIR spectra of 30% SD

In the FTIR spectra of 5%, 10%, and 20% SDs, there are no prominent peaks of CBZ since it was in less concentration (Fig. 5.35. to Fig. 5.39.). While in 30% SD, there is prominent peak of Aromatic C-H str. started coming out at 1592 cm^{-}. There is also a sharp peak at 3464 cm^{-1} in spectra of 30% SD (Fig.5.40.) which may be because of intramolecular hydrogen bonding of NH_2 of CBZ with nitrogen or C=O of acetate or pyrrolidone of Kollidon VA64 which indicates formation of solid dispersion (Czernicki and Baranska, 2013).

5.2.15. Powder X-ray diffraction results

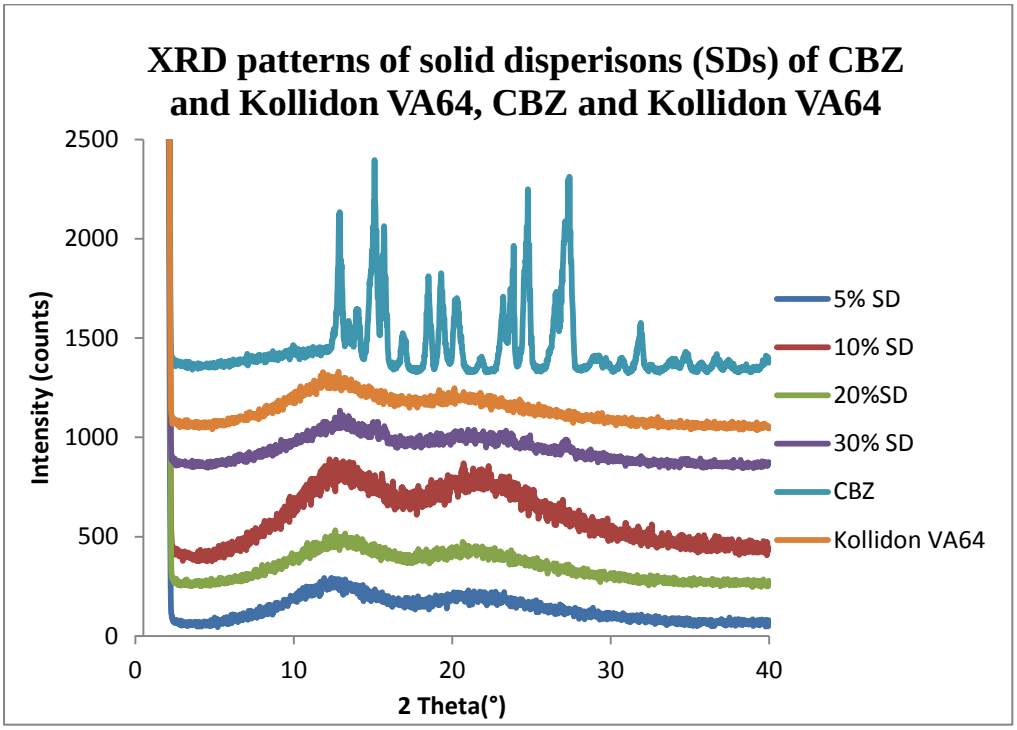

Fig.5.41. X-Ray diffraction patterns of CBZ, Kollidon VA64 and solid dispersions (5%, 10%, 20% and 30%)

The solid state of CBZ and its solid dispersions with Kollidon VA64 were studied by PXRD. The powder diffraction patterns of pure CBZ (Fig. 5.41.) showed characteristic high intensity diffraction peaks at 2θ values of 15.04°, 15.38°, 15.87°, 27.38°, 27.60°, and 32.10° which matched with previously reported value of CBZ (Krahn and Mielck, 1987; Lowes et al., 1987). The powder diffraction patterns of all the SDs did not show peaks corresponding to CBZ which indicate the conversion into amorphous form. This clearly indicates PXRD results have been able to confirm conversion of crystalline Carbamazepine in to amorphous solid dispersions along with Kollidon VA64. This analysis also gets supportive results from the indications of amorphous

form due to the differences in intensities and Raman shifts (wavenumbers) from Raman spectroscopic analysis.

To summarise, results obtained from preparation and characterization of solid dispersions of CBZ - Kollidon VA64 have found to be significant. The objective of the work was to get amorphous solid dispersions from crystalline active pharmaceutical ingredient along with the polymer. From DSC, XRD and Raman spectroscopic analysis, it has been found that amorphous solid dispersions have been formulated using hot melt extrusion with advantages such as a green and continuous process. Raman spectroscopy have been found superior to other analytical techniques in terms of quantification of CBZ in solid dispersions by TQ analyst generated correlation coefficient results (refer back to calibration curve results Fig. 5.34.). Based on the results obtained from these studies, we can conclude that Raman spectroscopy will be suitable as a PAT tool for in-line quantification of solid dispersions using other polymer combinations.

5.3. Preparation and characterisation of solid dispersions of Carbamazepine and Soluplus

5.3.1. DSC results

DSC analysis of Carbamazepine, Soluplus and Carbamazepine - Soluplus physical mixtures was carried out. Physical mixtures were prepared by using mortar and pestle in concentrations 5%w/w, 10%w/w, 20%w/w and 30%w/w. Thermal profiles were generated in the range of 20˚C - 220˚C using a Q2000 calorimeter from TA Instruments. Temperature calibration was performed using an indium metal standard supplied with the instrument at the respective heating rate. Accurately weighed samples (3-5mg) were placed in aluminium pans using similar empty pans as a reference. A heating rate of 10˚C min^{-1} was employed. Measurements were carried out in an inert atmosphere by purging nitrogen gas at the flow rate of 50 mL/min. The acquired thermo grams were analysed with TA Instruments Universal Analysis 2000 software.

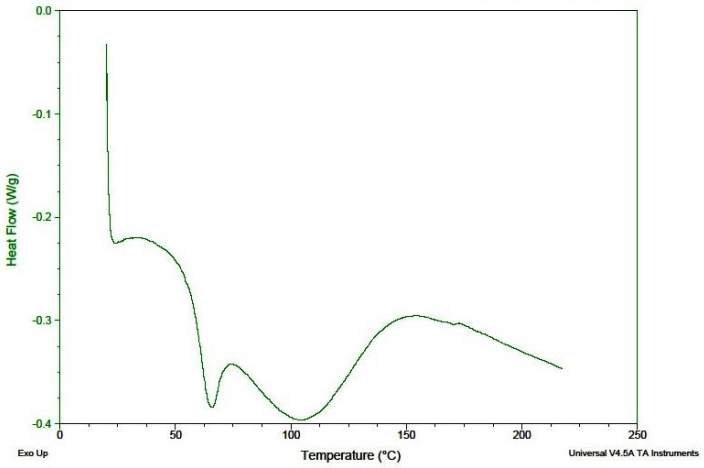

Fig. 5.42. DSC profile of Soluplus

The DSC thermogram of Soluplus shows an endothermic event at around 52˚C and reaching its peak at 75˚C (Fig.5.42.) which indicates transition of the polymer from the glassy to the rubbery state (Djuris et al., 2013).

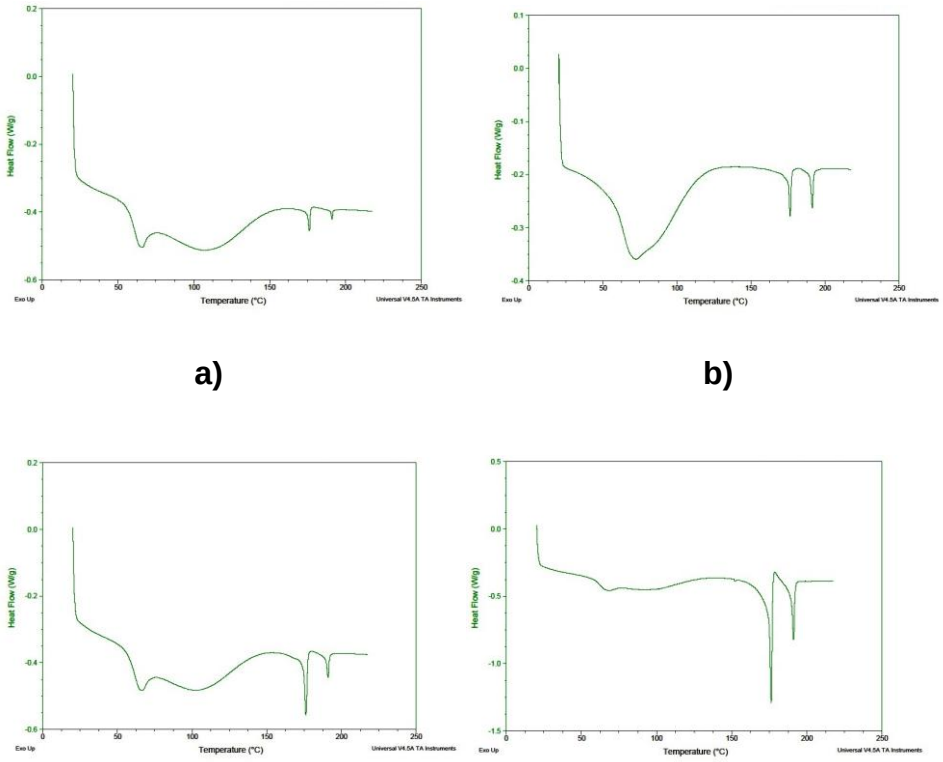

a) **b)**

c) **d)**

Fig.5.43. DSC profiles of physical mixtures of Carbamazepine and Soluplus: a) 5%, b) 10%, c) 20% and d) 30%

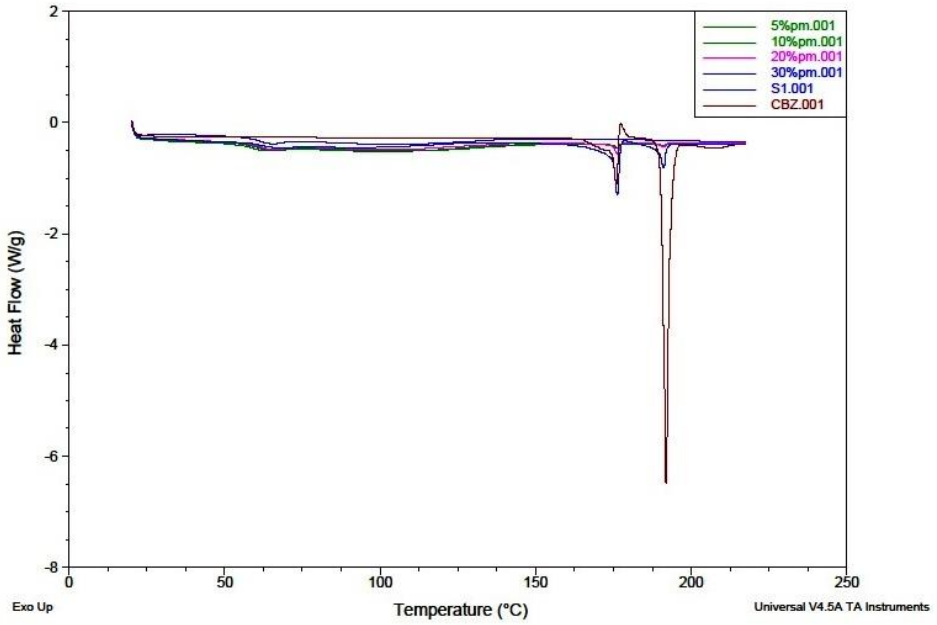

Fig.5.44. DSC profiles of Carbamazepine, Soluplus and physical mixtures of Carbamazepine and Soluplus (5%, 10%, 20%, and 30%)

It has been observed that in the DSC thermograms of Carbamazepine-Soluplus physical mixtures (Fig. 5.43., 5.44.), intensity of Carbamazepine melting endotherm decreases with the increase in Soluplus concentration. More intense melting peak can be seen in the DSC profile of 30 % physical mixture than that of other concentrations. These results indicate the suitability of Soluplus with Carbamazepine for further studies (hot melt extrusion). These results are in resemblance with that of reported in the literature (Djuris et al., 2013).

5.3.2. Rheological analysis

Rheological study of soluplus has been carried out at four temperatures (120°C, 140°C, 160°C and 180°C) to determine its stability.

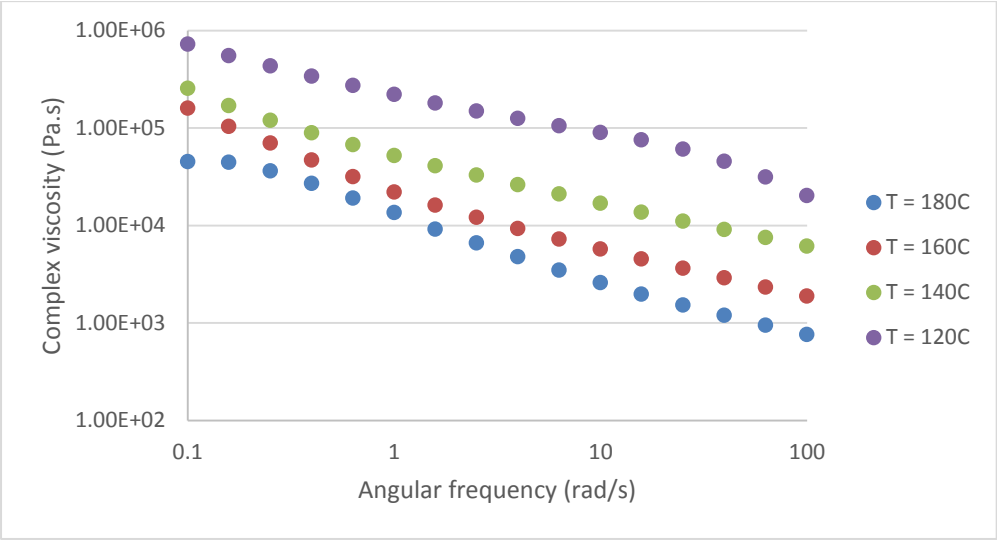

Fig. 5.45.Complex viscosity Vs angular frequency plot for Soluplus at 120°C, 140°C, 160°C and at 180°C

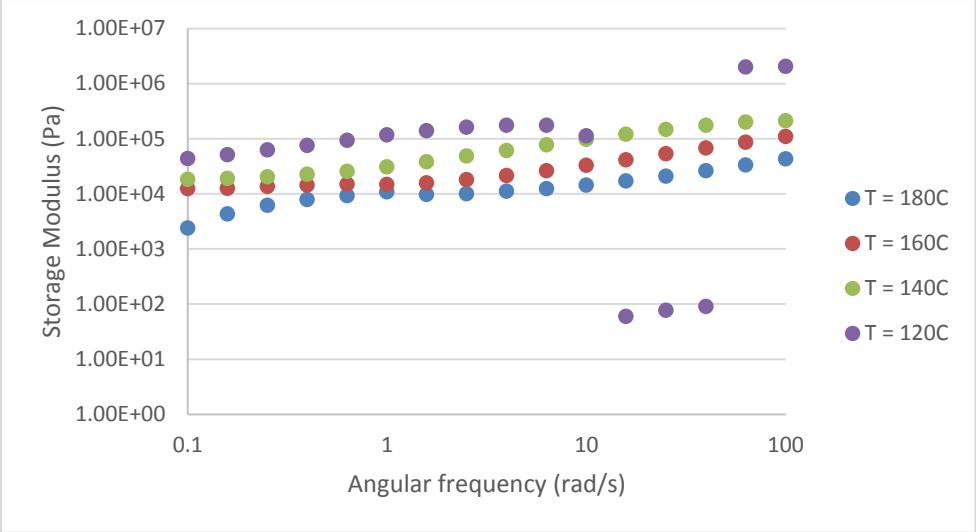

Fig. 5.46. Storage modulus Vs angular frequency plot for Soluplus at 120°C, 140°C, 160°C and at 180°C

Fig. 5.45. of complex viscosity Vs angular frequency shown good results at 120°C, 140°C, 160°C and at 180°C while when we plotted graph of storage modulus Vs angular frequency, results at 120°C have shown low stability of Soluplus which can be seen in Fig.5.46. Based on this we decided to choose temperatures above 120°C.

5.3.3. Preparation of solid dispersions of CBZ and Soluplus using Hot melt extrusion

To study effect of different polymer with Carbamazepine a new system - Carbamazepine and Soluplus was selected. Soluplus being a well extrudable polymer with the extrusion temperature range suitable with Carbamazepine melting was a good choice for study.

Solid dispersions of carbamazepine (5*H*-dibenzo [*b*, *f*] azepine-5-carboxamide) and Soluplus were prepared by a hot melt extrusion process using a twin screw extruder at a screw speed of 30rpm and at temperatures in the range of 130˚C to 170˚C (T1) and 120˚C to 170˚C with a feed rate of 0.180Kg/hr.(Table 5.10.).

	Zone									
T (°C)	**Die**	**10**	**9**	**8**	**7**	**6**	**5**	**4**	**3**	**2**
T1	**170**	**170**	**170**	**150**	**150**	**150**	**140**	**140**	**140**	**130**
T2	**170**	**160**	**160**	**160**	**150**	**140**	**120**	**120**	**120**	**120**

Table 5.10.Temperature (°C) profiles used during hot melt extrusion

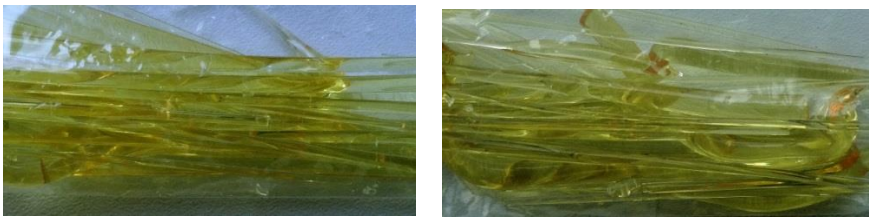

a) 5% SD b) 10%SD

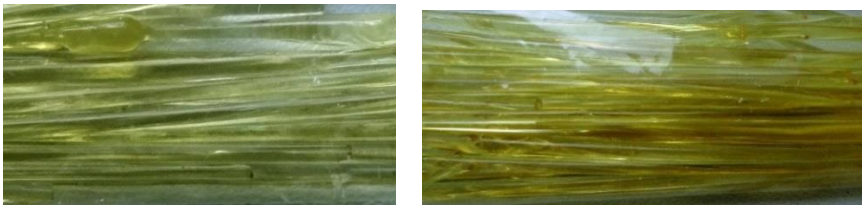

c) 20%SD d) 30%SD

Fig.5.47. Photographic images of Solid dispersions of CBZ – Soluplus

Photographic images of Solid dispersions of CBZ - Soluplus have been taken using digital camera (Sony 16.1 megapixel). As it can be seen from Fig. 5.47. a, b, c and d there was yellow coloration as per increase in concentration of extrudates was observed in SDs. To find out degradation mechanism based on these observations, comparative study of Raman spectra of extrudates with that of metabolite of carbamazepine, 5H-Dibenz (b, f) azepine (Iminostilbene) was carried out. In-line monitoring of Carbamazepine - Soluplus solid dispersion preparation using Raman spectroscopy during hot melt extrusion process.

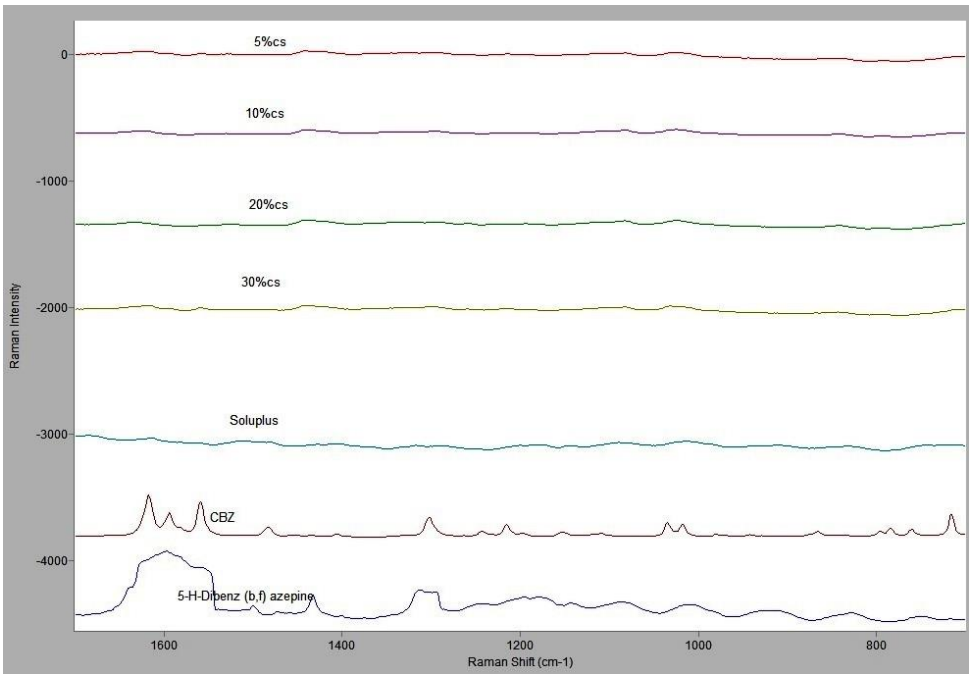

Fig.5.48. Raman spectra of CBZ, 5H-Dibenz (b, f) azepine, Soluplus and solid dispersions of CBZ-Soluplus (5, 10, 20, 30%) off-line

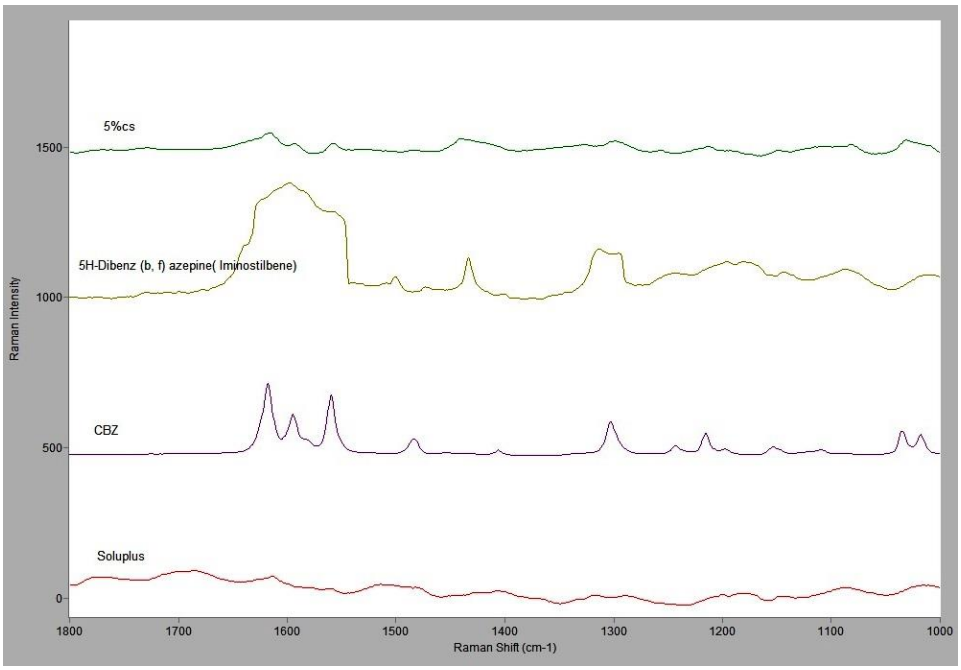

Fig.5.49.Raman Spectra of 5% CBZ-Soluplus (in-line 120-170°C)

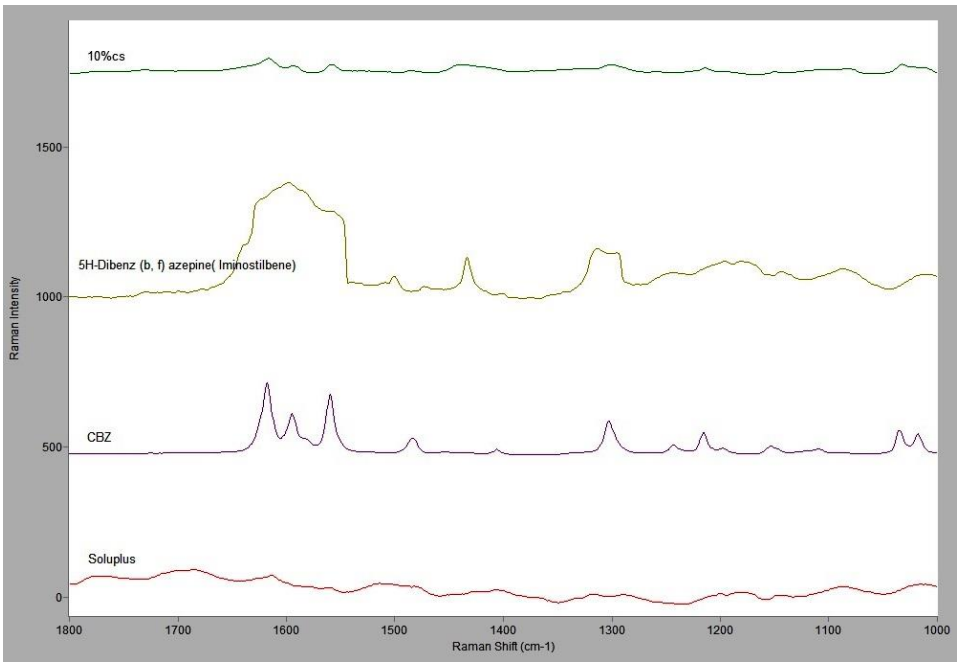

Fig.5.50.Raman Spectra of 10% CBZ-Soluplus (in-line 120-170°C)

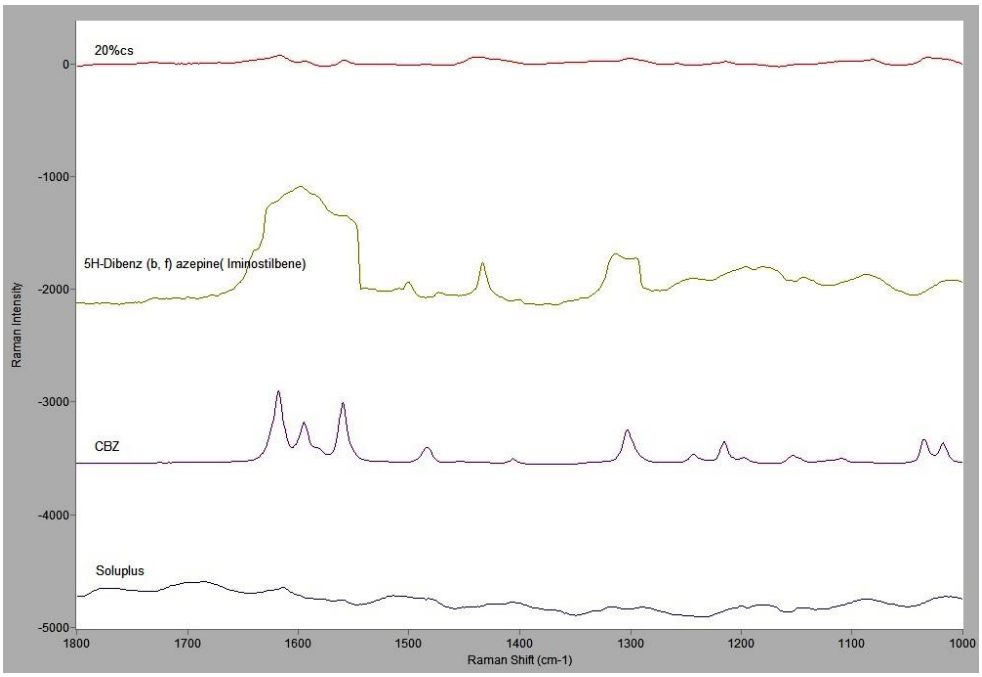

Fig.5.51.Raman Spectra of 20% CBZ-Soluplus (in-line 120-170°C)

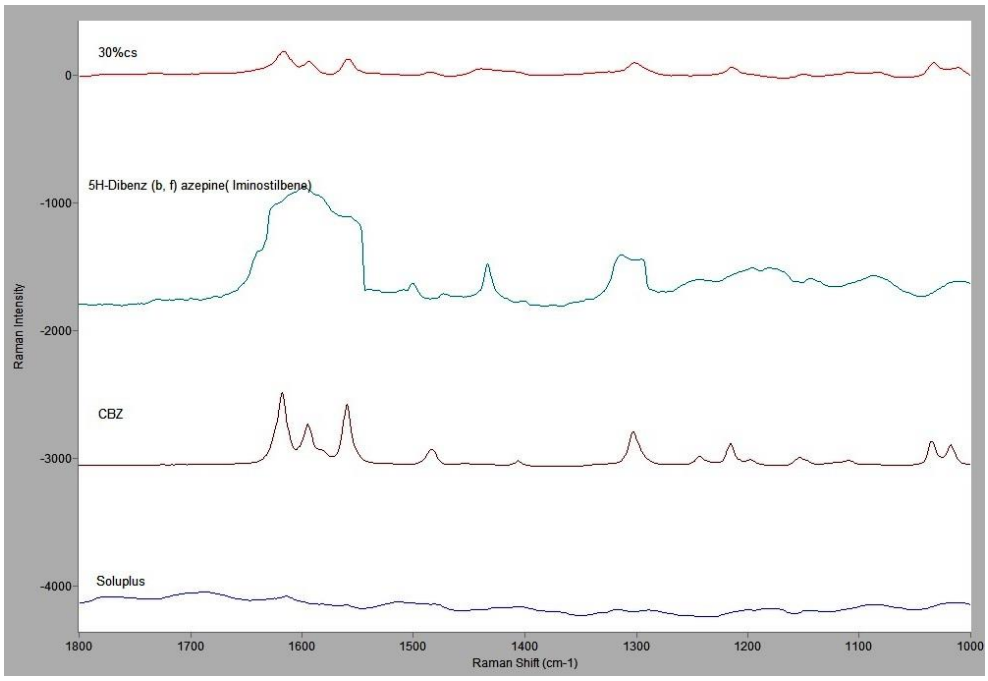

Fig.5.52.Raman Spectra of 30% CBZ-Soluplus (in-line 120-170°C)

In-line Raman spectroscopic analysis of CBZ, 5H-Dibenz (b, f) azepine, Soluplus and solid dispersions of CBZ-Soluplus (5, 10, 20, and 30%) has been carried out using Inphotonics Raman probe. Spectra were converted into Grams format using Grams 9.1 by Thermoscientific. From Fig.5.48. it can be seen that in the Raman spectra of solid dispersions there is no presence of peaks of 5H-Dibenz (b, f) azepine (Iminostilbene) which is a metabolite of carbamazepine. So even though extrudates are showing yellow colour, this data indicates absence of any metabolite as well as absence of crystallinity of CBZ in the extrudates. During in-line Raman spectroscopic analysis, resemblance in peaks of solid dispersions obtained and 5H-Dibenz (b, f) azepine (Iminostilbene) was observed (Fig. 5.49. to Fig. 5.52.) From these results we can conclude that there might be formation of metabolite of CBZ i.e. 5H-Dibenz (b, f) azepine (Iminostilbene) in the temperature profile used during hot melt extrusion in the range of 120- 170° C.

5.3.4. Raman spectroscopy results

Off-line Raman spectroscopic analysis

Off-line Raman analysis of Carbamazepine, Soluplus and Carbamazepine - Soluplus SDs was carried out using the Thermo Scientific DXR Smart Raman spectrophotometer by placing samples in transparent containers using universal platform after calibration and background corrections in the range of 200-3500cm^{-1}. Raman spectra were converted into Grams format for interpretation using GRAMS 9.1 spectroscopy software suite, Thermo Fisher Scientific Inc. Laser power of 80mW was used with warm up time of 5min. Two scans of 120s acquisition were collected. These results can be seen in Fig. 5.53, to Fig.5.56 .

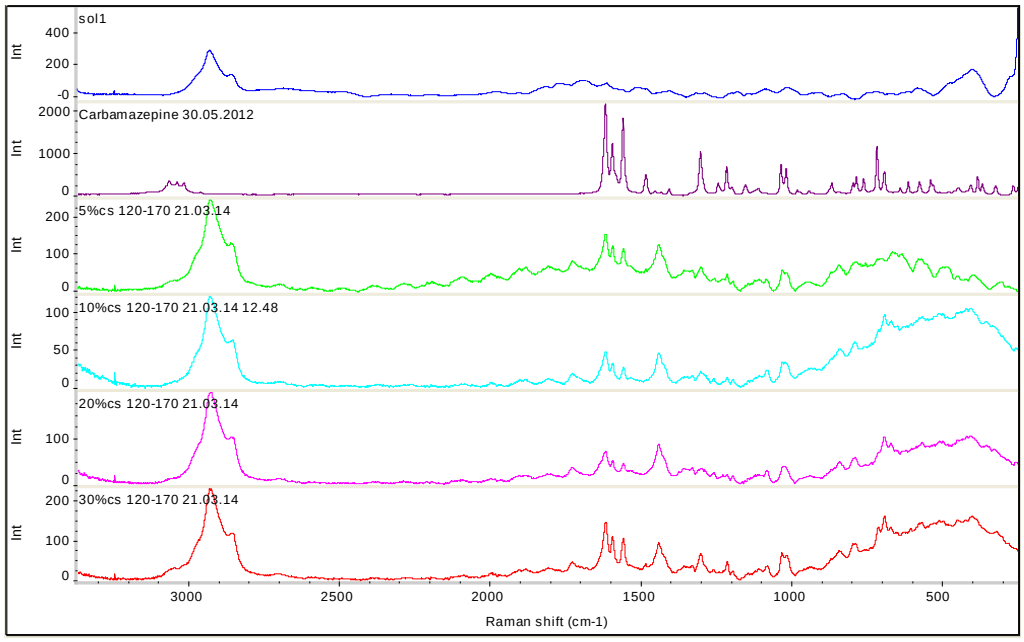

Fig.5.53. Off-line Raman spectra of CBZ – Soluplus SDs (T2 = 120-170°C)

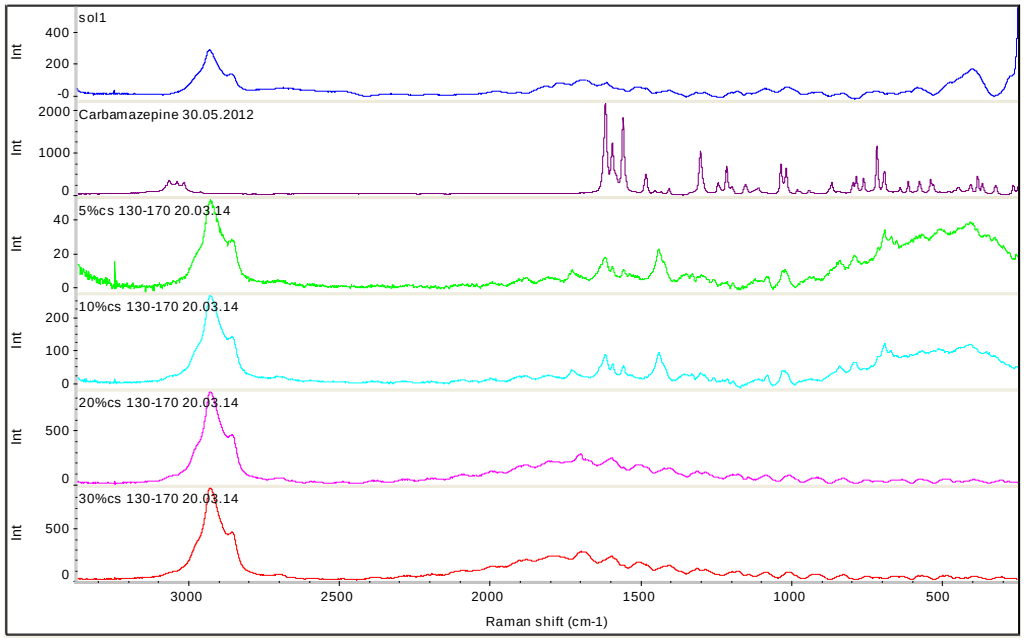

Fig.5.54. Off-line Raman spectra of CBZ – Soluplus SDs (T1 = 130-170°C)

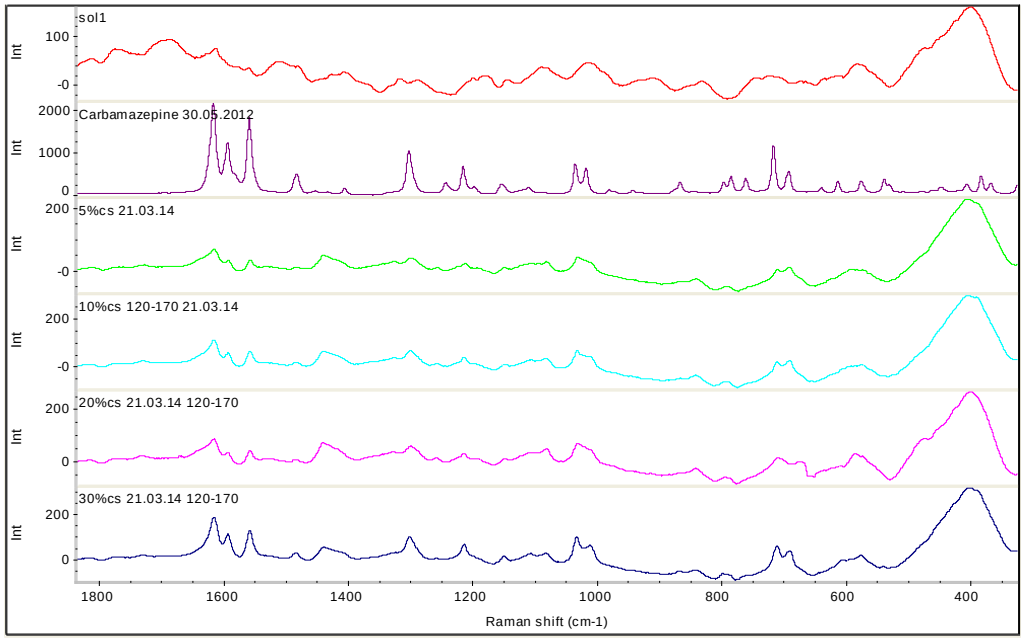

Fig.5.55. In-line Raman spectra of CBZ – Soluplus SDs (T2 = 120-170°C)

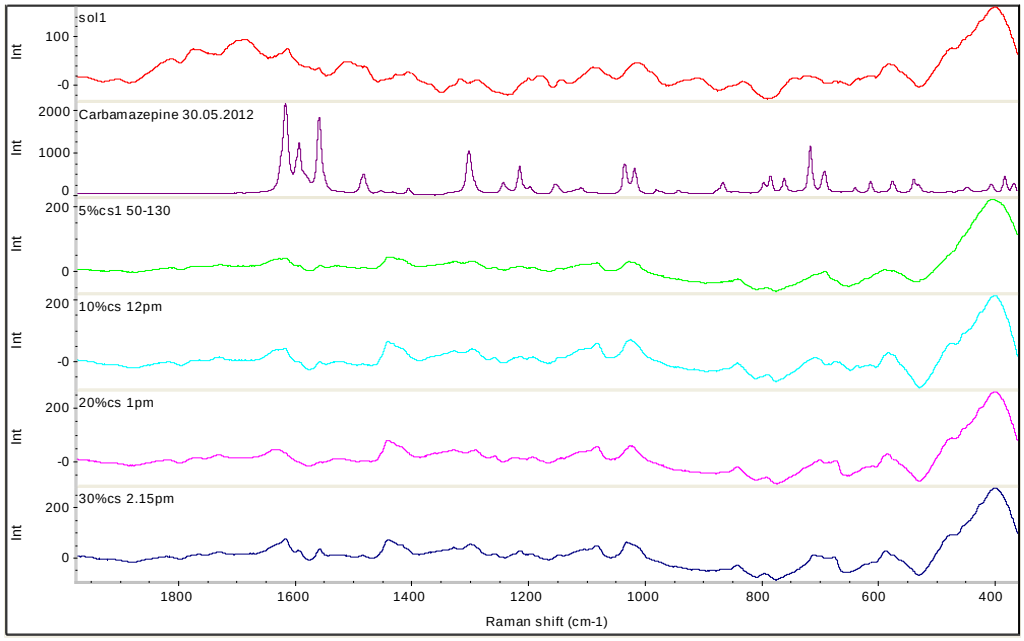

Fig. 5.56. In-line Raman spectra of CBZ – Soluplus SDs (T1 = 130-170°C)

In-line Raman spectroscopic analysis

In-line Raman spectroscopic analysis of Carbamazepine, Soluplus and solid dispersions of Carbamazepine - Soluplus (5, 10, 20, and 30%) has been carried out using Inphotonics Raman probe with 80mW laser power and 2 scans of 60s acquisition. Spectra were converted into Grams format using Grams 9.1 by ThermoScientific.

Prediction of Carbamazepine degradation during hot melt extrusion using in-line Raman spectroscopic monitoring an application of Process Analytical Technology has been carried out. A comparative study of Raman spectra of extrudates with that of metabolite of carbamazepine, 5H-Dibenz (b, f) azepine (Iminostilbene) was carried out.

Calibration curve - off-line Raman spectroscopic analysis of CBZ - Soluplus SDs

From the Raman spectra collected off-line using Thermoscientific Raman spectrophotometer using ups, a calibration curve has been generated. A

partial least square method was used 2 factors was found to give correlation coefficient value of 0.7433 for SDs prepared using temperature range of 120-170°C (T2). This can be seen in Fig.5.57., while SDs prepared in the range of 130-170°C (T1) found to show correlation coefficient value of 0.8226 (Fig. 5.58.).

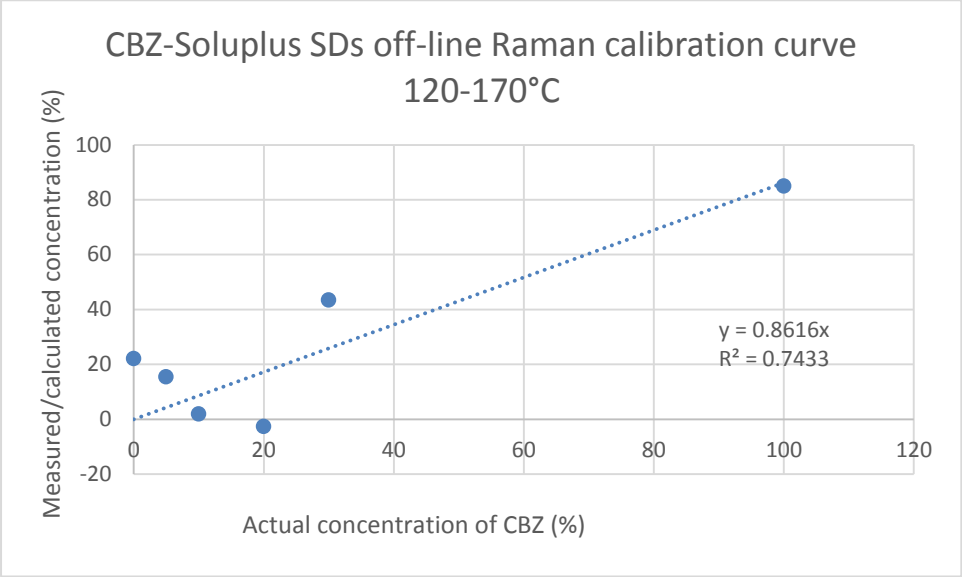

Fig. 5.57. CBZ - Soluplus SDs off-line Raman calibration curve 120-170°C

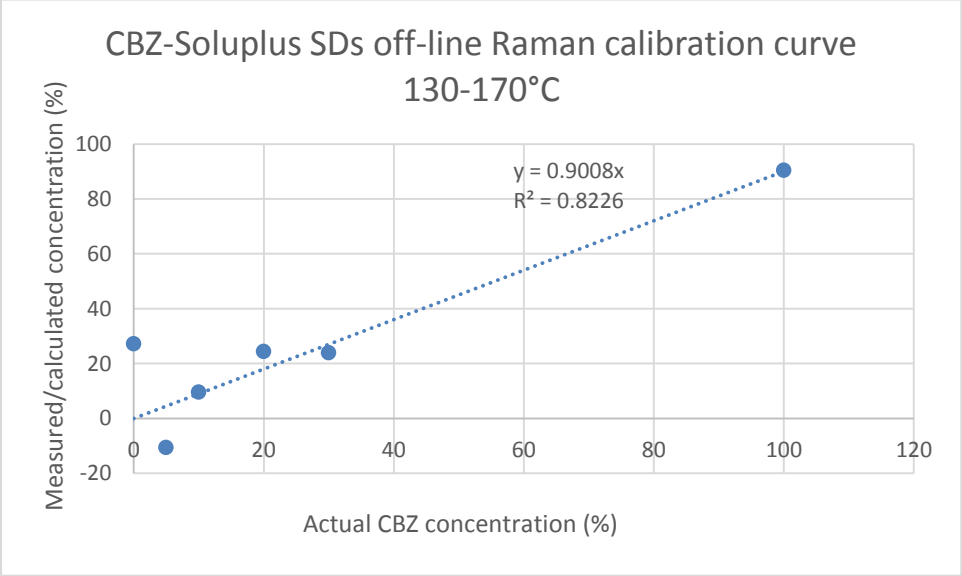

Fig. 5.58. CBZ - Soluplus SDs off-line Raman calibration curve 130-170°C

Calibration curve - In - line Raman spectroscopic analysis of CBZ - Soluplus SDs

From the Raman spectra collected using in-line Raman probe by Inphotonics during preparation of CBZ - Soluplus SDs using hot melt extrusion, a calibration curve has been generated. A partial least square method was used with standard normal variate and full spectra were selected for the study. Using 2 factors, the calibration curve was found to give correlation coefficient value of 0.9704 for SDs prepared using temperature range of 120-170°. This can be seen in Fig. 5.59. while SDs prepared in the range of 130-170°C found to show correlation coefficient value of 0.9478 (Fig. 5.60.).

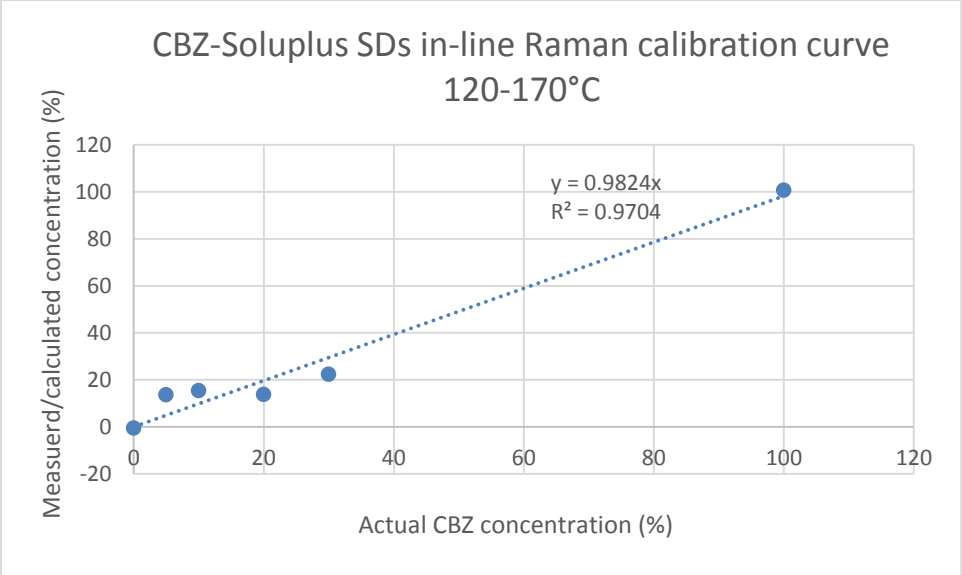

Fig. 5.59. CBZ - Soluplus SDs in-line Raman calibration curve 120-170°C

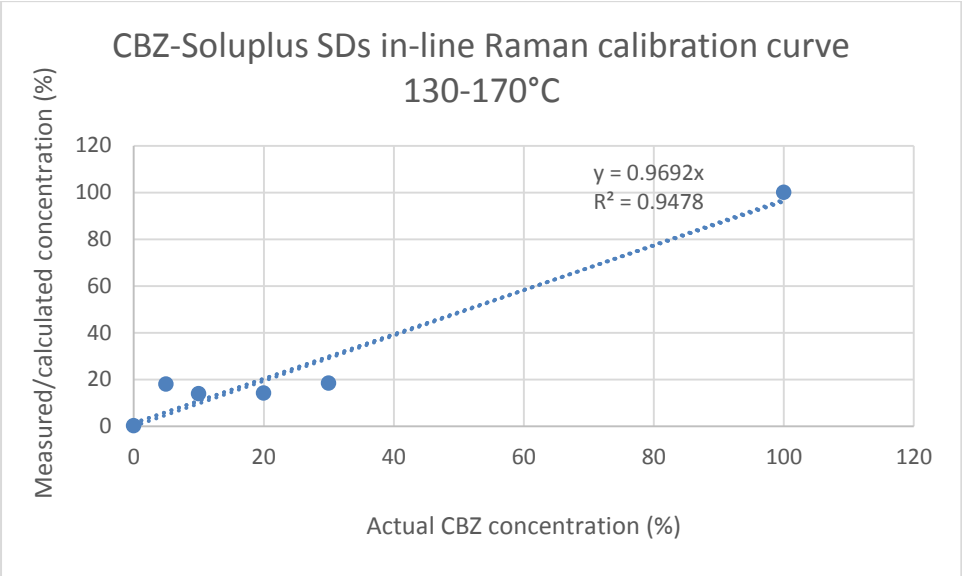

Fig. 5.60. CBZ - Soluplus SDs in-line Raman calibration curve 130-170°C

Correlation coefficient values obtained from calibration curves of CBZ - Soluplus SDs from in-line Raman spectroscopic monitoring have been found to be better than those of off-line analysis. These results show that Raman spectroscopy is a suitable technique for off-line as well as in-line monitoring of CBZ levels in solid dispersions of CBZ - Soluplus. It proves that in-line Raman can be used as a PAT tool during hot melt extrusion.

5.3.5. Hot stage microscopy (HSM) results

To understand effect of temperature and for the determination of crystalline nature of polymorphic forms of Carbamazepine and conversion of its forms (form I from heating of form III), hot melt microscopic studied have been carried out. Hot stage microscopic analysis of Carbamazepine, Soluplus and solid dispersions of carbamazepine and Soluplus obtained by hot melt extrusion was carried out. Axiovision software was connected with Link sys 32 for hot stage. Small amount of samples were placed on open glass slides fixed on hot stage with 10 x/0.20 magnifications with bifocal light and heated form 30°C to 220°C at 10°C per min.

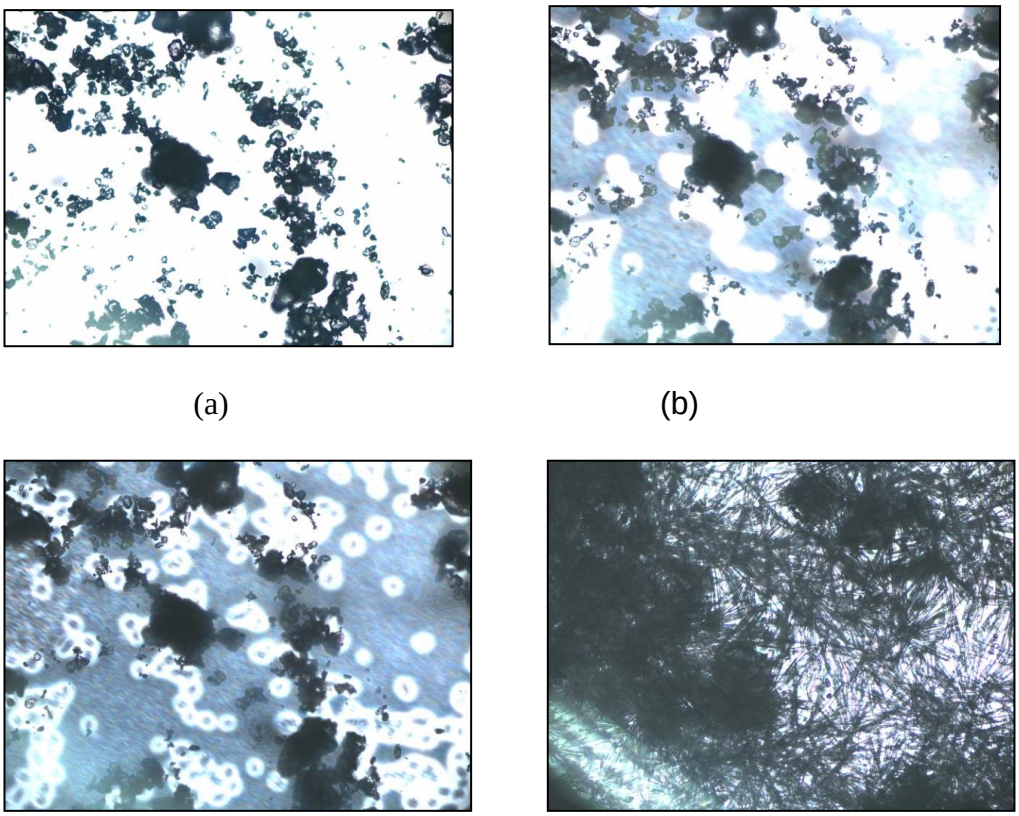

Fig.5.61. HSM images of CBZ at a) 165°C b) 179° C c) 190°C and d) 170°C (cooling)

Pure carbamazepine form III (*p*-monoclinic) form started melting (Fig.5.61.a) and started converting to form I (triclinic) (Fig.5.61.b). At 190°C melting of carbamazepine was observed (Fig.5.61.c). Crystallization on cooling was observed. Needle shaped CBZ form I crystals converted from commercial CBZ form III can be seen in Fig. 5.61.d. These results are in resemblance with those of literature (Djuris et al., 2013).

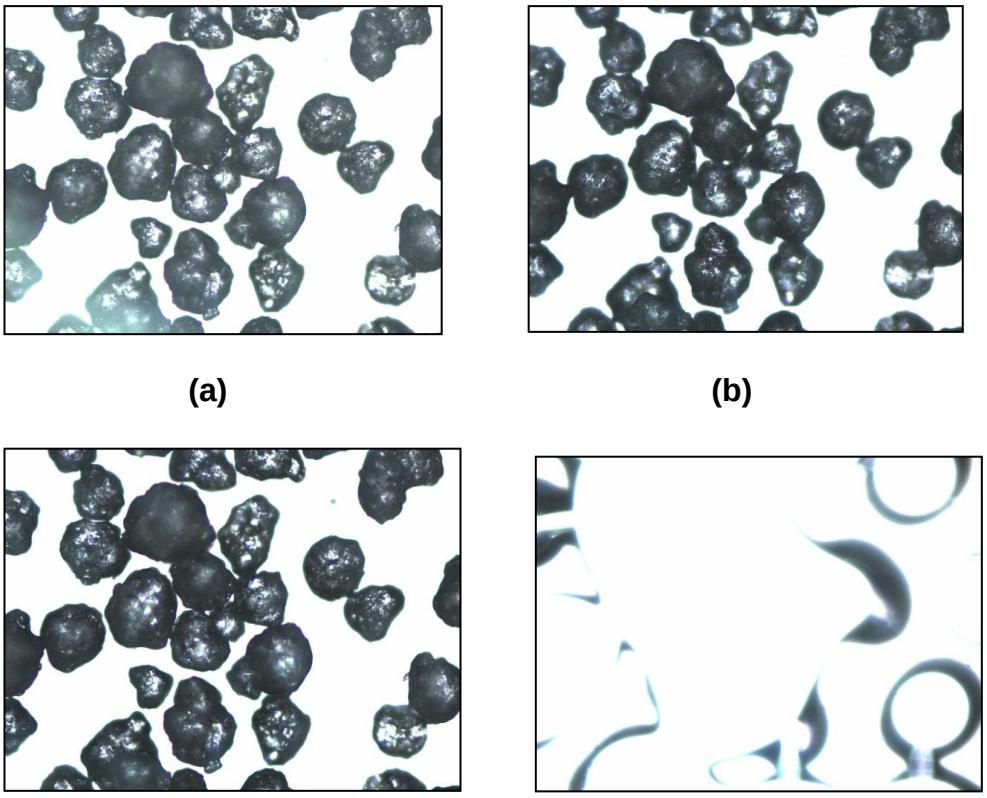

Fig.5.62. HSM images of Soluplus at a) ambient temperature, b) 50°C, c) 85°C and d) 185°C

Studying stability of soluplus was of great importance since it was selected to be used for preparation of solid dispersion with Carbamazepine. Soluplus was heated from 30°C to 220°C at 10°C per min. After 70°C it started showing changes and after 185°C it was completely disappeared which indicates complete melting. Based on the clear melt it has been concluded that there was no sign of degradation of Soluplus up to temperature of 220°C

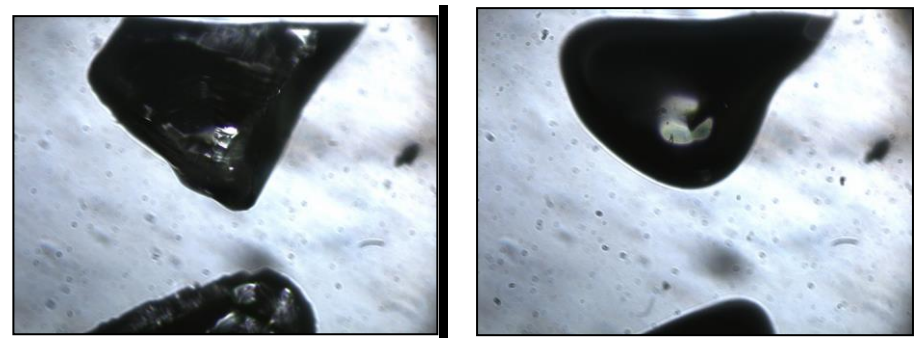

(a) (b)

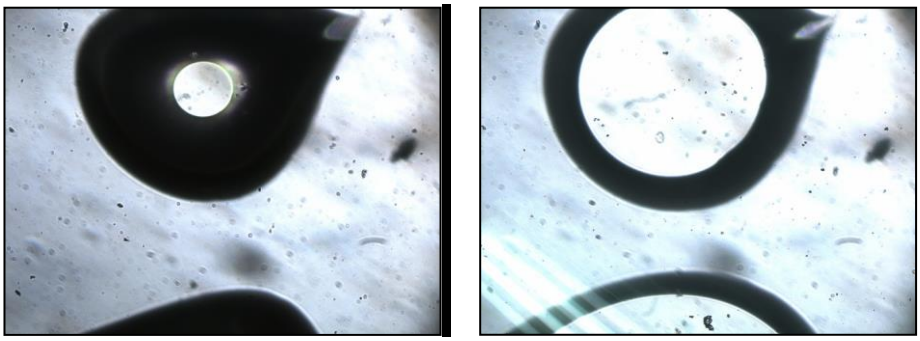

(c) (d)

Fig.5.63. HSM images of 5% SD at a) 126°C, b) 160°C, c) 179°C, d) 190°C

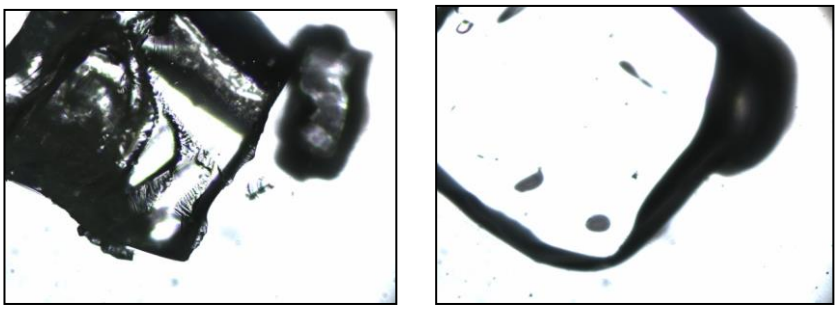

(a) (b)

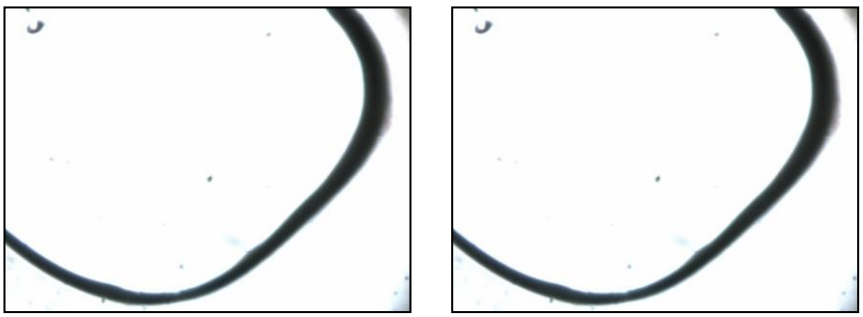

(c) (d)

Fig.5.64. HSM images of 10% SD at a) 126, b) 160, c) 179 and d) 190°C

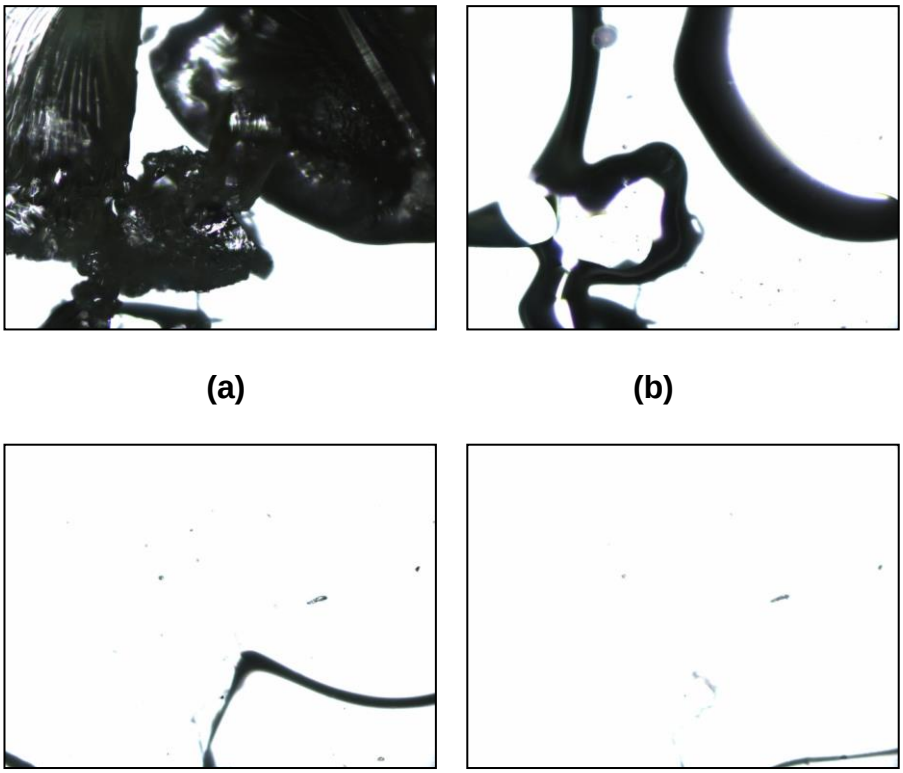

(a) **(b)**

(c) **(d)**

Fig.5.65. HSM images of 20% SD at a) 126°, b) 160°C, and c) 179°C d) 190°C

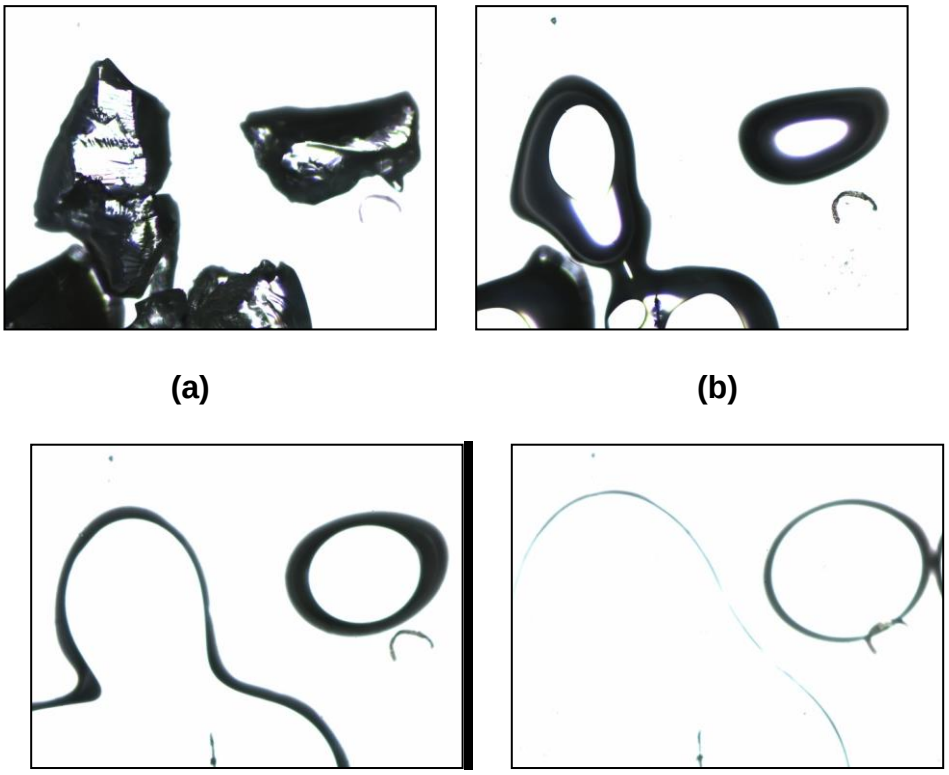

(a) **(b)**

(c) **(d)**

Fig.5.66. HSM images of 30% SD at a) 126°C, b) 160°C, c) 179°C, d) 190°C

From Fig 5.63. to 5.66. it can be seen that carbamazepine crystals in the solid dispersion samples prepared at 120°C-170°C were completely melted and got converted into amorphous form which was concluded based on absence of any crystals in results. These observations indicate complete dissolution of carbamazepine in molten Soluplus. This process might have enhanced by hot melt extrusion (shear) in case of SDs prepared by hot melt extrusion. After 126°C all solid dispersion samples started to show some changes and finally got melted with increase in temperature. Also up to 170°C - 190°C there was no degradation of carbamazepine was observed. Samples were completely got melted at this temperature range.

5.4. Preparation and characterization of co-crystals of Ibuprofen and Nicotinamide

Co-crystallization is carried out to obtain crystalline forms of molecules with improved quality and is of great importance in pharmaceutical industry in order to enhance material properties and in development of overall quality of formulations. Use of co-crystals has been reported in literature for stability and solubility enhancement, improvement of dissolution rate and bioavailability (Dhumal et al., 2010).

Preparation of co-crystals of Ibuprofen and Nicotinamide has been carried out to investigate possible applications of off-line and in-line Raman spectroscopy for quantification of co-crystal production during hot melt extrusion. The focus of this work was to get solvent free, scalable preparation of co-crystals and study of methods for confirmation purity of co-crystals.

5.4.1. DSC results

Thermal profiles of Ibuprofen and Nicotinamide were generated in the range of 40 - 170^{o}C using a Q2000 calorimeter from TA Instruments. Accurately weighed samples (3-5mg) were placed in aluminium pans using similar empty pans as a reference. A heating rate of 10^{o}C min^{-1} was employed. Measurements were carried out in an inert atmosphere by purging nitrogen gas at the flow rate of 50 mL/min. The acquired thermo grams were analysed with TA Instruments Universal Analysis 2000 software. Meting peak of Ibuprofen at 76°C and that of Nicotinamide at 129.5°C can be seen in Fig. 5.67. and Fig. 5.68. respectively.

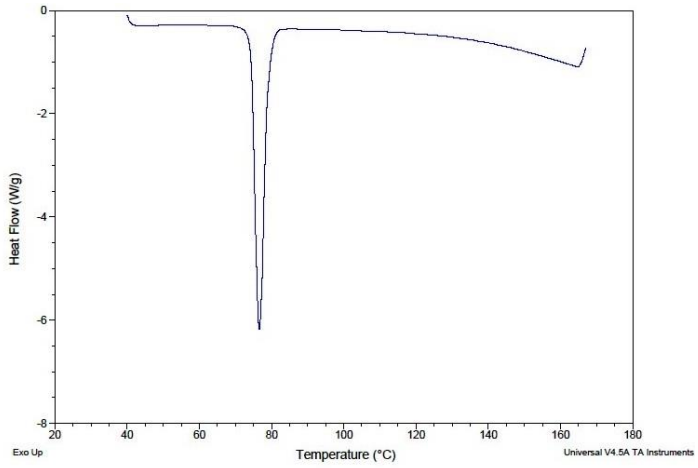

Fig.5.67. DSC profile of Ibuprofen (m.p. 76°C)

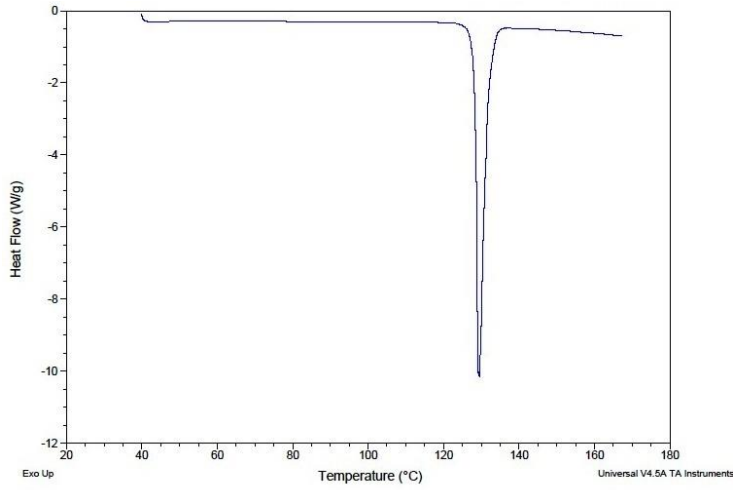

Fig.5.68. DSC profile of Nicotinamide (m.p. 129.5°C)

5.4.2. Preparation of pure Ibuprofen-Nicotinamide co-crystals by Microwave method

Microwave method has been selected for the preparation of co-crystals of Ibuprofen and nicotinamide based on its advantages such as quicker method, greener as there is no use of organic solvent as well as user friendliness and reproducibility.

Ibuprofen and Nicotinamide in molar ratio (1:1) were mixed with 82µL of distilled water and added in 30 mL capacity glass tube (glass vial type 30). Preparation of co-crystals was carried out using Monowave 300 microwave

synthesis reactor by Anton Paar. Initially, the temperature chosen was 70°C and samples were subjected to microwave irradiation with the holding time of 1 min and cooled at 40°C. DSC results of co-crystals obtained using these parameters did not show pure co-crystal single peak when compared with literature (Dhumal et al., 2010). To get pure co-crystals, various batches of co-crystals were prepared with different holding times and temperatures during microwave preparation as mentioned in the table 5.11. The obtained Ibuprofen – Nicotinamide co-crystals were finally analysed and their purity was confirmed by DSC. Batch C15 with the holding temperature of 80°C with cooling temperature of 40°C was found to produce pure co-crystals which was confirmed by DSC.

Batch name	Heating temperature △(°C)	Holding time ▷ (min)	Cooling temperature ▽ (°C)
C1	70	1	40
C2	70	2	40
C3	70	3	40
C4	75	1	40
C5	75	2	40
C6	75	3	40
C7	80	1	40
C8	80	2	40
C9	80	3	40
C10	70	5	40

C11	75	5	40
C12	80	5	40
C13	70	5	40
C14	75	5	0
C15	80	5	40
A,B,C,D,E	80	5	40

Table 5.11. Microwave reactor parameters used in the preparation of Ibuprofen-Nicotinamide co-crystals.

5.4.3. DSC results of co-crystals and calibration curve

Thermal profiles were generated in the range of 40 - 170°C using a Q2000 calorimeter from TA Instruments. Accurately weighed samples (3-5mg) were placed in aluminium pans using similar empty pans as a reference. A heating rate of 10°C min^{-1} was employed. Measurements were carried out in an inert atmosphere by purging nitrogen gas at the flow rate of 50 mL/min. The acquired thermo grams were analysed with TA Instruments Universal Analysis 2000 software. DSC profiles converted into text files and graphs were generated in Microsoft excel.

Melting endotherm of Ibuprofen can be seen at 76°C while melting endotherm of Nicotinamide can be seen in the range of 129°C -130°C (Fig.5.69., 5.70., 5.71).

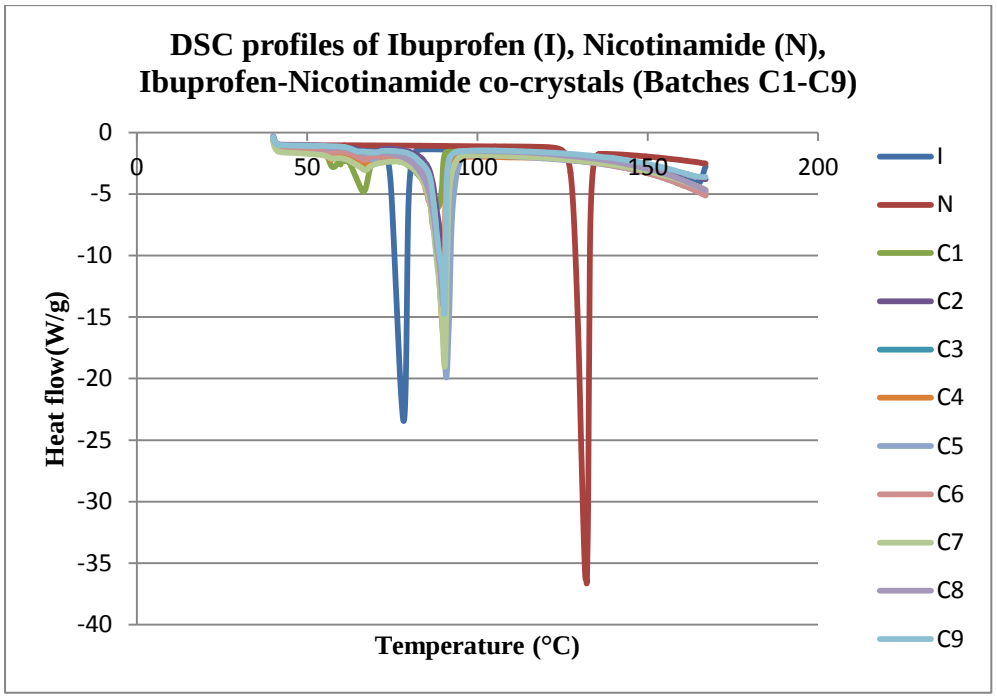

Fig. 5.69. DSC profiles of Ibuprofen (I), Nicotinamide (N) Ibuprofen-Nicotinamide co-crystals (Batches C1-C9)

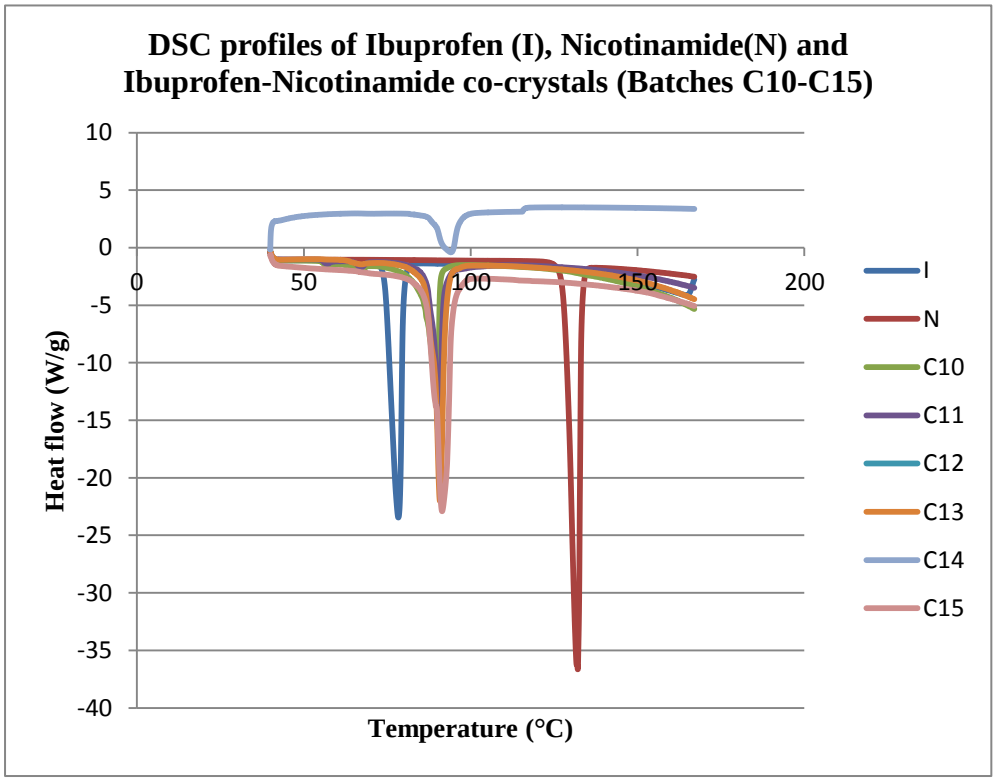

Fig.5.70. DSC profiles of Ibuprofen (I), Nicotinamide (N) Ibuprofen-Nicotinamide co-crystals (80°C, 5min, 40°C) Batches C10-C15

DSC profiles of Batches C1 To C14 were found to show impurity peaks below 80°C (Fig.5.69., Fig.5.70.) which disappeared in the DSC profile of Batch C15 (Fig 5.70.) at temperature 80°C with holding time of 5min. Based on this, settings which produced pure co-crystals (C15) were considered as the ideal settings. Using these settings, 5 batches of co-crystals A, B, C, D and E were prepared to get reproducibility of results and to get more sample for preparation of dilutions of Ibuprofen with co-crystals of Ibuprofen and nicotinamide. DSC profiles of batches A, B, C, D and E found to show pure co-crystals without any impure peaks (Fig.5.71.).

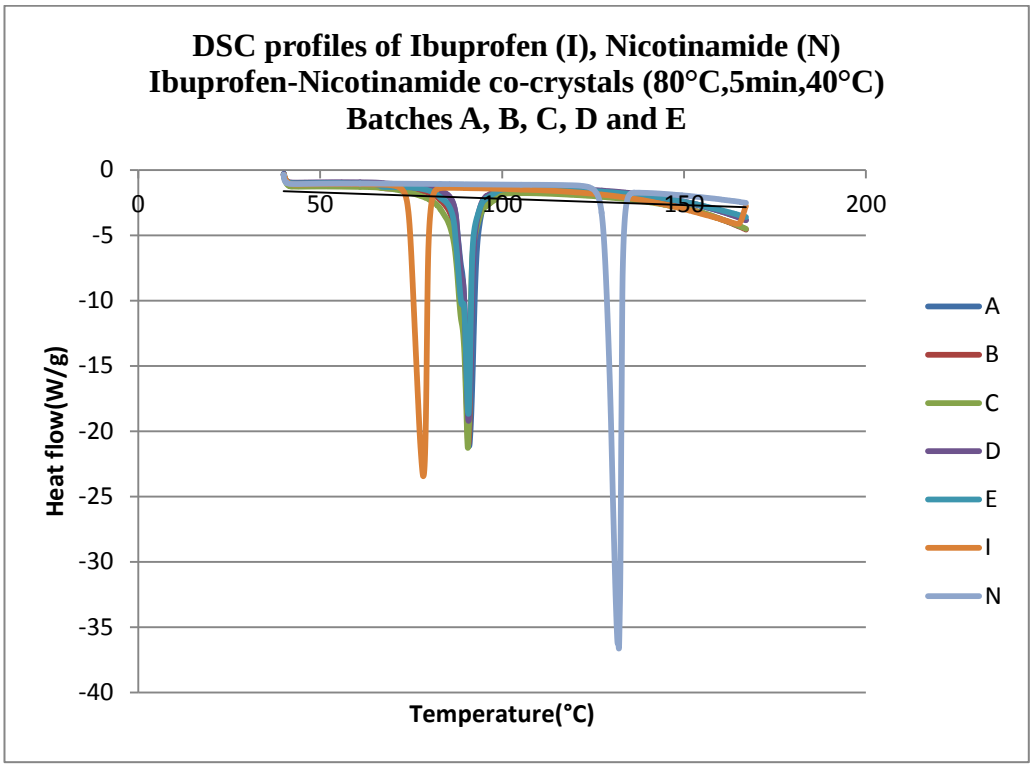

Fig.5.71. DSC profiles of Ibuprofen (I), Nicotinamide (N) Ibuprofen-Nicotinamide co-crystals (80°C, 5min, 40°C) Batches A, B, C, D, E

DSC profiles obtained in Trios format were exported in Microsoft excel for generation of calibration curve using enthalpy values. A calibration curve has been generated by plotting a graph of actual concentration of dilutions of

Ibuprofen-nicotinamide co-crystals with Ibuprofen against measured concentration of dilutions co-crystals with Ibuprofen from DSC enthalpy data.

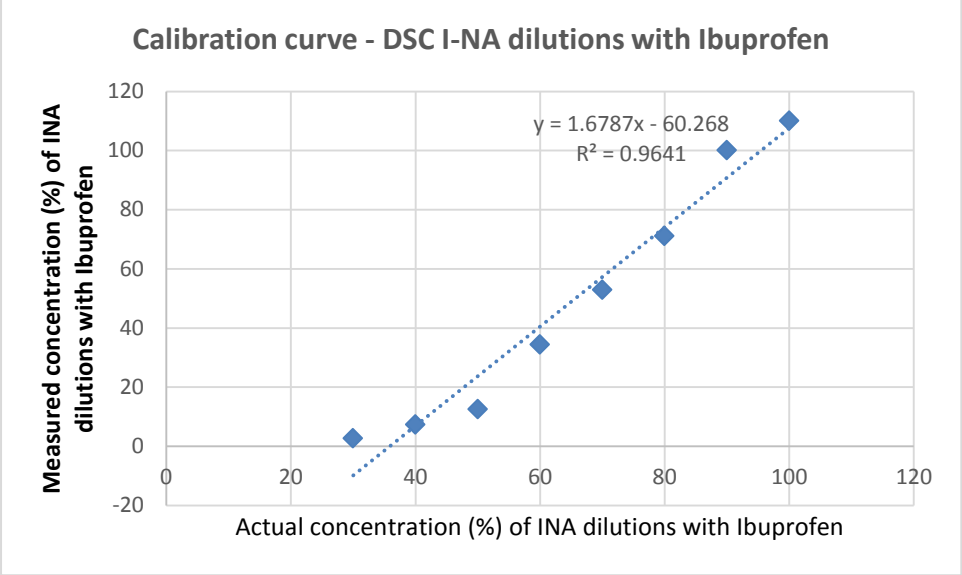

Fig.5.72. Calibration curve generated for INA dilutions with ibuprofen concentration (actual) Vs Measured concentration (%) from DSC enthalpy

Coefficient of correlation of 0.9641 was obtained from calibration curve (Fig. 5.72.).

5.4.4. PXRD results (co - crystals prepared by microwave reactor method)

Crystallinity of co-crystals along with pure ibuprofen and nicotinamide has been determined by X-ray powder diffraction using a Bruker D8 diffractometer (wavelength of X-rays 0.154 nm Cu source, voltage 40 keV, and filament emission 40 mA). Samples were scanned in the range of 2 to 40° (2θ) using a 0.01° step width and a 1s time count. The receiving slit was 1° and the scatter slit was 0.2°. PXRD patterns of co-crystals (C1), pure

ibuprofen and pure nicotinamide have been shown in the Fig. 5.73., 5.74. and 5.75.

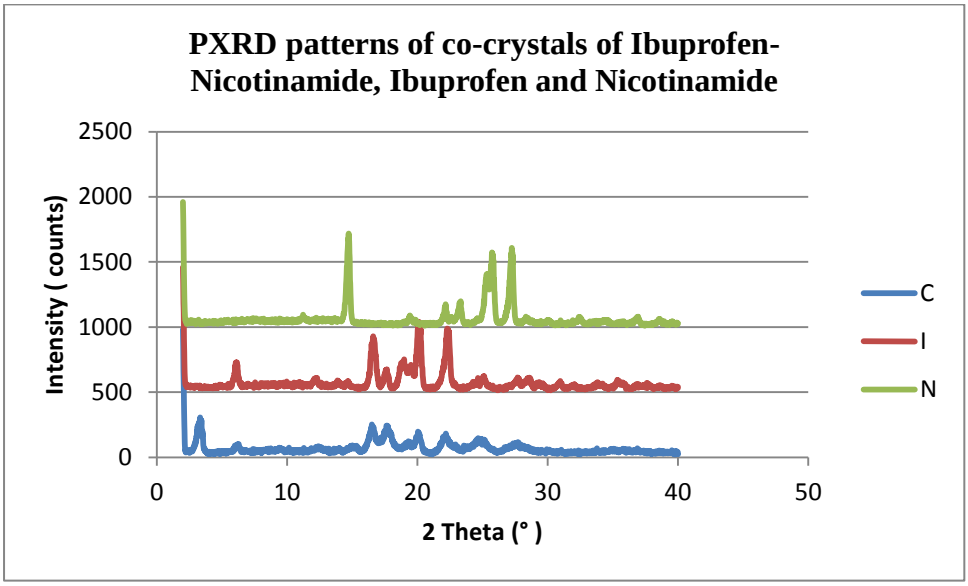

Fig.5.73. PXRD patterns of co-crystals of Ibuprofen- Nicotinamide, Ibuprofen and Nicotinamide

The characteristic peaks of ibuprofen at 6.10 and 12.21 2˚theta and characteristic peak of nicotinamide at 14.8 2˚theta are found to be reduced in co crystal diffractogram. Diffraction pattern of co-crystals was found to be different from that of its coformers ibuprofen and nicotinamide. These observations are found to be in resemblance with that of literature (Soares, F.L.F., 2013).

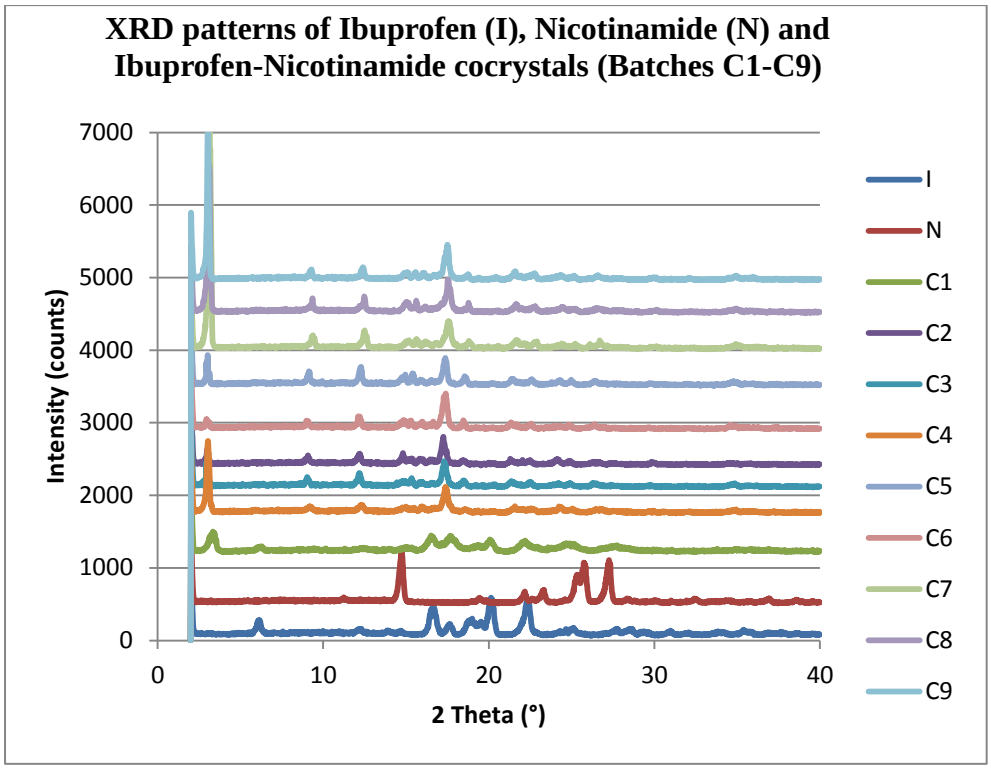

Fig.5.74. PXRD patterns of Ibuprofen, Nicotinamide and of co-crystals of Ibuprofen and Nicotinamide

In Fig. 5.74., Ibuprofen peak (6.10) was found to be present in some batches between C1-C9. After changing microwave synthesis parameters (temperature and holding time), Ibuprofen peak (6.10) was found to be absent in co-crystals (Batches A, B, C, D, E).

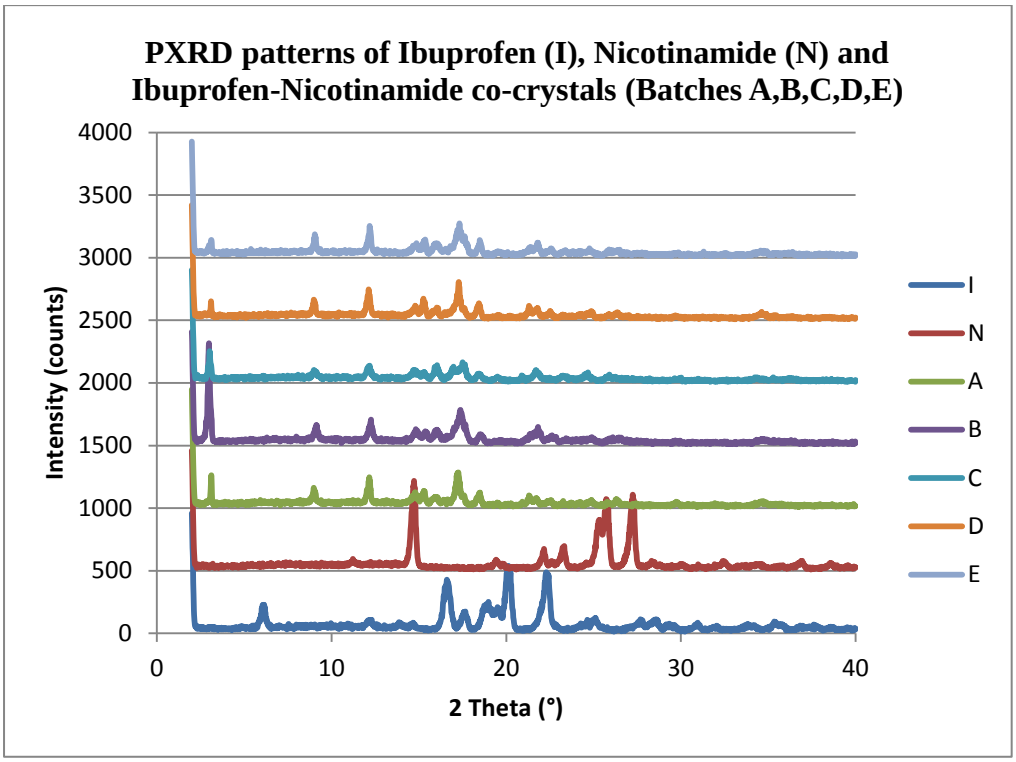

Fig.5.75. PXRD patterns of co-crystals of Ibuprofen- Nicotinamide, Ibuprofen and Nicotinamide

In the PXRD patterns of co crystals (Fig.5.75.) Ibuprofen peak (5-6.10) was found to be absent which indicates purity of co crystals.

5.4.5. FTIR results - calibration curve

FTIR analysis of Ibuprofen-Nicotinamide (IBU - NA) co-crystal dilutions with Ibuprofen (10-100%) has been carried out using Nicolet is50 ATR FTIR by Thermoscientific. Samples have been analysed at 32 scans with 4cm^{-1} resolution. Calibration curves have been generated from FTIR spectra using TQ analyst and Microsoft excel.

Correlation coefficient value of 0.4293 was obtained from the calibration curve generated using data obtained from TQ analyst using 2 factors for IBU-Na co-crystal dilutions with Ibuprofen (Fig. 5.76.) This was carried out for the accuracy of the results.

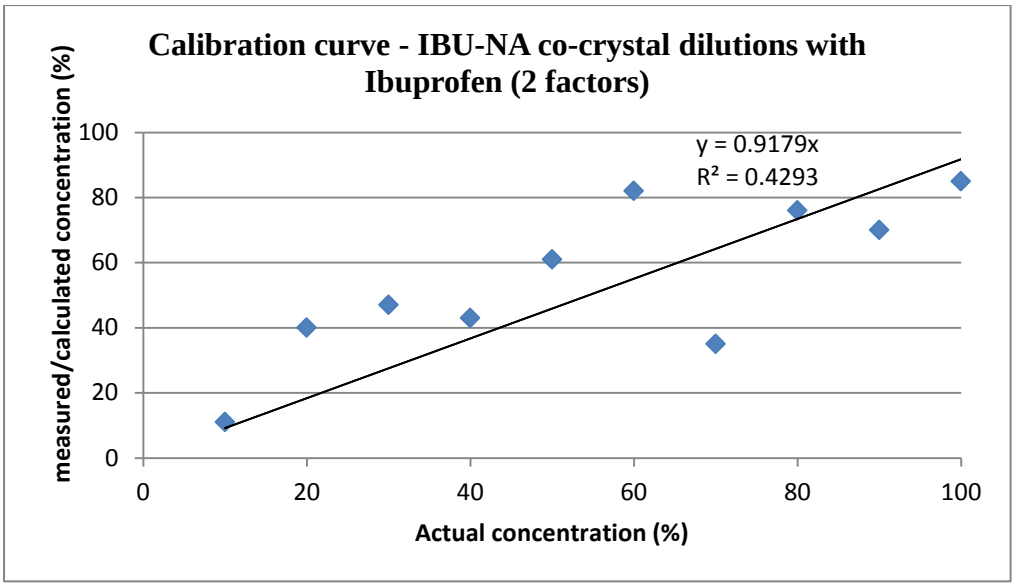

Fig.5.76. Calibration curve - IBU-NA co-crystal dilutions with Ibuprofen - 2 factors

Correlation coefficient value of 0.8385 was obtained from the calibration curve generated using data obtained from TQ analyst using 3 factors for IBU-NA co-crystal dilutions with Ibuprofen (Fig. 5.77.) This was carried out for the accuracy of the results.

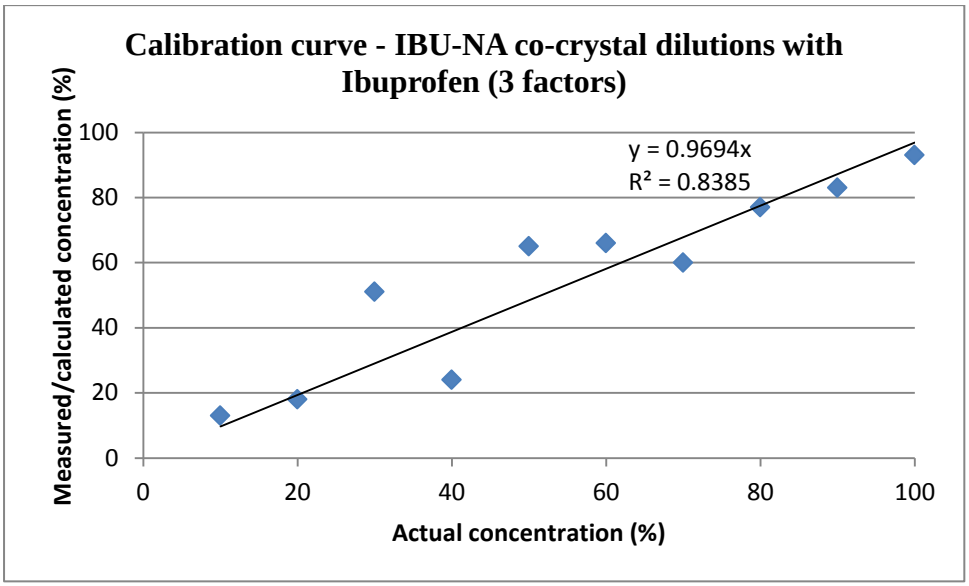

Fig.5.77. Calibration curve - IBU-NA co-crystal dilutions with Ibuprofen - 3 factors

5.4.6. Raman spectroscopy results

Raman spectroscopic analysis of Ibuprofen, Nicotinamide and IBU-NA co-crystals

Raman spectroscopic analysis of Ibuprofen, Nicotinamide and IBU-NA co-crystals was carried out using Thermo Scientific DXR Smart Raman spectrophotometer with softwares called OMNIC for dispersive Raman and TQ Analyst with Laser power of 80mW, aperture slit size of 25µm. 2 scans of 60s acquisition were collected. Offline Raman spectroscopic analysis of all physical mixtures of Ibuprofen-Nicotinamide co-crystals with Ibuprofen (CoC1 to CoC9 - table no. 5.12.) was carried out using Thermoscientic DXR smart Raman spectrometer universal platform.

Sample name	% of pure Ibuprofen	% of co-crystals of Ibuprofen and Nicotinamide
CoC1	10	90
CoC2	20	80
CoC3	30	70
CoC4	40	60
CoC5	50	50
CoC6	60	40
CoC7	70	30
CoC8	80	20
CoC9	90	10

Table 5.12. Table showing dilutions of 100% pure co-crystals of Ibuprofen-Nicotinamide with Pure Ibuprofen

Fig. 5.78. shows Raman spectra of Ibuprofen, nicotinamide and co-crystal of Ibuprofen - nicotinamide. Characteristic peak of Ibuprofen corresponding to C=O can be seen at 739-740cm $^{-1}$. (Fig.5.79. and 5.80.)

In Fig.5.81. Raman spectrum of Nicotinamide can be seen with characteristic -C-N-H stretching at 1034cm^{-1} whereas in Fig.5.82. and Fig. 5.83., Raman spectrum shows characteristic peak of 100% pure co-crystal at 792cm^{-1} with peak height and peak area respectively. Figures 5.84. to 5.101. Show Raman spectra of co-crystal dilutions with Ibuprofen which has been carried out to be used for determination of concentration of Ibuprofen by generating calibration curve.

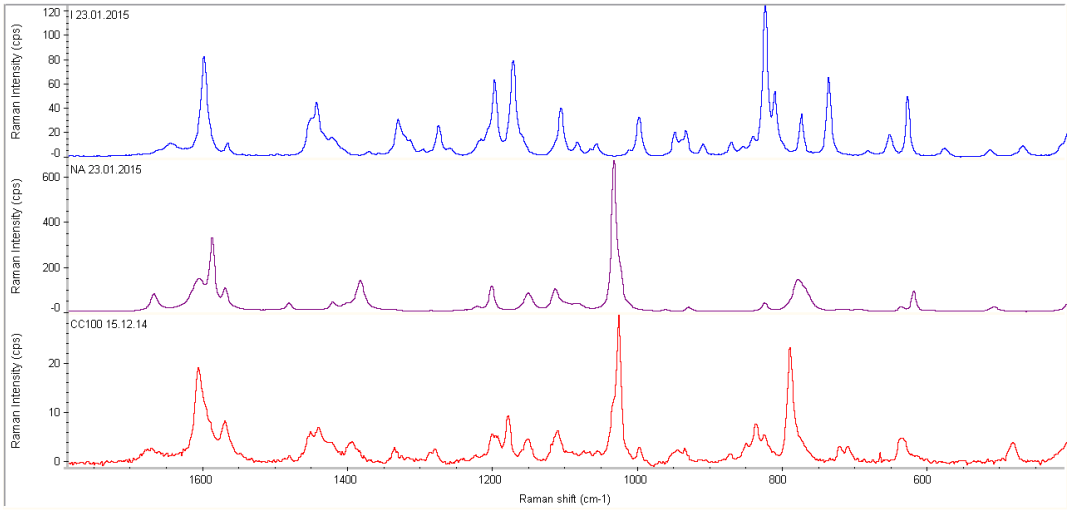

Fig. 5.78. Raman spectra of Ibuprofen (Blue), Nicotinamide (Purple) and co-crystal of Ibuprofen - Nicotinamide (Red)

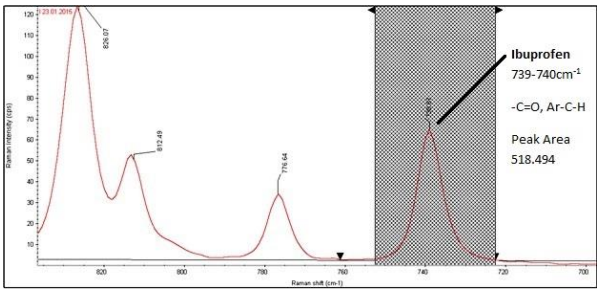

Fig 5.79. Raman spectrum of Ibuprofen showing -C=O, Ar- C-H peak area at 739-740cm^{-1}

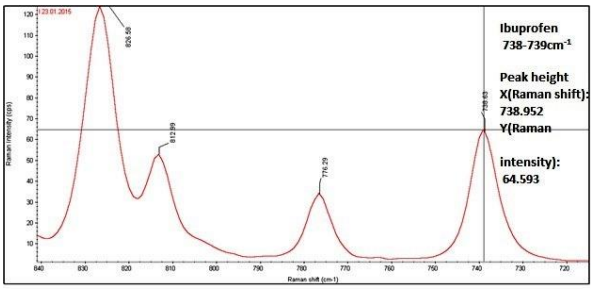

Fig.5.80. Raman spectrum of Ibuprofen showing -C=O, Ar- C-H peak height at 738-739cm^{-1}

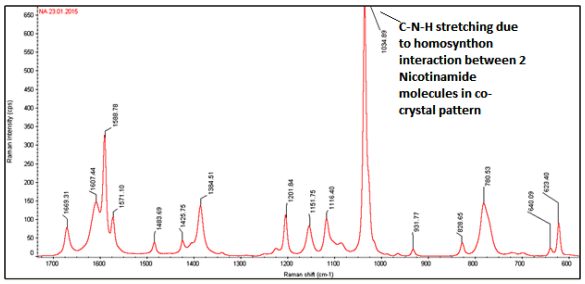

Fig.5.81. Raman spectrum of Nicotinamide showing -C-N- H stretching at 1034cm^{-1}

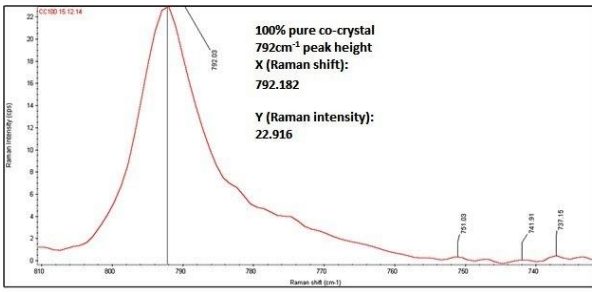

Fig.5.82. Raman spectrum showing characteristic peak (peak height) of 100% pure co-crystal at 792cm^{-1}

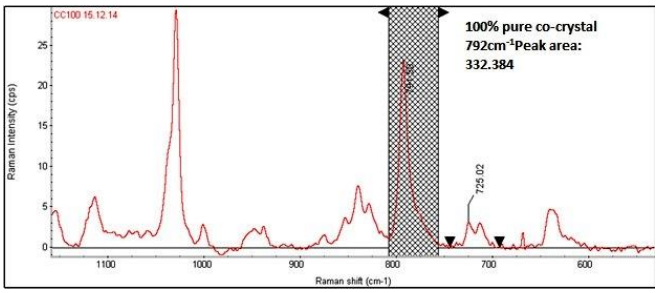

Fig.5.83. Raman spectrum showing characteristic peak (peak area) of 100% pure co-crystal at 792cm^{-1}

5.4.7. Raman spectroscopic analysis of dilutions of Ibuprofen with IBU-NA co-crystals - peak area and peak height analysis

The peak height and peak area analysis has been carried out using TQ Analyst from DXR Smart Raman spectrophotometer by Thermo Scientific from previously collected full Raman spectra (CoC1 to CoC9).

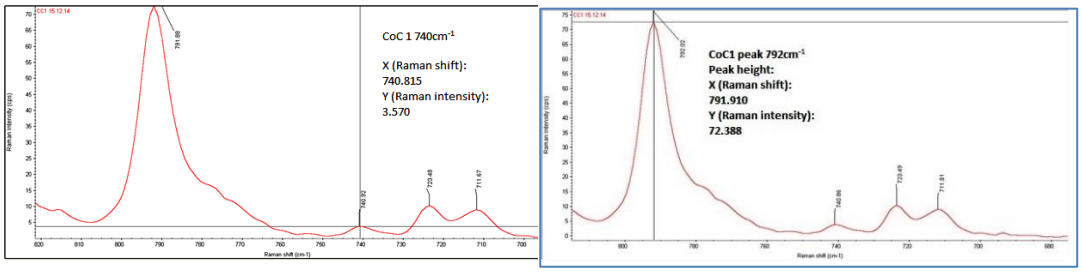

a) b)

Fig. 5.84. Raman spectra showing peak height of CoC 1 a) at 740cm^{-1} (3.570) and b) at 792cm^{-1} (72.388)

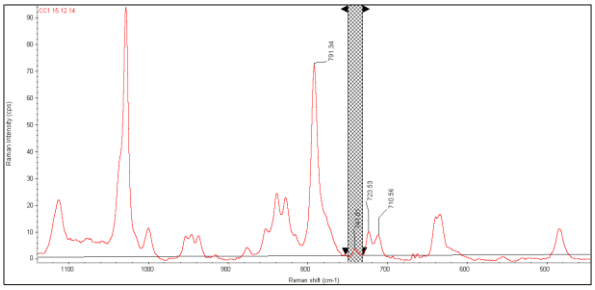

a)

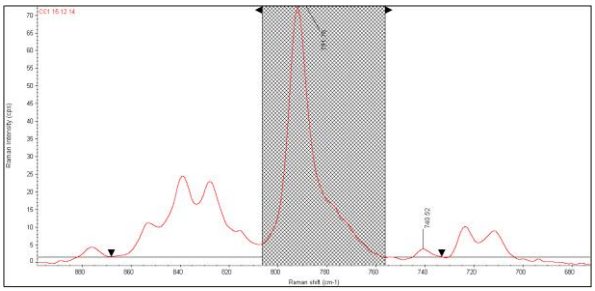

b)

Fig. 5.85. Raman spectra showing peak area of CoC 1 peak at a)740cm^{-1} (12.072) and b) 792cm^{-1} (960.085)

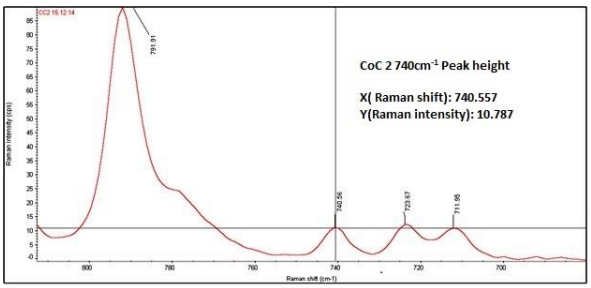

a)

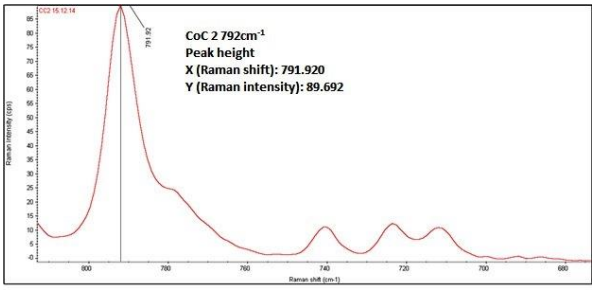

b)

Fig. 5.86. Raman spectra showing peak height of CoC 2 peak at a) 740cm^{-1} (10.787) and b) 792cm^{-1} (89.692)

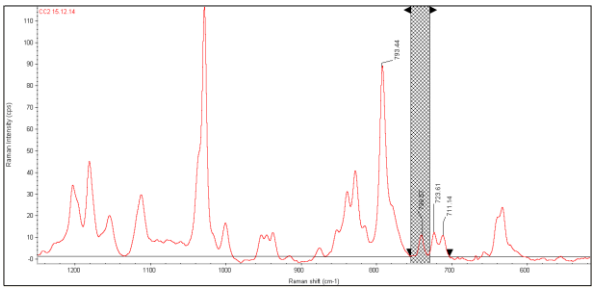

a)

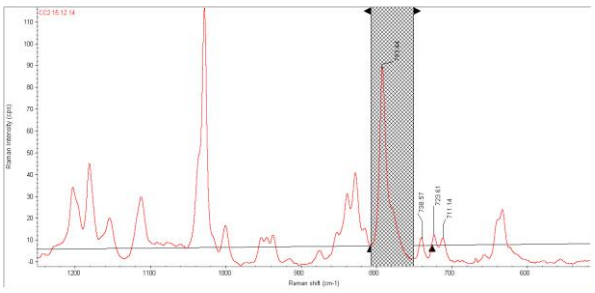

b)

Fig. 5.87. Raman spectra showing peak area of CoC 2 peak at a) 740cm^{-1} (74.786) and 792cm^{-1} (904.357)

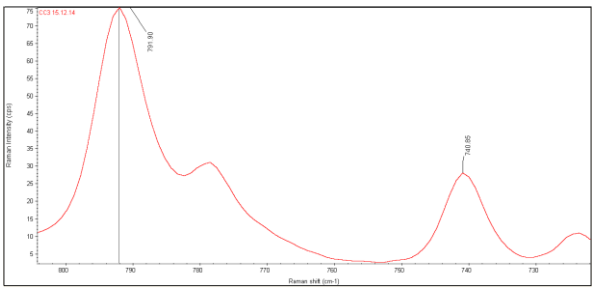

a)

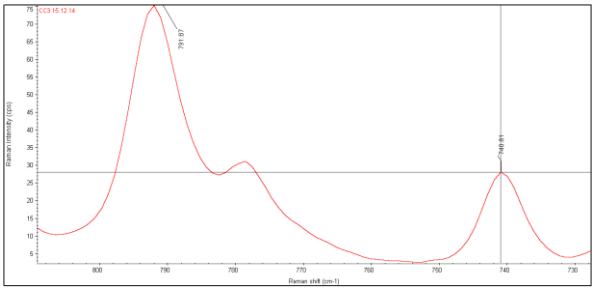

b)

Fig. 5.88. Raman spectrum showing peak height of CoC 3 peaks at a) 740cm^{-1} (7.152) and 792cm^{-1} (27.886)

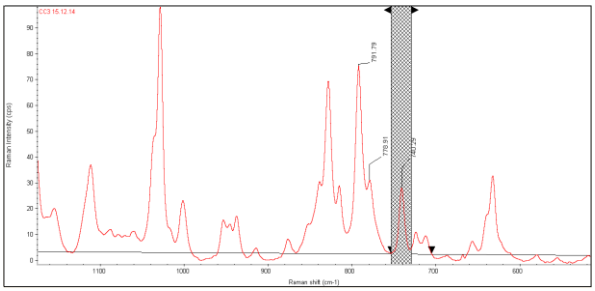

a)

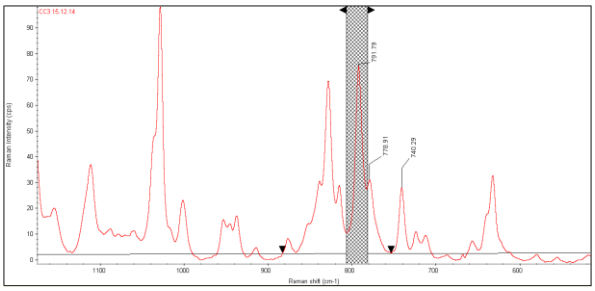

b)

Fig.5.89. Raman spectra showing peak area of CoC 3 peak at a) 739cm^{-1} (205.234) and b) 792cm^{-1} (852.881)

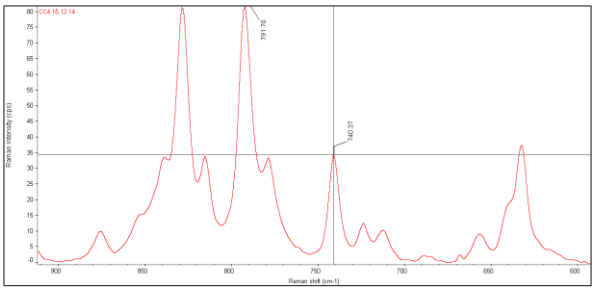

a)

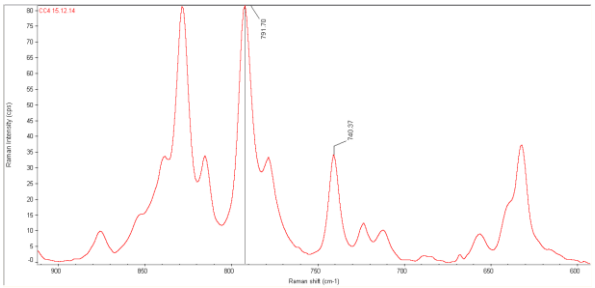

b)

Fig.5.90. Raman spectra showing peak height of CoC 4 peak at a) 740cm^{-1} (34.199) and b) 792cm^{-1} (81.499)

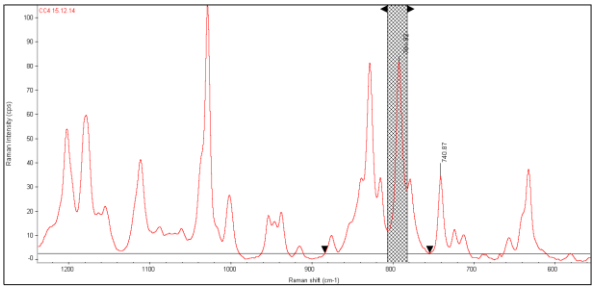

a)

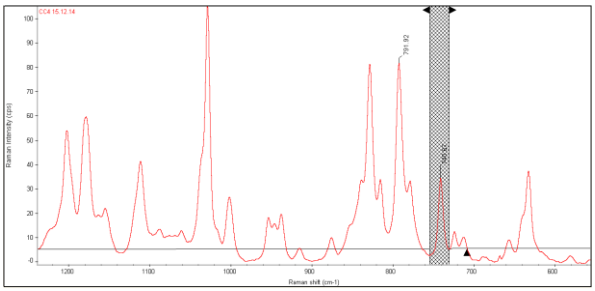

b)

Fig.5.91. Raman spectra showing peak area of CoC 4 peak at a) 739cm^{-1}

(181.011) and b) 792cm^{-1} (899.333)

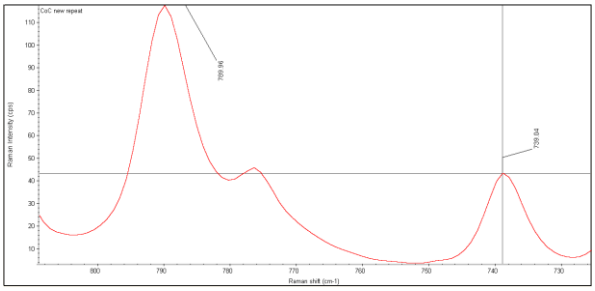

a)

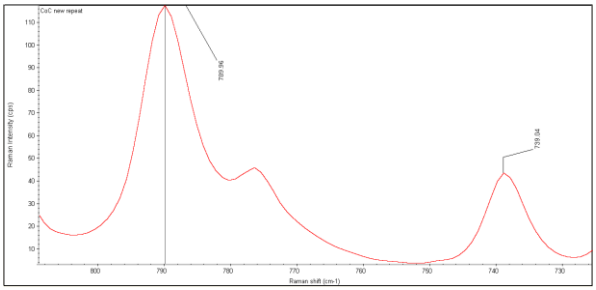

b)

Fig. 5.92. Raman spectra showing peak height of CoC 5 peak at a) 740cm^{-1} (43.194) and **b) 792cm^{-1} (117.359)**

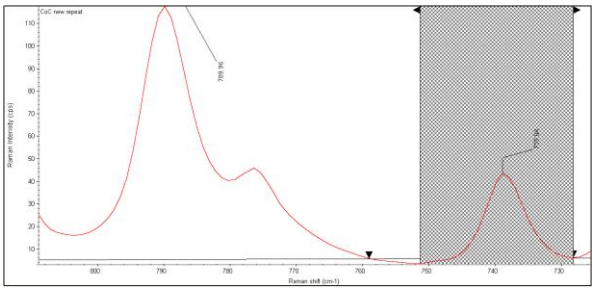

(a)

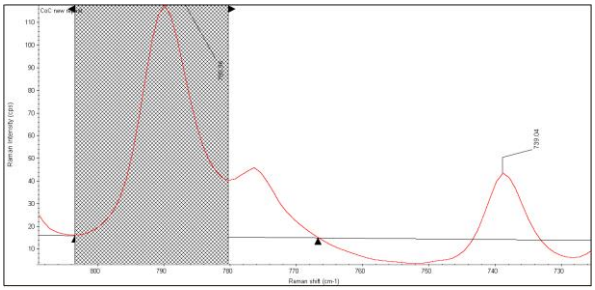

(b)

Fig.5.93. Raman spectra showing peak area of CoC 5 peak at

b) 740cm^{-1} (258.881) and b) 792cm^{-1} (Peak area: 985.634)

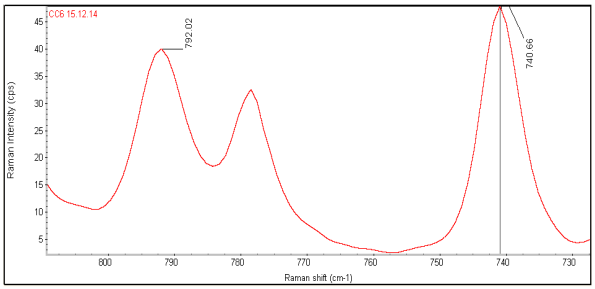

a)

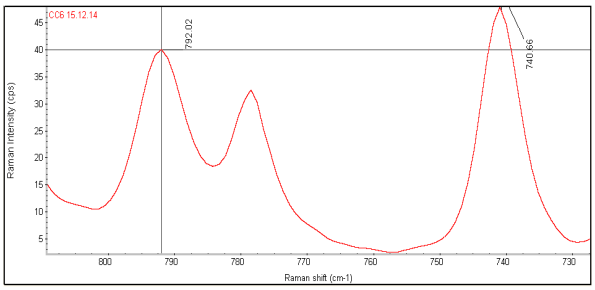

b)

Fig.5.94. Raman spectra showing peak height of CoC 6 peak at

a) 740cm^{-1} (47.832) and b) 792cm^{-1} (39.954)

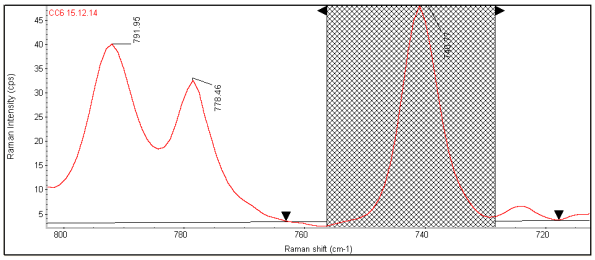

a)

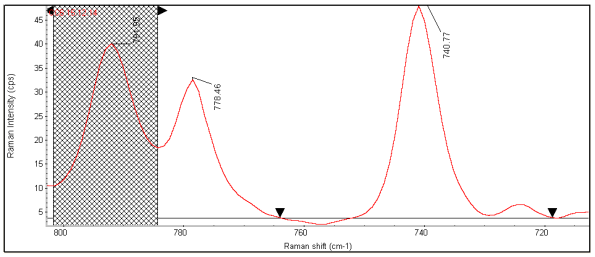

b)

Fig.5.95. Raman spectra showing peak area of CoC 6 peak at

a) 740cm^{-1} (346.333) and b) 792cm^{-1} (371.142)

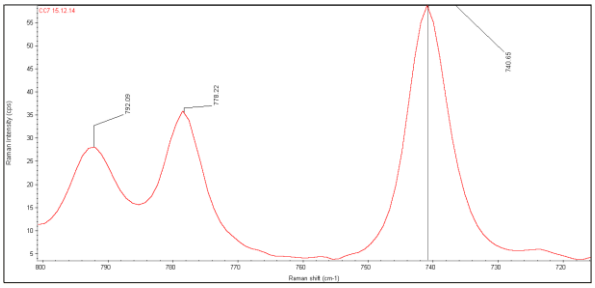

a)

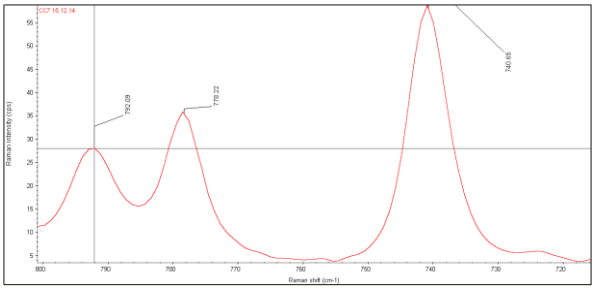

b)

Fig.5.96. Raman spectra showing peak height of CoC 7 peak at

a) 740cm^{-1} (58.597) and b) 792cm^{-1} (27.912)

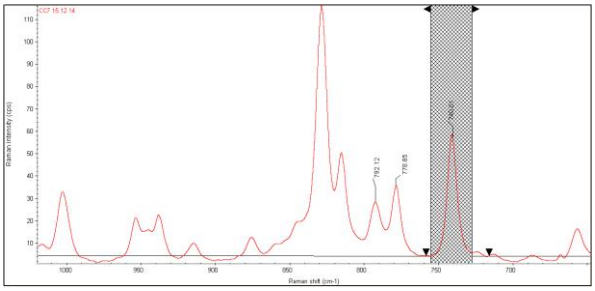

a)

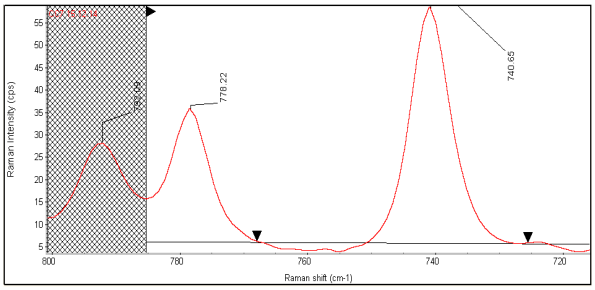

b)

Fig. 5.97. Raman spectra showing peak area of CoC 7 peak at

a) 740cm^{-1} (450.829) and b) 792cm^{-1} (209.074)

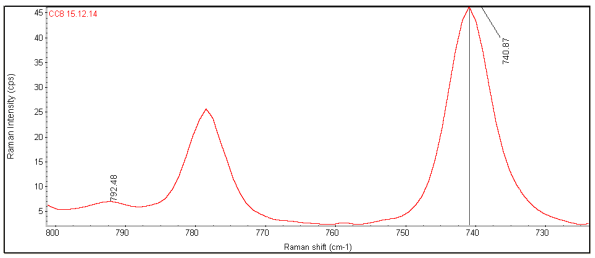

a)

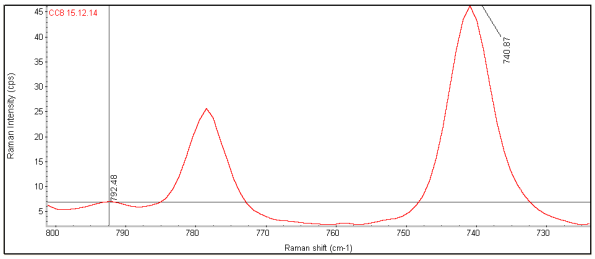

b)

Fig.5.98. Raman spectra showing peak height of CoC 8 peak at a) 740cm^{-1} (46.113) and b) 792cm^{-1} (6.775)

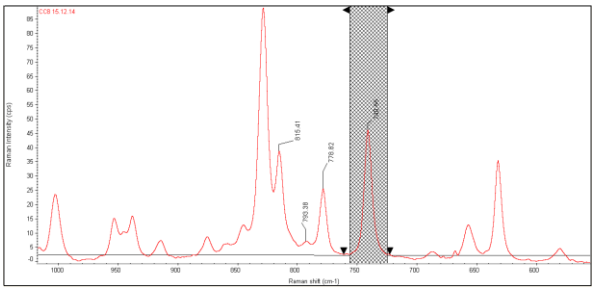

a)

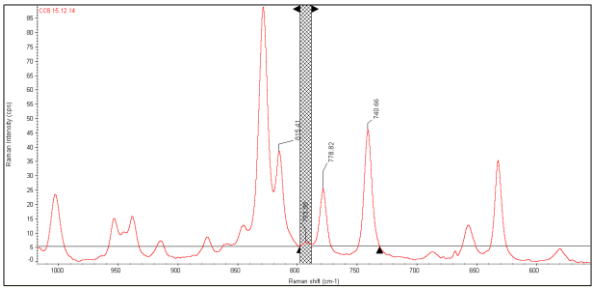

b)

Fig. 5.99. Raman spectra showing peak area of CoC 8 peak at a) 740cm^{-1} (372.309) and b) 792cm^{-1} (8.174)

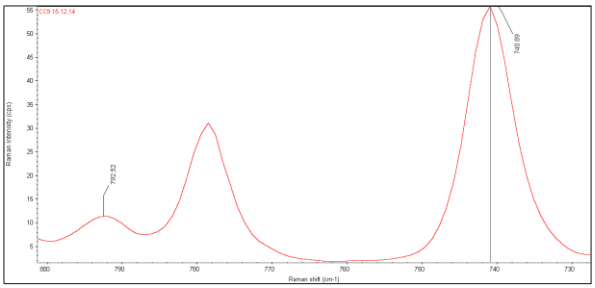

a)

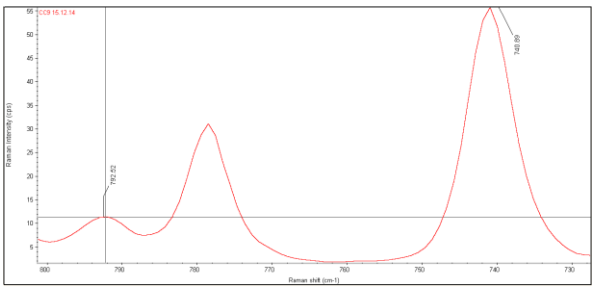

b)

Fig.5.100. Raman spectra showing peak height of CoC 9 peak at a) 740cm^{-1} (55.679) and b) 792cm^{-1} (11.237)

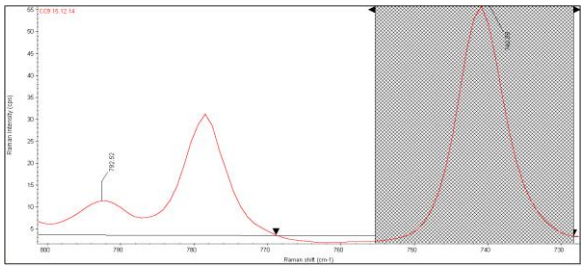

a)

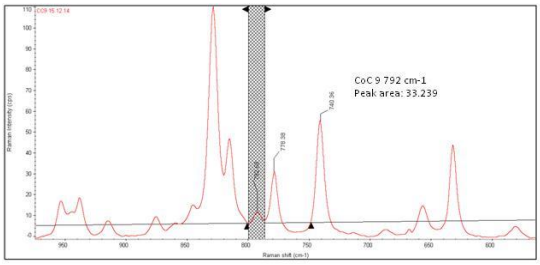

b)

Fig.5.101. Raman spectra showing peak area of CoC 9 peak at a) 740cm^{-1} (412.616) and 792cm^{-1} (33.239)

Generation of calibration curves has been carried out using peak height and peak area values obtained from Raman spectra of dilutions of Ibuprofen with IBU-NA co-crystals from this analysis (section 5.4.7.). Characteristic peaks corresponding to Ibuprofen (740 cm^{-1}) and pure co-crystal of IBU-NA (792 cm^{-1}) have been selected while selecting peak height and peak area values obtained from Raman spectra of all dilutions.

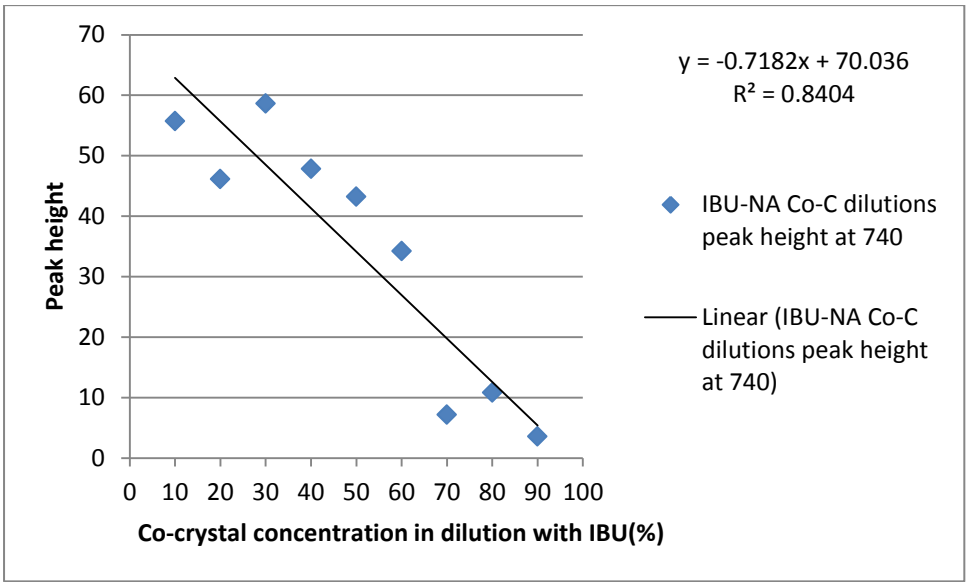

Fig.5.102. Calibration curve showing Ibuprofen and IBU-NA co-crystal concentration - peak height at 740cm^{-1}

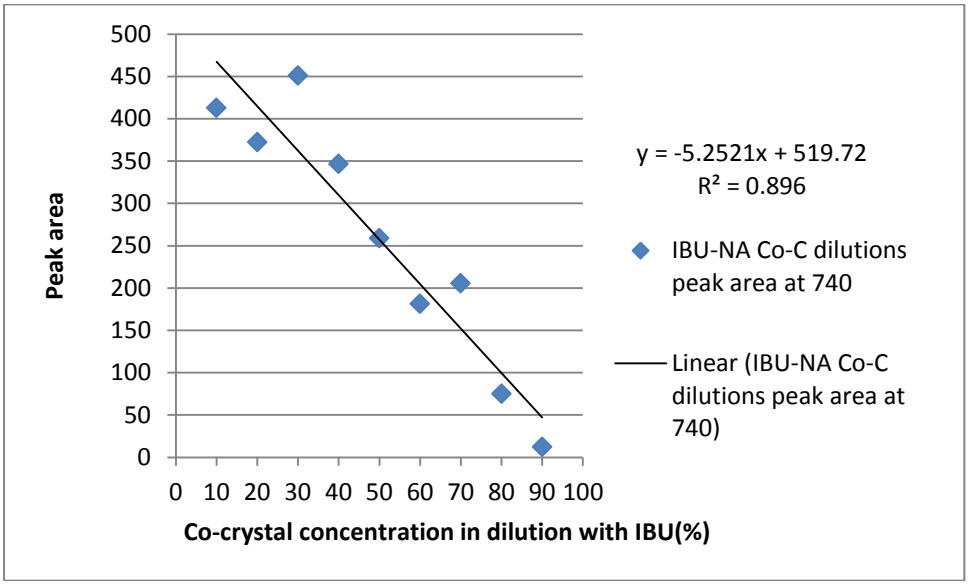

Fig. 5.103. Calibration curve showing Ibuprofen and IBU-NA co-crystal concentration - peak area at 740cm^{-1}

Correlation coefficient values were obtained from calibration curves generated for Ibuprofen and co-crystal concentration using peak height and peak area at 740cm^{-1} (Fig.5.102. and Fig.5.103) however the correlation coefficients determined for the fits are relatively low.

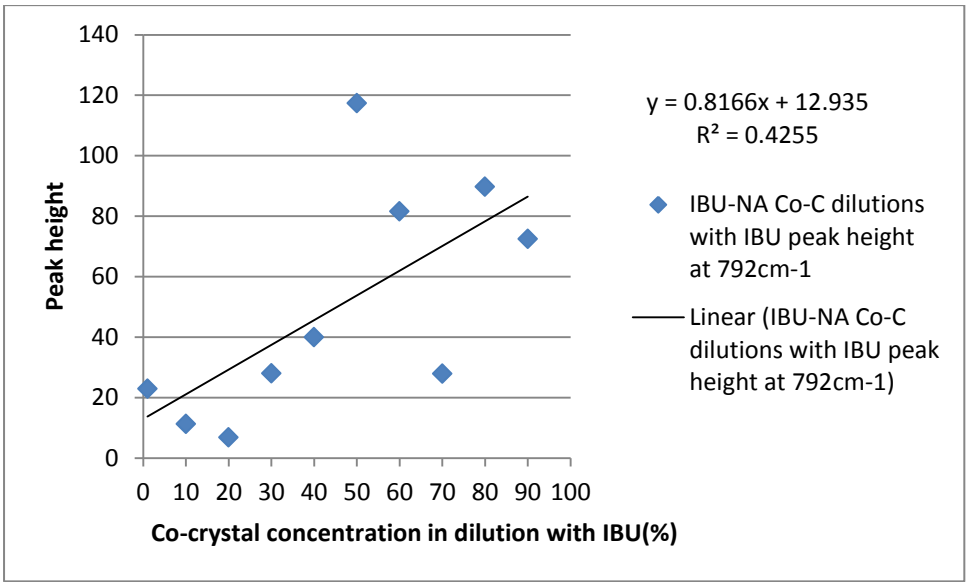

Fig.5.104. Calibration curve showing IBU-NA co-crystal concentration - peak height at 792cm^{-1}

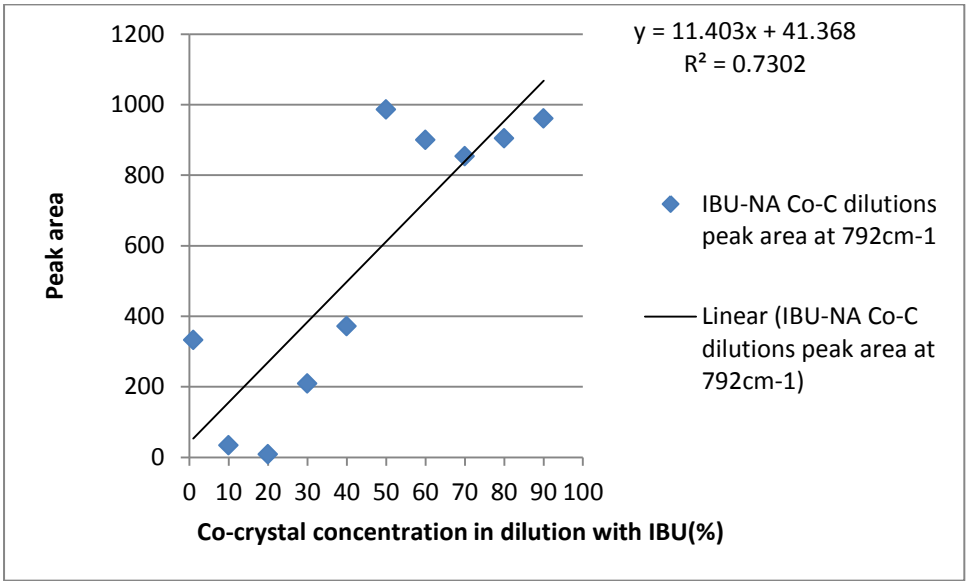

Fig.5.105. Calibration curve showing IBU-NA co-crystal concentration - peak area at 792cm^{-1}

From the calibration curves generated from peak height and peak area analysis of IBU-NA co-crystal concentration at 792cm^{-1} which corresponds to pure co-crystal of IBU-NA co-crystal, it was observed that low correlation coefficient values were obtained (Fig.104. and Fig.105.). This clearly indicates peak height and peak area analysis was not completely useful in

predicting co-crystal concentration in dilutions of IBU-NA co-crystal with Ibuprofen. Also it shows that this analysis is particularly inaccurate at lower concentrations of IBU-NA co-crystal. Hence, it was decided to generate a calibration curve using chemometric analysis of the full Raman spectra of dilutions of IBU-NA co-crystals with pure Ibuprofen (section 5.48).

5.4.8. Raman spectroscopy - Calibration curve

To determine purity of co-crystals of Ibuprofen and Nicotinamide and their correlation with pure Ibuprofen concentration calibration curve was generated using TQ Analyst using the full Raman spectra.

All spectra (CoC1 to CoC9) were collected using 80mW laser power, 25µm slit at 780nm with estimated spot size of 3.1µm and estimated resolution of 5.0 to 9.2cm^{-1}. 2 scans of 60s acquisition each were collected. New chemometric method was created for preparing calibration curve for prediction of concentration of Ibuprofen and co-crystals of Ibuprofen and Nicotinamide using TQ analyst 8 by Thermoscientific. Partial least squares (PLS) method was selected with standard normal variate and second derivative spectra were selected for the study. Spectral data normalization was carried out by using mean centering technique.

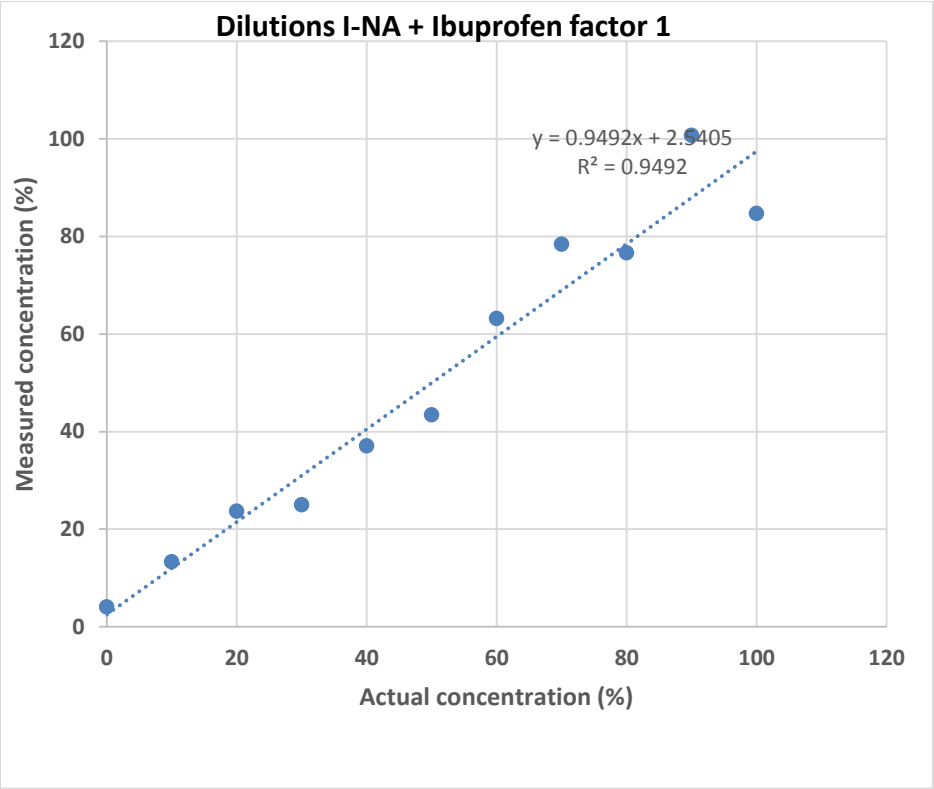

Fig.5.106. Calibration curve: Ibuprofen-Nicotinamide co-crystals + Ibuprofen using data exported from TQ Analyst to Microsoft excel from Raman spectroscopy results

Coefficient correlation (r^2) of 0.9492 with RMSEC (Root mean square error of calibration) value of 7.13 was obtained with 1 factor (Fig.5.106.) indicating a much better fit than for the peak area and height calibration curves discussed in the previous section.

5.5. Preparation and characterization co-crystals of Carbamazepine and Nicotinamide

5.5.1. DSC results

DSC analysis of co-crystals of Carbamazepine-Nicotinamide has been carried out to study thermal properties of co-crystals. In the DSC profile of physical mixture a peak at 127ºC indicates melting of Nicotinamide (Fig.

5.107.). Presence of a sharp peak at 161.118 ºC indicates melting of pure co-crystal of CBZ-NA (Fig. 5.108).

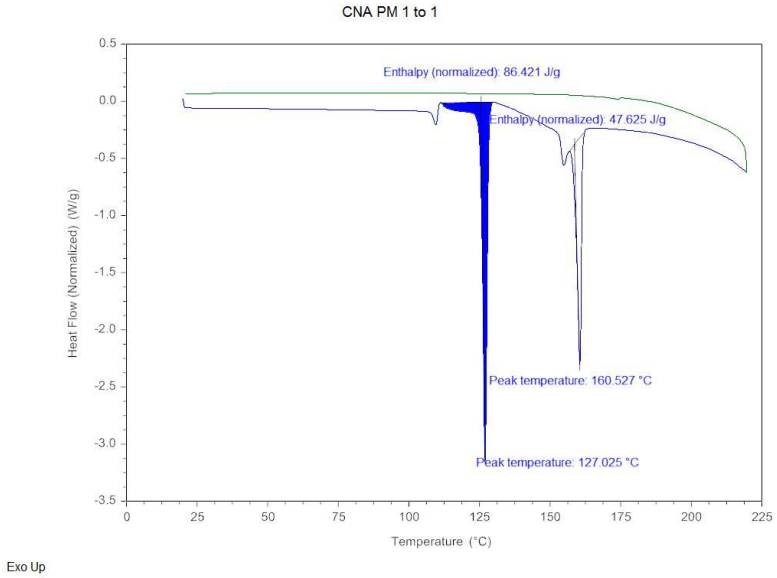

Fig.5.107. DSC profile of Carbamazepine-Nicotinamide physical mixture

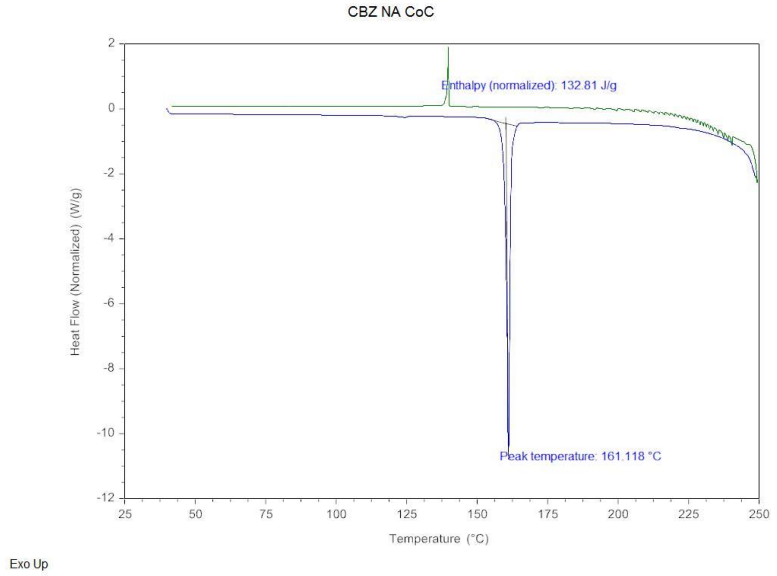

Fig.5.108. DSC profile of Carbamazepine-Nicotinamide co-crystal

5.5.2. Calibration curve generation from DSC results

DSC profiles obtained in Trios format were exported in Microsoft excel for generation of calibration curve using enthalpy values. A calibration curve has

been generated by plotting a graph of actual concentration of dilutions co-crystals with CBZ Vs measured concentration of dilutions co-crystals with CBZ from DSC enthalpy data.

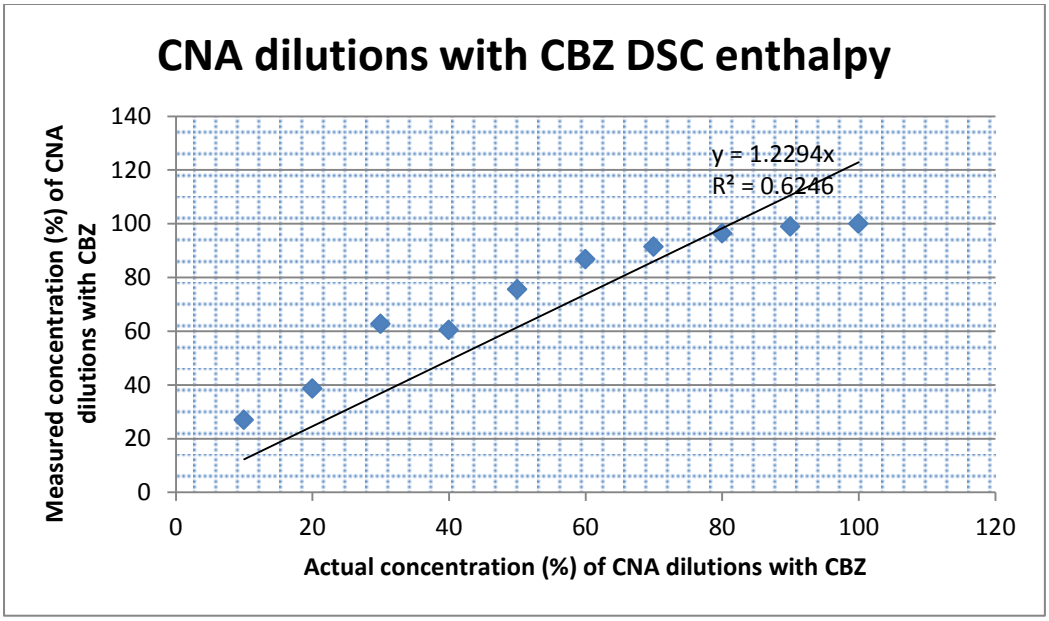

Fig.5.109. Calibration curve generated for CNA dilutions with CBZ concentration (actual) Vs Measured concentration (%) from DSC enthalpy

Coefficient of correlation of 0.6246 was obtained from calibration curve (Fig.5.109.).

5.5.3. FTIR analysis - calibration curve

FTIR analysis of Carbamazepine-Nicotinamide (CBZ - NA) co-crystal dilutions (10-100%) with Carbamazepine has been carried out using Nicolet is50 ATR FTIR by Thermoscientific. Samples have been analysed at 32 scans with 4cm^{-1} resolution. Calibration curve has been generated from FTIR spectra using TQ analyst and Microsoft excel.

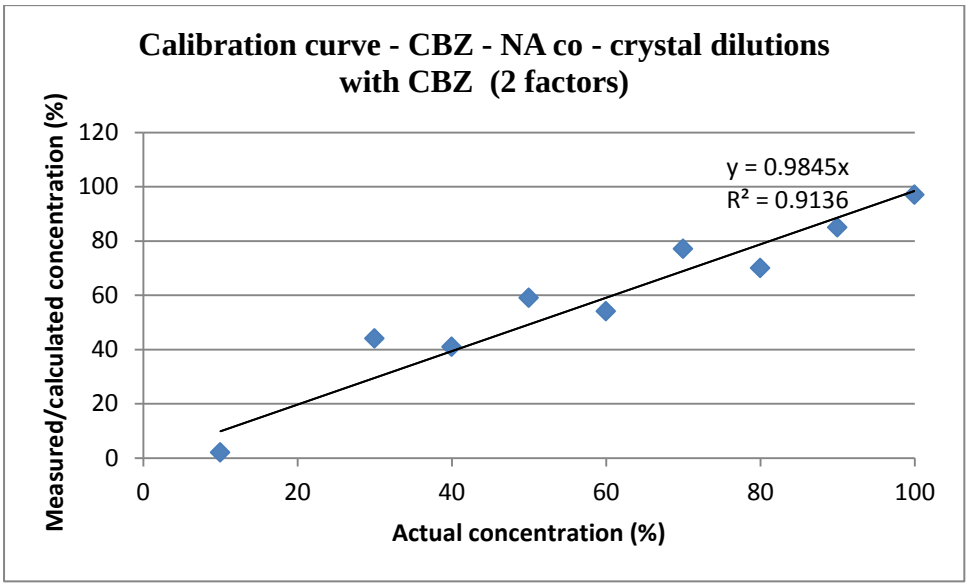

Fig.5.110. Calibration curve – CBZ-NA co-crystal dilutions with CBZ using Microsoft excel (2 factors)

Correlation coefficient value of 0.9136 was obtained from the calibration curve generated using data obtained from TQ analyst using 2 factors for CBZ-NA co-crystal dilutions with Ibuprofen (Fig. 5.110.). This was carried out for the accuracy of the results.

5.5.4. Raman spectroscopy - Calibration curve

Dilutions of co-crystals of Carbamazepine-Nicotinamide (Table 5.13.) with Carbamazepine have been prepared by making physical mixtures using mortar and pestle. Off-line Raman spectroscopic analysis of these dilutions along with physical mixture of Carbamazepine - Nicotinamide (1:1) and co-crystals has been carried out using DXR smart Raman spectrophotometer by Thermoscientific.

All spectra were collected using 80mW laser power, 25µm slit at 780nm with 2 scans of 10s acquisition each.

New chemometric method was created for generating calibration curve for prediction of concentration of Carbamazepine and co-crystals of

Carbamazepine and Nicotinamide using TQ analyst 8 by Thermoscientific. Partial least squares (PLS) method was selected with standard normal variate and second derivative spectra were selected for the study. Spectral data normalization was carried out by using mean centering technique.

Sample name	% of co-crystals of Carbamazepine - Nicotinamide	% of pure Carbamazepine
CNA1	90	10
CNA2	80	20
CNA3	70	30
CNA4	60	40
CNA5	50	50
CNA6	40	60
CNA7	30	70
CNA8	20	80
CNA9	10	90

Table 5.13. Dilutions of physical mixtures of co-crystals of Carbamazepine and Nicotinamide with Carbamazepine.

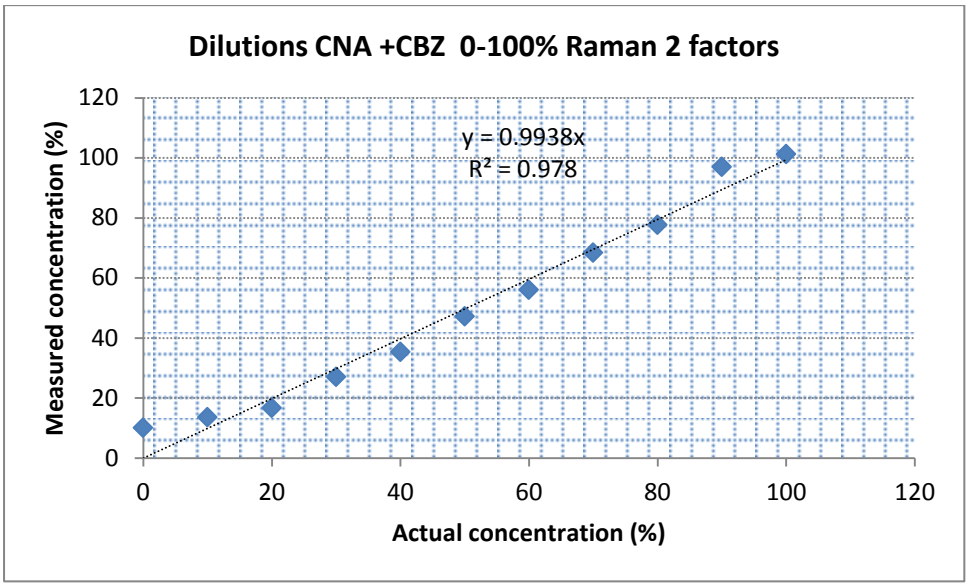

Fig. 5.111. Calibration curve obtained from Raman spectra of dilutions of co-crystals of Carbamazepine-Nicotinamide (0-100%) with Carbamazepine

Using TQ analyst 8, coefficient correlation (r^2) of 0.978 with RMSEC (Root mean square error of calibration) value of 4.66 was obtained with 2 factors (Fig. 5.111).

The value of coefficient of correlation obtained from calibration curve using DSC enthalpy data generated from CBZ - NA co - crystals was 0.6246 (Fig.5.109.) whereas the correlation coefficient value obtained from Raman spectroscopic result - generated calibration (Fig 5.111.) was 0.978. A good correlation value has been obtained using Raman spectroscopy. From this we can conclude that Raman spectroscopy is more sensitive than DSC.

5.5.5. Comparison of FTIR, DSC and Raman curves for CBZ-NA co-crystal quantity determination

Co - crystals of CBZ - NA were analysed by DSC, FTIR and Raman spectroscopy. Calibration curves were generated using the data obtained from these studies.

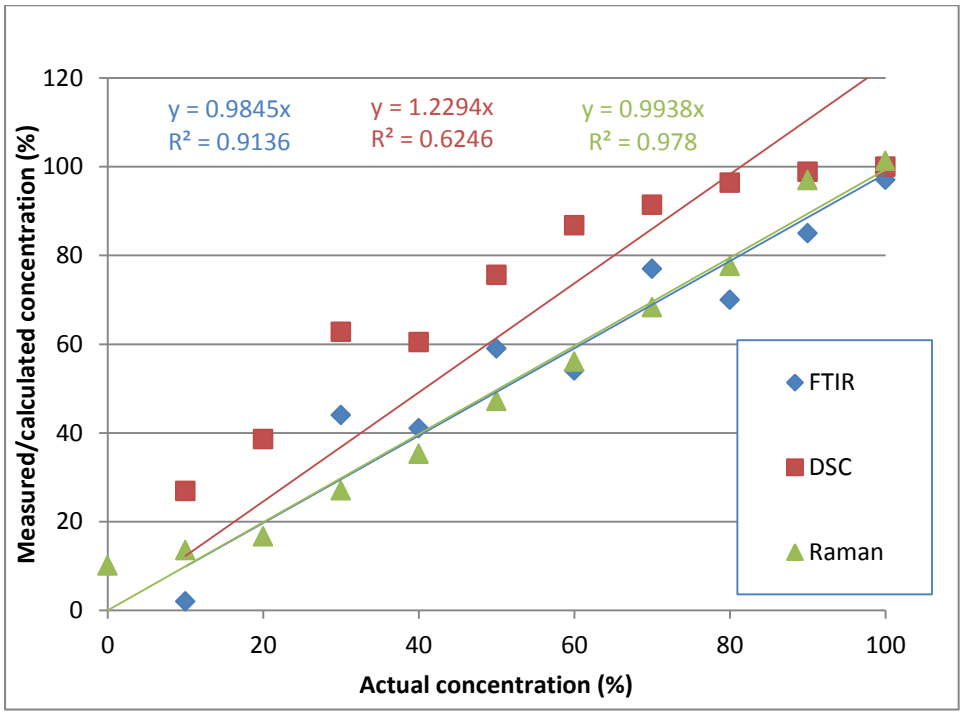

Fig.5.112. Comparison of FTIR, DSC and Raman calibration curves for CBZ-NA co-crystal

Fig.5.112. shows difference between coefficient of correlation obtained from calibration curves obtained using these methods. Coefficient of correlation value obtained from Raman spectroscopic studies has been found to be higher than the coefficient correlation valued obtained from the DSC and FTIR calibration curves. This indicates superiority of Raman spectroscopy over DSC and FTIR analysis for co-crystal concentration determination in addition to its being able to measure this in-line during the manufacture.

Chapter 6 - Conclusions and Further work

The present work was focused on studying suitability of Raman spectroscopy as a PAT technique for monitoring of solid dispersion preparation using hot melt extrusion. Raman spectroscopy has been used for studying solid dispersions of Carbamazepine - Kollidon VA64, Carbamazepine - Soluplus as well as co-crystals of Ibuprofen - Nicotinamide and Carbamazepine - Nicotinamide. To conclude, key findings from the present work are listed below and further work on these topics has been suggested.

Conclusions

Experiment 1

- Solid dispersions of CBZ - Kollidon VA64 with drug loading up to 30% were extrudable during HME while 40% drug loading SDs produced a liquid not suitable for extrusion.
- An increase in the concentration of CBZ decreased the solid dispersion Tg.
- Decrease in complex viscosity with increasing drug loading indicates the platicising effect of the drug upon the formulation.
- Complex viscosity also decreases with increasing shear rate indicating shear thinning of the formulation.
- In order to extrude the formulations it was still necessary to add Triethyl acetate (5%) to gain the desired plasticisation for SD preparation. Differences between Raman spectra for physical mixtures and solid dispersions show the formation of solid dispersions.

- From FTIR and Raman spectroscopy there exists the possibility of hydrogen bonding between the NH_2 group of CBZ with nitrogen or C=O of acetate or pyrrolidone of Kollidon VA64.

- From PXRD it can be confirmed that solid dispersions were prepared and the drug was in the amorphous form.

Experiment 2

- From rheological studies, Soluplus was found to be stable (for extrusion) above 140°C.

- During hot stage microscopic studies no sign of degradation of Soluplus up to a temperature of 220°C was observed.

- The correlation coefficient value from the off-line Raman calibration for CBZ- Soluplus SDs was found to be reduced when compared to the calibration value obtained from in-line Raman calibration.

- Degradation mechanism of CBZ was studied based on yellow colouration of SDs.

Experiment 3

- An optimised and reproducible method was developed for the preparation of IBU-NA co-crystals using microwave radiation. Variation of temperature and holding time confirm the impact of microwave power on co-crystal purity as confirmed by DSC, PXRD as well as Raman and FTIR spectroscopies.

- IBU-NA co-crystals were diluted with further IBU to produce calibration samples of known percentage co-crystals. Calibration curves for these were produced using DSC as well as Raman and FTIR spectroscopies.

Experiment 4

- CBZ-NA co-crystals were prepared using a solvent method and dilutions with further CBZ were prepared for the construction of calibration curves using Raman and FTIR spectroscopies as well as DSC.

- A higher correlation coefficient value for the calibration curve produced using Raman spectroscopy, compared to those for DSC and FTIR calibration curves, indicates the potential for the use of Raman as an accurate in-line PAT tool.

Further work

- In-line Raman spectroscopic monitoring of solid dispersions of CBZ - Kollidon VA64 should be carried out using series collection tool in Omnic software. Preliminary work using this technique with CBZ-Soluplus SD manufacture has been carried out since thesis submission showing promising results.
- Analysis of co-crystals of IBU-NA prepared using solvent-evaporation method needs to be completed (PXRD, DSC, FTIR and Raman spectroscopic analysis). These results can then be compared to the extrusion-based manufacturing of IBU-NA co-crystals (after preparation) as well as to the co-crystals manufactured using microwave radiation.

- PXRD analysis of co-crystals of CBZ-NA was not carried out due to the working condition of the Bruker diffractometer and this should be performed to further prove efficient co-crystal manufacture.
- Microwave method for the preparation of co-crystals of CBZ-NA can be developed through variation in temperature and holding time in the similar manner used for the preparation of IBU-NA co-crystals.
- Preparation of CBZ - NA co-crystals by HME and its in-line monitoring using Raman spectroscopy should be performed. As part of this study, in-line Raman spectroscopic monitoring results should be compared to off-line Raman spectroscopic analysis carried out on samples collected from various zones of extrusion (feeding/mixing/towards die etc.). This would allow application of Raman as a PAT tool for co-crystal manufacture as well as determining the mechanism of co-crystal formation.

References

Agarwal, P. and Berglund, K. A. (2003) In-situ Monitoring of Calcium carbonate polymorphs during batch crystallization in the presence of polymeric additives using Raman spectroscopy. *Crystal Growth and Design,* 3 (5)**,** 941-946.

Ahuja, N., Katare, O. P. and Singh, B. (2007) Studies on dissolution enhancement and mathematical modeling of drug release of a poorly water- soluble drug using water - soluble carriers. *Eur.J.Pharm.Biopharm,* 65**,** 26-38.

Al- Khanbashi, A., Dhamdere, M. and Hansen, M. (1998) Application of in-line fiber-optic Raman spectroscopy to monitoring emulsion polymerization reactions. *Appl. Spectrosc. Rev.,* 33**,** 115-131.

Al-Zoubi, N., Koundourellis, J. E. and Malamataris, S. (2002) FTIR and Raman spectroscopic methods for identification and quantification and quantitaton of orthorhombic and monoclinic paracetamol in powder mixes. *J.Pharm.Biomed.Anal.,* 29**,** 459-467.

Ali, S., Velaga, S. and Jouyban, A. (2014) solubility of carbamazepine - nicotinamide cocrystal in ethanol - water mixtures. *Fluid Phase Equilibria,* 363**,** 97-105.

Alig, I., Fischer, D., Lellinger, D. and Steinhoff, B. (2005) Combination of NIR. Raman, Ultrasonic and dielectric Spectroscopy for in-line monitoring of the extrusion process. *Macromol. Symp,* 230**,** 51-58.

Amidon, G. L., Lennernas, H., Shah, V. P. and Crison, J. R. (1995) Theoretical basis for a biopharmaceutical drug classificaton: the

correlation of in vitro drug product dissolution and in vitro bioavailability. *Pharm.Res.,* 12 (3)**,** 413-420.

Andrew, J. J., Browne, M. A., Clark, I. E. and Hancewicz, A. M. (1998) Raman imaging of emulsion systems. . *Appl.Spectrsc.,* 52**,** 790-6.

Anton Paar (2015) *Anton Paar home page.* Available from: www.anton-paar.com

Arruebarren de Baez, M., Hendra, P. J. and Judkins, M. (1995) The Raman spectra of oriented isotactic polypropylene. *Spectrochim Acta,* 51A (12)**,** 2117-2124.

Arunachalam, A. M., Karthikeyam, M., Kishore Konam, K., Prasad, P., Sethuraman, S. and Ashutoshkumar, S. (2010) Solid dispersions: a review. *Current Pharma Research,* 1**,** 1-9.

Auer, M. E., Griesser, U. J. and Sawatzki, J. (2003) Qualitative and quantitative study of polymorphic forms in drug formulations by near infrared FT-Raman spectroscopy. *J.Mol.Str.,* 661**,** 307-317.

Barman, H. (2013) The blue mystery and the Raman effect.

Barnes, S., Gillian, J., Diederich, J. and Ertl, E. (2008) In process monitoring of polymorphic form conversion by raman spectroscopy and turbidity measurements. *American pharmaceutical review,* 11 (3)**,** 82-5.

Barnes, S. E., Brown, E. C., Sibley, M. G., Edwards, H. G. M. and Coates, P. D. (2005) Vibrational spectroscopic and ultrasound analysis for the in-line monitoring of poly (ethylene vinyl acetate) copolymer during melt extrusion. *Analyst* 130**,** 286-292.

BASF (2011) *BASF Homepage.* Available from: http://www.pharma-ingredients.basf.com/

Bauer, C., Amram, B., Agnely, M., Charmot, D., Sawatski, J., Dupuy, D. and Huvenne, J. P. (2000) On- line monitorng of a latex emulsion polymerization by fiber-optic FT- Raman spectrscopy. *Appl Spectrosc,* 54**,** 528-535.

Bolton, B. P. and Prasad, P. N. (1978) Phase transitions of polyphenyls. *Chem Phys,* 35**,** 331-344.

Bower, D. I. and Maddams, W. F. (1989) *The vibrational spectroscopy of polymers.* Cambridge: Cambridge Unversity Press.

Braatz, R. D. (2002) Advanced control of Crystallzation process. *Annual Reviews in Control,* (26)**,** 87-99.

Breitenbach, J. (2002) Melt extrusion: from process to drug delivery technology. *Eur.J.Pharm.Biopharm,* 54 (2)**,** 107-117.

Breitenbach, J. and J., L. (2003) Two concepts: one technology: controlled release and solid dispersion with meltrex. *Modified Drug delivery technology*.

Breitkreutz, J., El-Saleh, F., Kiera, C., Kleinebudde, P. and Wiedey, W. (2003) Pediatric drug formulations of sodium benzoate: II. Coated granules with a lipophilic binder. *Eur. J. Pharm. Biopharm,* 56**,** 255–260.

Ceballos, A. (2005) Influence of formulations and process variables on in-vitro release of theophylline from directly compressed Eudragit matrix tablets. *Il Farmaco,* 60**,** 913-918.

Ceolin, R. T. S., Gardette, M., Agafonov, V., Dzyabchenkoo, A. and Bachet, B. (1997) X-ray characterization of the triclinic polymorph of carbamazepine. *J.Pharm.Sci.,* 86**,** 1062.

Chalmers, J. M. (2000) *Spectroscopy in process analysis.* New York: Wiley-Blackwell.

Chemburkar, S. R., Spiwek, J. B., Patel, K., Morris, J., Henry, R., Spanton, S., Dziki, W., Porter, W., Quick, J., Bauer, P., Donaubauer, J., Narayanan, B. A., Soldani, M., Riley, D. and McFarland, K. (2000) Dealing with the impact of ritonavir polymorphs on the last stages of bulk drug process development. . *Org. Process Res.Dev.,* 4**,** 413-417.

Chiou, W. L. and Riegelmann, S. (1970) Oral absorption of griseofulvin in dogs: increased absorption via solid dispersionin polyethylene glycol 6000. *J.Pharm.Sci.,* 59**,** 937-942.

Chiou, W. L. and Riegelmann, S. (1971) Pharmaceutical applications of solid dispersion systems. *J. Pharm.Sci.,* 60**,** 1281-1302.

Chokshi, R. and Zia, H. (2004) Hot-Melt Extrusion Technique: A Review. *Iranian Journal of Pharmaceutical Research,* (3)**,** 3-16.

Claybourn, M., Massey, T., Highcock, J. and Gogma, D. (1994) Analysis of processes in latex systems by FT- Raman spectroscpy. *J.Raman Spectrosc.,* 25**,** 123-129.

Coates, P. D. (1995) In-line Rheological Rheological Measurements for Extrusion Process Control. *Measurement and Control,* 28**,** 10-16.

Cox, P. J. (1990) Pharmaceutical thermal analysis—techniques and applications. *Talanta,* 37 (7)**,** i-ii.

Croker, D. M., Hennigan, M. C., Maher, A., Hu, Y., Ryder, A. G. and Hodnett, B. K. (2012) A comparative study of the use of powder X-ray diffraction, Raman and near infrared spectroscopy for quantification of

binary polymorphic mixtures of piracetam. *Journal of Pharmaceutical and Biomedical Analysis,* 63 (0)**,** 80-86.

Cutmore, E. A. and Skett, P. W. (1993) Application of Fourier - transform Raman spectroscopy to a range of compounds of phamaceutical interest *Spectrochim Acta,* 49A**,** 809-818.

Czernicki, W. and Baranska, M. (2013) Carbamazepine polymorphs: Theoretical and experimental spectrscopy studies. *Vibratonal spectr.,* 65**,** 12-23.

Damian, F., Blaton, N., Kinget, R. and Van den Mooter, G. (2002) Physical stability of solid dispersions of the antiviral agent UC-781 with PEG 6000,Gelucire 44/14 and PVP K30. *Int.J. Pharm.,* 244 (1-2)**,** 87-98.

Damian, F., Blaton, N., Naesens, L., Balzarini, J., Kinget, R., Augustijns, P. and Van den Mooter, G. (2000) Physicochemical characterization of solid dispersons of the antiviral agent UC-781 with polyethylene glycol 6000 and Gelucire 44/14. *Eur.J.Pharm.Sci.,* 10**,** 311-322.

Danley, R. L. and Caulfield, P. A. (2015) *DSC Baseline Improvements Obtained by a New Heat Flow Measurement Technique.*

de Beer, T. D. M., Dejaegher, C. B., Walczak, B., Vercruysse, P., Burggraeve, A., Lemos, L., Delattre, Heyden, Y. V., Remon, J. P., Vervaet, C. and Baeyens, W. R. G. (2008) *J.Pharm.Biomed.Anal.,* 48**,** 772-779.

de Waard, H., De Beer, T., Hinrichs, W. L. J., Vervaet, C., Remon, J.-P. and Frijlink, H. W. (2010) Controlled crystallization of the lipophilic drug fenofibrate during freeze-drying: elucidaton of the mechanism by in-line Raman spectroscopy. *AAPS Journal,* 12 (4)**,** 569-575.

Deeley, C. M., Spragg, R. A. and Threlfall (1991) A comparison of FT Raman infra-red and NIR FT Raman spectroscopy for quantitative measurements. *Spectrochim Acta,* 47A**,** 1217-1223.

Desai, J. (2006) Characterization of polymerc dispersions of dimenhydrinate in ethyl cellulose for controlled release. *Int.J. Pharm.,* 308**,** 115-123.

Dhumal, R. S., Kelly, A. L., York, P., Coates, P. D. and Paradkar, A. (2010) Cocrystalization and Simultaneous Agglomeration Using Hot Melt Extrsuion. *Pharm Res,* 27.

Djuris, J., Nikolakakis, I., Ibric, S., Djuric, Z. and Kachrimanis, K. (2013) Preparation of carbamazepine-Soluplus solid dispersions by hot-melt extrusion, and prediction of drug-polymer miscibility by thermodynamic model fitting. *Eur J Pharm Biopharm,* 84 (1)**,** 228-37.

Dong, Z., Sandhu, A. C. H., Choi, D. S., Chikshi, H. and Shah, N. (2007) Evaluation of solid state properties of solid dispersions prepared by hot-melt extrusion and solvent co-precipitation. *Int.J.Pharm.,* 355**,** 141-149.

Douglas, P., Andrews, G. P., Jones, D. S. and Walker, G. (2010) Analysis of in vitro drug dissolution from PCL melt extrusion. *Chemical Engineering Journal*., 164 (2-3), 359- 370.

DrugBank (2005) Drug Bank Version 3.0. Available from: http://www.drugbank.ca/drugs/DB00564.

Eliasson, C., Macleod, N. A., Jayes, L. C., Clarke, F. C., Hammond, S. V., Smith, M. R. and Matousek, P. (2008) Non-invasive quantitative assessment of the content of pharmaceutical capsules using transmission Raman spectroscopy. *J.Pharm.Biomed.Anal.,* 47**,** 221.

Eriksson, L., Johansson, E., Wold, N. and Wold, S. (2001) *Multi and megavariate Data Analysis, Principles and Applications.* Svea: Umetrics AB.

Exeter, U. o. (2013) *Physics and Astronomy.* Exeter, United Kingdom: Available from: newton.ex.ac.uk

FDA (2002) *General Principles of Software Validation; Final Guidance for Industry and FDA Staff* [US Food and Drug Administration (CDER & CBER)]

FDA (2004a) *Guidance for industry: PAT - A framework for innovative pharmaceutical development, manufacturing and quality assurance.*

FDA (2004b) *Pharmaceutical cGMPs for the 21st century- A risk based approach;Final report*

Fevotte, G., Calas, J., Puel, F. and Hoff, C. (2004) Applications of NIR spectroscopy to monitoring and Analyzing the solid state during industrial crystallization Process. *Int. J. Pharm.,* 273**,** 159-169.

Fini, G. (2004) Applications of Raman spectroscopy. *J. Raman Spectroscopy,* 35**,** 335-337.

Ford, J. L. and Mann, T. E. (2012) Fast-Scan DSC and its role in pharmaceutical physical form characterisation and selection. *Adv Drug Deliv Rev,* 64 (5)**,** 422-30.

Frank, C. J. (1998) Raman analysis in Pharmaceuticals in Raman Review. In: *Ann Arbor, MI: Kaiser Optical Systems.* pp. 1-3.

Frank, C. J. (1999) Raman spectroscopy for identity testing: Applications from development to production in the pharmaceutical industry. In:

Biomedical Applications of Raman Spectroscopy. Bellingham, WA: SPIE Press.,

Gervaso, G. J. and Pelletier, M. J. (1997) On-line Raman analysis of PCl_3 reactor material. *At Process* 3**,**7-11.

Gilbert, A. S., Hobbs, K. W., Reeves, A. H. and Hobsn, P. P. (1994) Automated headspace analysis for quality assurance of pharmaceutical vials by Laser raman spectroscopy. *SPIE***,** 391-398.

GNR (2013) *GNR Analytical Instruments Group.* Novara, Italy: Available from: http://www.gnr.it

Goldberg, A. H. (1966) Increasing dissolution rates and gastrointestinal absorption of drugs via solid solutions and eutectic mixtures IV Chloramphenicol-urea system. *J.Pharm.Sci.,* 55**,** 581-583.

Gryczke, S., Schminke, S., Maniruzzaman, M., Beck, J. and Douroumis, D. (2011) Development and evaluation of orally disintegrating tablets (ODTs) containing Ibuprofen granules prepared by hot melt extrusion. *Colloids Surf. Biointerf. ,* 86**,** 275–284

Hernandez-Trejo, N., Hinrichs, W. L. J., Visser, M. R., Muller, R. H., Kayser, O. and Frijlink, E. (2005) Enhancement of in-vitro dissolution rate of the lipophilic drug buparvaquone by incorporation into solid dispersions. *In: PharmSci.Fair.Nice,France*.

Hodges, C. M., Hendra, P. J., Willis, H. A. and Farley, T. (1989) Fourier transform Raman spectroscopy of illicit drugs. *J.Raman Spectrosc.,* 20**,** 745-749.

Hu, Q., Rohani, S. and Jutan, A. (2005) Optimal control of batch cooling seeded crystallizer. *Powder Technology,* 156 (1-2)**,** 170-176.

I., G.-S. and E., M. C. (2003) (Pharmaceutical Extrusion Technology) New York: Marcel Dekker.

ICH (2009) International Conference on Harmonisation(ICH) of Technical requirements for Registration of Pharmaceuticals for Human use, Topic Q8(R2), Pharmaceutical development, Geneva.

Kalantri, P. P., Somani, R. S. and Makhija, D. T. (2010) Raman spectroscopy: a potential technique in analysis of pharmaceuticals. *Pelegia Research Library. Der Chemica Sinica,* 1 (1)**,** 1-12.

Kanig, J. L. (1964) Properties of fused Mannitol in compressed tablets. *J.Pharm.Sci.,* 53**,** 188-192.

Kelly, A. L., Gough, T., Dhumal, R. S., Halsey, S. A. and Paradkar, A. (2012) Monitoring ibuprofen-nicotinamide cocrystal formation during solvent free continuous cocrystallization (SFCC) using near infrared spectroscopy as a PAT tool. *International Journal of Pharmaceutics,* 426 (1-2)**,** 15-20.

Kepa, C., Vallejuelo, D. S. F. and Madariaga, J. M. (2012) Freworks: composition and chemistry through Raman spectroscopy and SEM-SDZ imaging. *Spectroscopy Europe,* 24 (3)**,** 6.

Kobayashi, R., FujiMaki, Y., Ukita, T. and Hiyama, Y. (2006) "Monitoring of Solvent-Mediated Polymorphic Transitions Using in-situ Analysis Tools". *Organic Process Research and Development,* 10**,** 1219-1226.

Kobayashi, Y., Ito, S., Itai, S. and Yamamoto, K. (2000) Physicochemical properties and bioavailability of carbamazepine polymorphs and dihydrate. *Int. J. Pharm.,* 193 (2)**,** 137-146.

Krahn, F. U. and Mielck, J. B. (1987) Relations between several polymorphs and the dihydrate of carbamazepine. *Pharm. Acta Helv.,* 67**,** 247-254.

Langkilde, F. W. (1995) Identification of celluloses with Fourier-transform (FT) mid-infrared, FT-Raman, and near-infrared spectrometry. . *J. Pharm. Biomed. Anal.,* 13**,** 409-14.

Langkilde, F. W., Tekenbergs-Hjelte, L. and Mrak, J. (1997) Quantitative FT-Raman analysis of two crystal forms of a pharmaceutical compound. *J.Pharm.Biomed.Anal.,* 15**,** 687.

Lewis, S., Dhirendra, K., Udupa, N. and Atin, K. (2009) Solid dispersions: A Review. *Pak. J. Pharm. Sci.,* 22 (2)**,** 234-246.

Li, F. (2006) In vitro controlled release of sodium ferulatefrom compritol 888 ATO based matrix tablets. *Int.J. Pharm.,* 324**,** 152-157.

Li, L., AbuBaker, O. and Shao, Z. J. (2006) Characterization of poly(ethylene oxide) as a drug carrier in hot-melt extrusion. *Drug Dev. Ind.Pharm.,* 32 (8)**,** 991-1002.

Lowes, M. M. J., Caira, M. R., Lotter, A. P. and Van Der Watt, J. G. (1987) Physicochemical properties and X-ray structural studies of the trigonal polymorph of carbamazepine. *J.Pharm.Sci.,* 76**,** 744-752.

Mantanus, J., Rozet, E., Van Butsele, K., De Bleye, C., Ceccato, A., Evrard, B., Hubert, P. and Ziemons, E. (2011) Near infrared and Raman spectroscopy as Process Analytical Technology tools for the manufacturing of silicone-based drug reservoirs. *Analytica Chimica Acta,* 699**,** 96-106.

McCreery, R. L. (2000) Raman spectroscopy for chemical analysis.

McGinity, J. W., Zhang, F., Repka, M. and Koleng, J. J. (2001) Hot melt extrusion process as a pharmaceutical process. *American pharmaceutical review,* 4**,** 25-36.

Meyer, M. C., Straughn, A. B. and Jarvi, E. J. (1992) Bioequivalence of Carbamazepine tablets with a history of clinical failures. *Pharm.Res.,* 9 (12)**,** 1612-1616.

Mezger, T. G. (2006) *The Rheology Handbook.* 2 ed. Hannover, Germany: Vincentz.

Michalk, A., Kanikanti, V. R., Hamann, H. J. and Kleinebudde, P. (2008) Controlled release of active as a consequence of the die diameter in solid lipid extrusion. *J. Control. Release* 132 35-41.

Muller, J. and Knop, K. (2010) Feasibility of Raman spectroscopy as PAT tool in active coating. *Drug Dev. Ind. Pharm.,* 36**,** 234-243.

Netzsch (2015) *Functional principle of a heat flux DSC.* Available from: https://www.netzsch-thermal-analysis.com/en/landing-pages/principle-of-a-heat-flux-dsc/

Niemczyk, T. M. and Delgadolopez, M. M. (1998) Quantitative assay of bucinodolol in gel capsules using infrared and raman spectroscopy. *Appl Spectrosc,* 52**,** 513-518.

Norman, C., Thomas, R. and Jaako, A. (2011) *J.Pharm.Biomed.Anal.,* 55**,** 618-644.

O'Brien, L., E., Timmins, P., Williams, A. C. and P., Y. (2004) "Use of in-situ FT Raman spectroscopy to study the kinetics of the Transformation of Carbamazepine polymorphs.". *Journal of Pharmaceutical and Biomedical Analysis,* 36 (2)**,** 335-340.

Ohara, T., Kitamura, S., Kitagawa, T. and Terada, K. (2005) Dissolution mechanism of poorly water soluble drug from extended release solid dispersion system with ethylcellulose and hydroxypropylmethylcellulose. *Int.J. Pharm.,* 302 (1-2)**,** 95-102.

Owusu-Ababio, G., Ebube, N. K., Reams, R. and Habib, M. (1998) Comparative dissolution studies for mefenamic acid-polyethylene glycol solid dispersion systems and tablets. *Pharm.Dev.Technol.,* 3 (3)**,** 405-412.

Particle sciences (2011) *Hot Melt Extrusion.* Bethlehem, USA: Available from: www.particlesciences.com

Patil, S. P. (2014) Generation of 1:1 Carbamazepine -Nicotinamide co-crystal by spray drying. *Eur.J.Pharm Sci.,* 62**,** 251-257.

Perissutti, B., Newton, J. M., Podczeck, F. and Rubessa, F. (2002) Preparation of extruded carbamazepine and PEG 4000 as a potential rapid release dosage form. *Eur. J.Pharm. and Biopharm.,* 53**,** 125-132.

PerkinElmer (2012) *Beginner's guide to thermogravimetric analysis.* Available from:http://www.perkinelmer.co.uk/CMSResources/Images/44-74556GDE_TGABeginnersGuide.pdf

Pokharkar, V. B., Mandpe, L. P., Padamwar, M. N., Ambike, A. A., Mahadik, K. R. and Paradkar, A. (2006) Development,characterization and stabilization of amorphous form of a low Tg drug. *Powder Technol.,* 167 (1)**,** 20-25.

Porter, W. W., Elie, S. C. and Matzger, A. J. (2008) Polymorphism in carbamazepine co-crystals. *Cryst Growth Des,* 8**,** 14-16.

Qiao, N., Wang, K., Schlindwein, W., Davies, A. and Li, M. (2013) In situ monitoring of carbamazepine - nicotinamide cocrystal intrinsic dissolution behaviour *Eur. J. Pharm. Biopharm,* 83**,** 415-426.

Rahman, Z., Agarabi, C., Zidan, A. S., Khan, S. R. and Khan, M. A. (2011) Physico-mechanical and Stability Evaluation of Carbamazepine Cocrystal with Nicotinamide. *Aaps Pharmscitech,* 12 (2)**,** 693-704.

Raman, C. V. and Krishnan, K. S. (1928) A New Type of Secondary Radiation. *Nature,* 121 (3048)**,** 501-502.

Rasanen, E. and Sandler, N. (2007) Near infra-red spectroscopy in the develpment of solid dosage forms. *J.Pharm.Pharmacol.,* 59**,** 147-159.

Rauwendaal, C. (1986b) *Twin screw extruders, in: Rauwendaal, C. (Ed.), Polymer extrusion.* 4 ed*.* cincinnati, Ohio, USA: Hanser.

Rodier, E., Lochard, H., Sauceau, M., Letourneau, J. J., Freiss, B. and Fages, J. (2005) A three step supercritical process to improve the dissolution rate of Eflucimibe. *Eur.J.Pharm.Sci.,* 26 (2)**,** 184-103.

Rodriguez-Hornedo, N. N., S.J.; Seefeldt, K.F. Pagan, T. (2006) Reaction crystallization of pharmaceutical molecular complexes. *Mol.Pharm.,* 3 (3)**,** 362-367.

Rodriguez - Hornedo, N., Nehm, SJ., Seefeldt, KF., Pagan -torres, Y. Falkiewicz, CJ. (2006) Reaction crystallization of pharmaceutical molecular complexes *Mol.Pharm.,* 3**,** 362 - 367.

Romero, T., Perez, R., Morris, K. R. and Grant, E. R. (2005) Raman spectroscopic measurement of tablet to tablet variability. *J.Pharm.Biomed.Anal.,* 38**,** 270-274.

Romero, T., Wikstrom, H., Grant, E.R., Taylor, L.S. (2007) Monitoring of Mannitol phase behaviour during freez drying using non- invasive Raman spectroscopy. *J.Pharm.Sci.,* 61**,** 131-145.

Rosen, S. L. (1993) *Fundamental principles of polymeric materials.* 2 ed*.* John Wiley and Sons.

Rull, F., Prieto, A. C., Casado, J. M., Sobrano, F. and Edwards, H. G. M. (1993) Estimates of crystallinity in polyethylene by Raman spectrscopy *J.Raman Spectrosc.,* 24**,** 545-550.

Rutter, N. (2012) *Thermal analysis of materials.* Cambridge: Univeristy of Cambridge.

Sabir, A. M., Moloy, M. and Bhasin, P. (2013) HPLC Method development and Validation: A review. *Int. Res. J. Pharm.,* 4 (4)**,** 39 - 46.

Saerens, L., Dierickx, L., Lenain, B., Vervaet, C., Remon, J. P. and Beer, T. D. (2011) Raman spectroscopy for the in-line polymer-drug quantification and solid state characterization during a pharmaceutical hot melt extrusion process. *Eur. J. Pharm. Biopharm,* 77**,** 158-163.

Salameh, A. K. and Taylor, L. S. (2006) Physical stabiility of crystal hydrates and their unhydrates in the presence of excipiients. *J.Pharm.Sci.,* 95 (2)**,** 446-461.

Savolainen, M., Kogermann, K. and Heinz, A. (2009) Better understanding of dissolution behaviour of amorphous drugs by in situ solid-state

analysis using Raman spectroscopy *Eur.J.Pharm and Biopharm.,* 71 (1)**,** 71-79.

Schmeling, N., Konietzny, R., Sieffert, D., Rölling, P. and Staudt, C. (2010) Functionalized copolyimide membranes for the separation of gaseous and liquid mixtures. *Beilstein J. Org. Chem.,* 6**,** 789–800.

Scott, B. and Wilcock, A. (2006) Process analytical technology in the pharmaceutical industry: A toolkit for continuous improvement. *PDA journal of pharmaceutical science and technology / PDA,* 60 (1)**,** 17-53.

Sekhon, B. S. (2009) Pharmaceutical co-crystals - A review. *Ars Pharmaceutica,* 50 (3)**,** 99-117.

Sekiguchi, K. and Obi, N. (1961) Studies on absorption of eutectic mixtures I A comparison of the behaviour of eutectic mixtures of sulphathiazole and that of ordinary sulphathiazole in man. *Chem.Pharm.Bull.,* 9**,** 866-872.

Sekiguchi, K. and Obi, N. (1964) Studies on absorption of Eutectic mixture II Absorption of Fused Conglomerates of Chloramphenicol and Urea in Rabbits. *Chem.Pharm.Bull.,* 12**,** 134-144.

Seo, A. (2003) The preparation of agglomerates coontaining solid dispersions of diazepam by melt agglomeration in a high shear mixer. *Int.J. Pharm.,* 259**,** 161-171.

Serajuddin, A. (1999) Solid dispersion of poorly water-sluble drugs: early promises, subsequent problems and recent breakthroughs. *J. Pharm.Sci.,* 88**,** 1058- 1066.

Shodor (2015) *Shodor home page.* Available from: http://shodor.org

Simonson, P. D. (2004) An Introduction to Raman Spectroscopy and the Development of SERS. [Physics 598 OS University of Illinois at Urbana-Champaign]. Available from

Skoog, D. A., Holler, F. J. and Crouch, S. R. (2007) *Principles of Instrumental analysis.* 6th ed. Thomson publisher.

Soares, F. L. F. and Carneiro, R. L. (2013) Green Synthesis of Ibuprofen-Nicotinamide Cocrystals and In-Line Evaluation by Raman Spectroscopy. *Crystal Growth & Design,* 13 (4)**,** 1510-1517.

Spragg, R. A. (1995) Pharmaceutical Analysis using FT-Raman spectroscopy. *Am Lab,* 27**,** 35-37.

Sreekanth, B. R., Vishweshwar, P. and Vyas, K. (2007) Supramolecular synthon polymorphism in 2:1 co-crystal of 4- hydroxybenzoic acid and 2,3,5,6 - tetramethylpyrazine. *Chem commun,* (23)**,** 3375-3377.

Starbuck, C., Spartalis, A. and Wai, L. (2002) Process optimization of a complex pharmaceutical polymorphic system via in situ Raman spectroscopy. *Cryst. Growth,* 2 (6)**,** 515-522.

Strachan, C. J., Howell, S. L., Rades, T. and Gordon, K. C. (2004) A theoretical and spectroscopic study of carbamazepine polymorphs. . *J.Raman Spectrosc.,* 35 (5)**,** 401-408.

Szelagiewicz, M., Marcolli, C., Cianferani, S., Hard, A. P., Vit, A., Burkhard, A., Von Raumer, M., Hofmeier, U. C., Zilian, A., Francotte, E. and Schenker, R. (1999) In Situ Characterization of Polymorphic Forms The Potential of Raman Techniques. *Journal of Thermal Analysis and Calorimetry,* 57 (1)**,** 23-43.

TA Instruments (2012) *Thermal Analysis.* TA Instruments. (Accessed 26.06.2015).

Tanaka, N., Imai, K., Okimoto, K., Ueda, S., Tokunaga, Y., Ohike, A., Ibuki, R., Higaki, K. and Kimura, T. (2005) Development of novel sustained-release system, disintegration- controlled matrix tablet (DCMT) with solid dispersion granules of nilvadipine. *J.Contr. Release,* 108 (2-3)**,** 386-395.

Taylor, L. S. and Zografi, G. (1997) Spectroscopic characterization of interactions between PVP and indomethacin in amorphous molecular dispersions. *Pharm Res,* 14**,** 1691-1698.

Taylor, L. S. and Zografi, G. (1998) The Quantitative Analysis of Crystallinity Using FT-Raman Spectroscopy. *Pharm.Res.,* 15 (5)**,** 755-761.

Tensmeyer, L. G. and Heathman, M. A. (1989) Analytical applications of Raman spectroscopy in the pharmaceutical field. *Trends anal Chem,* 8**,** 19-24.

Thermoscientific (2015) *Nicolet iS50 FTIR* Available from: www.thermoscientific.com

Thomas, L. C. (2005) MDSC paper #2, Modulated DSC, Basics: Calculation and Calibration of MDSC signals. Available from

Tian, F. J., Strachan, C. J., Saville, D. J., Gordon, K. C. and Rades, T. (2006) Characterizing the conversion kinetics of carbamazepine polymorphs to the dihydrate in aqueous suspension using Raman spectroscopy *J.Pharm.Biomed.Anal.,* 40**,** 271.

Urbanetz, N. A. (2006) Stablization of solid dispersions of nimodipine and polyethylene glycol 2000. *Eur.J.Pharm.Sci.,* 28**,** 67-76.

USFDA (2005) *Process Analytical Technology(PAT) Initiative.*

Van den Mooter, G., Weuts, I., De Ridder, T. and Blaton, N. (2006) Evaluation of Inutec SP1 as a new carrier n the formulation of solid dispersionsfor poorly sooluble drugs. *Int.J. Pharm.,* 316 (1-2)**,** 1-6.

van Drooge, D. J., Hinrichs, W. L. J., Visser, M. R. and Frijlink, H. W. (2006) Characterization of the molecular distribution of drugs in glassy solid dispersions at the nano-meter scale, using differential scanning calorimetery and gravimetric water vapour sorption techniques. *Int.J. Pharm.,* 310 (1-2)**,** 220-229.

Vasconcelos, T., Sarmento, B. and Costa, P. (2007) Solid dispersions as strategy to improve oral bioavailability of poor water soluble drugs. *Drug Discovery Today,* 12**,** 1068-1075.

Vergote, G. J., Beer, d. and Vervaet, C. (2004) In-liine monitoring of a pharmaceutical blending proocess using FT-Raman spectroscopy. *Eur.J.Pharm Sci.,* 21 (4)**,** 479-485.

Verreck, G., Decorte, A., Heymans, K., Adriaensen, J., Liu, D., Tomasko, D., Arien, A., Peeters, J., Van den Mooter, G. and Brewster, M. E. (2006) Hot stage extrusion of *p*- amino salicylic acid with EC using CO_2 as a temporary plasticizer. *Int.J. Pharm.,* 327 (1-2)**,** 45-50.

Verreck, G., Decorte, A., Heymans, K., Adriaensen, J., Liu, D., Tomasko, D. L., Arien, A., Peeters, J., Rombaut, P., Van den Mooter, G. and Brewster, M. E. (2007) The effect of supercritical CO_2 as a reversible plasticizer and foaming agent on the hot stage extrusion of itraconazole with EC 20 cps. *J.Supercrit.Fluids,* 40 (1)**,** 153-162.

Vitez, I. M., Newman, A. W., Davidovich, M. and Kiesnowski, C. (1998) The evolution of hot-stage microscopy to aid solid-state characterizations of pharmaceutical solids. *Thermochimica Acta,* 324 (1-2)**,** 187 - 196.

Walker, G. and Bell, S. E. (2009) Characterization of fludized bed granulation processes using in-situ Raman spectroscopy. *Chem.Eng.Sci,* 64**,** 91-98.

Wang, F., Watcher, J. A., Antosz, f. J. and Berglund, K. A. (2000) An investigation of Solvent mediated polymorphic transformation of Progesterone Using in-situ Raman spectroscopy. *Organic Process Research and Development,* 4 (5)**,** 391–395.

Wang, X., Michoel, A. and G., V. d. M. (2005) Solid state characteristics of ternary solid dispersions composed of PVP VA64, Myrj 52 andtraconazole. *Int.J. Pharm.,* 303**,** 54-61.

Ward, N. J., Edwards, H. G. M., Johnson, A. F., Fleming, D. J. and Coates, P. D. (1996) Applications of Raman spectroscopy for determining residence time distribution in extruder reactors. *Appl. Spectrosc.,* 50**,** 812-815.

Wijk, R. J., de Wejer, A. P., Klarenberg, D. A., de Jonge, R. and Jongerden, G. J. (1999) Technique for measuring properties of polymeric fibers. *International patent WO 99/12019*.

Wikstrom, H., Marsac, P. J. and Taylor, L. S. (2005) In-line monitoring of hydrate formation during wet granulation using Raman spectroscopy. *J.Pharm.Sci.,* 94**,** 209-219.

Wilkinson, A. N. and J., R. A. (1998) *Polymer processing and structure development.* The Netherlands: Kluwer Academic publishers.

Williams, M. (2010) Hot Melt Extrusion Technology: Optimizing Drug Delivery. *European Industrial pharmacy,* 4 (7)**,** 7-9.

Wilson, R. J. and Haines, P. J. (2002) *Principles of Thermal analysis and calorimetry.* Cambridge, United Kingdom: Royal society of Chemistry.

Wishart DS, Knox C, Guo AC, Shrivastava S, Hassanali M, Stothard P, Chang Z, Woolsey J. *DrugBank: a comprehensive resource for in silico drug discovery and exploration.* Nucleic Acids Res. 2006 Jan 1; 34 (Database issue):D668-72. 16381955.

Witzleb, R., Kanikanti, V. R., Hamann, H. J. and Kleinebudde, P. (2011) Solid lipid extrusion with small die diameters – electrostatic charging, taste masking and continuous production. *Eur. J. Pharm. Biopharm,* 77**,** 170–177.

Won, D. H., Kim, M. S., Lee, S., Park, J. S. and Hwang, S. J. (2005) Improved physicochemical characteristics of felodipine solid dispersion particles by supercrtical anti-solvent precipitation process. *Int.J. Pharm.,* 301 (1-2)**,** 199-208.

www.dscsolution.net Available from: www.dscsolution.net

www.slideshare.net *www.slideshare.net*

Yao, W. W., Bai, T. C., Sun, J. P., Zhu, C. W., Hu, J. and Zhang, H. L. (2005) Thermodynamic properties for the system of silybin and poly(ethylene glycol)6000. *Thermochim. Acta,* 437 (1-2)**,** 17-20.

Yoshihashi, Y., Iijima, H., Yonemochi, E. and Terada, K. (2006) Estimation of physical stability of amorphous solid dispersion using differential scanning calorimetry. *J.Therm.Anal.Calorim.,* 85 (3)**,** 689-692.

Zaworotko, M. (2008) Crystal engineering of co-crystals and their relevance to pharmaceuticals and solid - state chemistry. *Acta Cryst,* A- 64**,** C11-C12.

Appendices

Appendix

A - 1

Published work at conference

Presented a poster entitled “Prediction of Carbamazepine metabolite formation during hot melt extrusion using Raman spectroscopy - an application of Process Analytical Technology” at APS UK Pharm Sci 2014.

A - 2

HPLC

Simultaneous estimation of Carbamazepine and Iminostilbene by HPLC and calibration curve generation

During preparation of solid dispersions of Carbamazepine and Kollidon VA64 by hot melt extrusion yellow colour have been noticed which gave a reason to find out degradation mechanism of Carbamazepine. To understand Carbamazepine degradation or formation of its metabolite Iminostilbene, simultaneous HPLC of Carbamazepine and Iminostilbene was carried out using HPLC.

HPLC separations were carried out using Waters alliance e2695 HPLC system with Empower software. UV absorbance was monitored at 210nm and 219nm using Photodiode Array detector. Mobile phase was prepared (Table A - 2.1.) and allowed to sonicate for 10 minutes to remove air bubbles using Fisher brand sonicator. Table A - 2.2. indicates gradient proportions used for HPLC.

HPLC parameters:

Column	Symmetry C18 100°A 4.6mm×250mm 1pKg reversed phase by Waters
Mobile phase	A: Distilled water + 0.1% Formic acid B: Acetonitrile + 0.1% Formic acid
Column temperature	27°C
Sample injection volume	20µL (3 injections of each dilution and 2 injections of stock solutions)
Needle wash	Acetonitrile

Table A - 2.1. HPLC parameters (Mobile phase)

Time (min)	Flow	A%	B%	C%	D%
-	1.50	98.0	2.0	0.0	0.0
6	1.50	2.0	98.0	0.0	0.0
10	1.50	98.0	2.0	0.0	0.0
15	1.50	98.0	2.0	0.0	0.0

Table A - 2.1. Gradient proportions used for HPLC

Mean values of area µV sec were obtained from the values obtained from 3 injections of each dilutions and 2 injections of stock solutions. A graph of area Vs concentration (µg/mL) was plotted. Fig. A - 2.1. shows the calibration curve for simultaneous estimation of Carbamazepine and Iminostilbene.

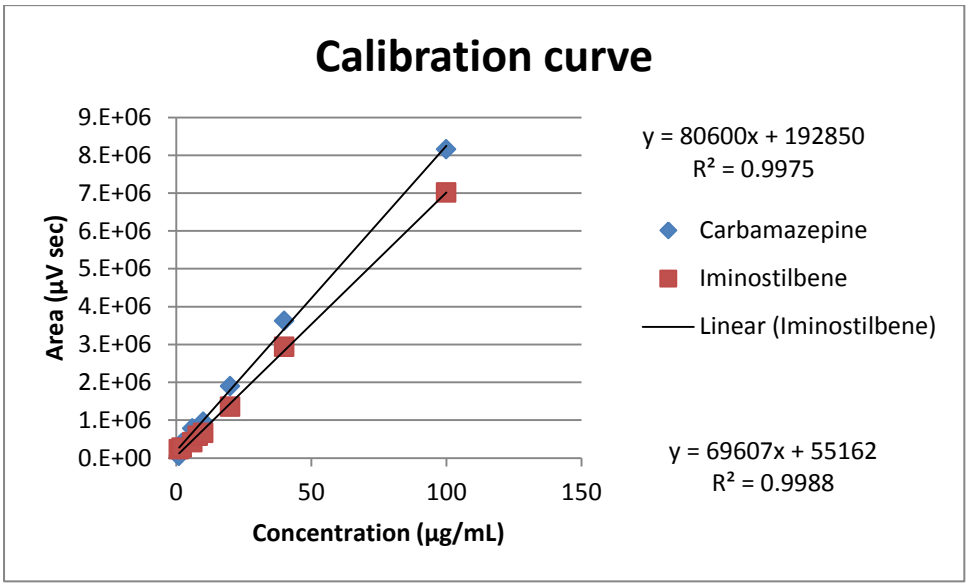

Fig. A - 2.1. Calibration curve for simultaneous estimation of Carbamazepine and Iminostilbene

From the calibration curve a straight line equation was obtained. Good linearity response was obtained with correlation coefficient of 0.9975 with the Carbamazepine. While Iminostilbene trend line has found to show correlation coefficient of 0.9988.

Unfortunately, after producing these preliminary calibration curves, the HPLC failed and had to go under service. Hence there was not enough time to fully characterize the solid dispersions for degradation during the project. This data will be useful further to detect % degradation content of Carbamazepine in solid dispersions. See further work section for more details.